



TECHNICAL UNIVERSITY OF CRETE  
School of Environmental Engineering  
Water Resources Management  
and Coastal Engineering Laboratory

# **Spatiotemporal drought analysis and climate change impact on hydrometeorological variables for the island of Crete**

A thesis submitted to the School of Environmental Engineering  
of Technical University of Crete  
in partial fulfillment of the requirements for the Degree of Doctor of Philosophy

**By**

**Angeliki-Eleni K. Vrochidou**

Supervisor: Professor Ioannis K. Tsanis

Chania, 2013

© 2013 Technical University of Crete

Angeliki-Eleni K. Vrochidou

All rights reserved

### ***Επταμελής επιτροπή***

- Τσάνης Ιωάννης (επιβλέπων),  
Καθηγητής Τμήματος Μηχανικών Περιβάλλοντος, Πολυτεχνείο Κρήτης
- Γκίκας Πέτρος,  
Επίκουρος Καθηγητής Τμήματος Μηχανικών Περιβάλλοντος, Πολυτεχνείο Κρήτης
- Καρατζάς Γεώργιος,  
Καθηγητής Τμήματος Μηχανικών Περιβάλλοντος, Πολυτεχνείο Κρήτης
- Λαζαρίδης Μιχαήλ,  
Καθηγητής Τμήματος Μηχανικών Περιβάλλοντος, Πολυτεχνείο Κρήτης
- Λουκάς Αθανάσιος (external),  
Καθηγητής Τμήματος Πολιτικών Μηχανικών, Πανεπιστήμιο Θεσσαλίας
- Τσούτσος Θεοχάρης,  
Αναπληρωτής Καθηγητής Τμήματος Μηχανικών Περιβάλλοντος, Πολυτεχνείο Κρήτης
- Χριστόπουλος Διονύσιος,  
Καθηγητής Τμήματος Μηχανικών Ορυκτών Πόρων, Πολυτεχνείο Κρήτης

**Χανιά, 19/11/2013**

# Abstract

---

The Mediterranean climate has been the focus of intense research on climate related issues. Climate change is expected to increase the risk of high drought frequency and duration. The Mediterranean region has been characterized as one of the main climate change “Hot-Spots” while it is quite vulnerable to its effects. The increasing frequency of extreme drought events in comparison to the past conditions constitutes one of the biggest concerns. The present PhD thesis focuses on the study of drought phenomena on the island of Crete. At first, combined methodology helped investigating the influence of elevation and longitude on precipitation distribution, offering valuable information about the linkage between these geographical factors and droughts. This connection provides an important clue for the respective spatial drought pattern, which is produced with the aid of the Spatially Normalized Standardized Precipitation Index (SN-SPI) for the period 1974–2005. Further analysis with the use of three Global Climate Models (GCMs) output (precipitation and temperature) and results from hydrological model IHMS-HBV for drought assessment at a basin scale was carried out. The produced hydrological variables (flow, soil moisture and lower groundwater reservoir volume) were used for the hydrological regime assessment, drought identification and projection till 2100 from two emission scenarios aspects. In addition, drought assessment and projection for the island of Crete was performed with the aid of thirteen GCMs output (precipitation), using the new scenarios based on the Representative Concentration Pathways (RCPs) 2.6, 4.5 and 8.5. The above findings aim to an improved understanding of drought mechanisms as well as to the future strategic planning for drought management.

## Περίληψη

---

Τα τελευταία χρόνια το μεσογειακό κλίμα αποτελεί το επίκεντρο εντατικής έρευνας σε θέματα που σχετίζονται με το κλίμα. Η κλιματική αλλαγή αναμένεται να αυξήσει τον κίνδυνο της υψηλής συχνότητας και διάρκειας ξηρασιών. Η περιοχή της Μεσογείου έχει χαρακτηριστεί μια από τις κύριες «εστίες» της κλιματικής αλλαγής, ενώ είναι αρκετά ευάλωτη στις επιπτώσεις της. Η αύξηση της συχνότητας των ακραίων φαινομένων ξηρασίας σε σύγκριση με τις παρελθοντικές συνθήκες αποτελεί μία από τις μεγαλύτερες ανησυχίες. Η παρούσα διδακτορική διατριβή επικεντρώνεται στη μελέτη φαινομένων ξηρασίας στο νησί της Κρήτης. Αρχικά, συνδυασμένη μεθοδολογία οδήγησε στην έρευνα της επίδρασης του υψομέτρου και του γεωγραφικού μήκους στην κατανομή της βροχόπτωσης, προσφέροντας πολύτιμες πληροφορίες σχετικά με τη συσχέτιση μεταξύ αυτών των παραγόντων και της ξηρασίας. Αυτή η συσχέτιση παρέχει μια σημαντική ένδειξη για το αντίστοιχο χωρικό πρότυπο της ξηρασίας, το οποίο παράγεται με τη βοήθεια του Χωρικά Κανονικοποιημένου - Τυποποιημένου Δείκτη Βροχόπτωσης (SN-SPI) για την περίοδο 1974-2005. Περαιτέρω ανάλυση διεξήχθη με τη χρήση των αποτελεσμάτων τριών παγκόσμιων κλιματικών μοντέλων (GCMs) (βροχόπτωση και θερμοκρασία) και του υδρολογικού μοντέλου IHMS-HBV για την αξιολόγηση της ξηρασίας σε επίπεδο λεκάνης απορροής. Οι παραγόμενες υδρολογικές παράμετροι (απορροή, εδαφική υγρασία και όγκος υπογείων υδάτων) χρησιμοποιήθηκαν για την εκτίμηση του υδρολογικού καθεστώτος, του εντοπισμού της ξηρασίας και μελλοντικών προβλέψεων μέχρι το 2100 βάσει δύο κλιματικών σεναρίων. Επιπλέον, η εκτίμηση της ξηρασίας και της πρόβλεψής της για το νησί της Κρήτης πραγματοποιήθηκε με τη βοήθεια των αποτελεσμάτων δεκατριών GCMs (βροχόπτωση), χρησιμοποιώντας τρία νέα κλιματικά σενάρια (RCPs) 2.6, 4.5 και 8.5. Τα αποτελέσματα της μελέτης στοχεύουν στην καλύτερη κατανόηση των μηχανισμών που διέπουν τις ξηρασίες και στον μελλοντικό σχεδιασμό στρατηγικής για τη διαχείριση της ξηρασίας.

*...Dedicated to my parents.*

# Acknowledgments

---

First and foremost I want to thank my supervisor Ioannis Tsanis for showing confidence in me by giving me the chance to work in his lab. It has been an honor to be his Ph.D. student. I appreciate all his contributions of time, ideas, and funding to make my Ph.D. experience productive and stimulating. The joy and enthusiasm he has for his research was contagious and motivational for me, even during tough times in the Ph.D. pursuit. I am also thankful for the excellent example he has provided as a successful engineer and professor.

The members of the laboratory have contributed immensely to my personal and professional time all these years. The group has been a source of friendships as well as good advice and collaboration. I gratefully acknowledge Aristeidis Koutroulis, Manolis Grillakis, Kostas Seiradakis, Ioannis Daliakopoulos, Sotiris Tsitsilonis and Vasiliki Iordanidou for their insightful advice and help as well as for enriching my experience and enabling the success of this thesis. My gratitude is also extended to the WATCH project for providing the WFD data, the World Climate Research Programme's Working Group on Coupled Modelling, within the context of CMIP, for producing and making available the model output of various climate modelling groups. Moreover, special thanks to SMHI for providing the IHMS version of the HBV hydrological model.

Lastly, I would like to thank my family for all their love, encouragement and support in all my pursuits. Without them, none of this would have been meaningful.

Technical University of Crete, 2013

Angeliki-Eleni K. Vrochidou

# Contents

---

Abstract .....	1
Περίληψη .....	2
Acknowledgments.....	4
Contents .....	5
List of Figures .....	7
List of Tables .....	10
1. Introduction .....	11
1.1 Climate and climate change .....	11
1.2 Droughts .....	14
1.3 Drought indices .....	15
1.4 Climate models.....	16
1.5 Objectives.....	17
1.6 Thesis outline .....	18
1.7 Innovative points .....	18
1.8 Case study .....	19
2. Precipitation distribution impacts on droughts .....	20
2.1 Methodology .....	21
2.1.1 Multiple linear regression .....	21
2.1.2 Clustering method.....	22
2.1.3 The SPI.....	24
2.1.4 The SN-SPI .....	29
2.2 Data .....	31
2.3 Results .....	34
2.3.1 Influence of elevation and longitude on precipitation .....	34

2.3.2	Precipitation shortage and excess .....	40
2.3.3	Spatiotemporal drought analysis.....	42
3.	The impact of hydrometeorological parameters on droughts.....	49
3.1	Methodology .....	52
3.1.1	Blaney-Criddle method.....	52
3.1.2	The hydrological model HBV.....	53
3.1.3	Threshold level method .....	56
3.2	Study area and data .....	58
3.3	Results .....	63
3.3.1	Hydrological model calibration and validation results and regime .....	63
3.3.2	Drought in different hydrometeorological variables.....	68
3.3.3	Frequency distributions.....	72
4.	Drought assessment based on multi-model precipitation projections .....	78
4.1	Methodology .....	81
4.1.1	Bias correction .....	81
4.1.2	The SN-SPI.....	82
4.2	Study area and data .....	82
4.3	Results and discussion.....	87
5.	Conclusions and recommendations for future research.....	95
5.1	Conclusions .....	95
5.2	Recommendations for future research.....	99
	Bibliography .....	101
	Publication list .....	121

## List of Figures

---

<b>Figure 1-1:</b> Projected changes in annual mean surface air temperature (K) under the A1B scenario, multi-model ensemble mean of RCM simulations for the time period 2071-2100 relative to the 1961-1990 mean (Van der Linden and Mitchell, 2009). .....	12
<b>Figure 1-2:</b> Projected changes in annual (left) and summer (right) precipitation (%) between 1961-1990 and 2071-2100 as simulated by ENSEMBLES Regional Climate Models for the IPCC SRES A1B emission scenario (European Environment Agency, 2012).....	13
<b>Figure 1-3:</b> Schematic representation of a General Circulation Model. The planet is divided into a 3-dimensional grid (horizontal and vertical grid) on which the basic equations are applied (www.noaa.gov). .....	16
<b>Figure 2-1:</b> Example of equiprobability transformation from fitted gamma distribution to the standard normal distribution. ....	26
<b>Figure 2-2:</b> Fitting of a representative dataset (observed values) to the expected values of gamma distribution. ....	28
<b>Figure 2-3:</b> Monthly SPI and SN-SPI (48-month time scale) time series for 2 representative watersheds.....	31
<b>Figure 2-4:</b> Area of study, 56 stations used in MLR and 18 representative stations for SPI Crete, Greece.....	33
<b>Figure 2-5:</b> a) Elevation versus mean annual precipitation plot and b) Longitude versus mean annual precipitation plot for Crete .....	35
<b>Figure 2-6:</b> Spatial distribution of a) precipitation for a long-term average of the period 1974-2005, b) precipitation shortage concerning the year 1989-1990 and c) precipitation excess concerning the year 2002-2003. ....	41
<b>Figure 2-7:</b> a) Monthly precipitation time series for drought events b) 48-month time scale SN-SPI and c) SPI for two representative stations of north-western Crete based on the period 1974-2005 .....	43
<b>Figure 2-8:</b> a) Monthly precipitation time series for drought events b) 48-month time scale SN-SPI and c) SPI for two representative stations of south-central Crete based on the period 1974-2005 .....	44
<b>Figure 2-9:</b> a) Monthly precipitation time series for drought events b) 48-month time scale SN-SPI and c) SPI for two representative stations of eastern Crete based on the period 1974-2005.....	46

<b>Figure 2-10:</b> Spatial separation of 55 stations using cluster analysis. a) Stations plot illustrating drought months as the dependent variable and b) silhouette plot of the clusters. .48	
<b>Figure 3-1:</b> Adjustment of WFD PET to measured values.....53	53
<b>Figure 3-2:</b> Schematic presentation of the HBV model for one subbasin (SMHI, 2006).....56	56
<b>Figure 3-3:</b> Determination of different flow curves for the threshold level definitions a) calendar units (day, month, season) and b) moving window (daily) (Hisdal and Tallaksen, 2000).....57	57
<b>Figure 3-4:</b> Platis basin location and relief.....59	59
<b>Figure 3-5:</b> a) Monthly and b) annual precipitation time series for Platis basin for the period 1974-1999.....60	60
<b>Figure 3-6:</b> Long-term daily averages derived from local and WFD datasets for Platis basin for the period 1974-1999. Top panel: temperature and precipitation; second panel: observed and simulated flow; third panel: soil moisture; lower panel: lower groundwater storage.....66	66
<b>Figure 3-7:</b> Seasonal variability between the past (observed and 3-model average) and future periods for precipitation and temperature climatic variables concerning A2 and B1 scenarios.....67	67
<b>Figure 3-8:</b> Seasonal variability between the past (observed and three-model average) and future periods for flow, soil moisture and lower groundwater climatic variables concerning A2 and B1 scenarios.....68	68
<b>Figure 3-9:</b> Example of drought propagation in Platis catchment for the hydrological year 1989-1990. Top panel: Mean annual precipitation; second panel: observed flow, dashed line = daily observed flow threshold d; third panel: simulated flow, dashed line = daily simulated flow threshold; fourth panel: soil moisture storage, dashed line = daily soil moisture threshold; lower panel: lower groundwater storage, dashed line = daily lower groundwater threshold.....71	71
<b>Figure 3-10:</b> Cumulative frequency distribution of drought duration (in days) for observed dataset and WFD regarding simulated flow (top), soil moisture (middle) and lower groundwater (bottom) during the past period 1974-1999.....73	73
<b>Figure 3-11:</b> Cumulative frequency distribution of drought duration (in days) for three models (CNCM, ECHAM5 and IPSL) regarding simulated flow (top), soil moisture (middle) and lower groundwater (bottom) during the past period 1974-2001 and future period 2001-2100 (Scenario A2), divided into four 25-year sub-periods.....74	74
<b>Figure 3-12:</b> Cumulative frequency distribution of drought duration (in days) for three models (CNCM, ECHAM5 and IPSL) regarding simulated flow (top), soil moisture (middle) and lower groundwater (bottom) during the past period 1974-2001 and future period 2001-2100 (Scenario B1), divided into four 25-year sub-periods.....75	75
<b>Figure 4-1:</b> The models grids and 50 stations over Crete a) $2.8^{\circ} \times 2.8^{\circ}$ : BCC-CSM1, CanEsm2, MIROC-ESM, MIROC-ESM-CHEM, FGOALS-g2, BNU-ESM, b) $3.75^{\circ} \times 1.89474^{\circ}$ : IPSL-CM5A-LR c) $1.40625^{\circ} \times 1.40625^{\circ}$ : MIROC5, d) $1.875^{\circ} \times 1.875^{\circ}$ : MPI-	

ESM-LR, MPI-ESM-MR, e) 1.125° x 1.125° : MRI-CGCM3, f) 2.5° x 1.89474° : NorESM1-M,	
g) 2.5° x 1.26° : IPSL-CM5A-MR. ....	83
<b>Figure 4-2:</b> Observed mean annual precipitation of three representative stations over Crete for the period 1973-2005. ....	84
<b>Figure 4-3:</b> a) Raw precipitation data versus bias corrected time series for a representative station (Kalives) for RCP4.5. ....	86
<b>Figure 4-4:</b> Ensemble of annual precipitation and temperature of all GCMs and scenarios for Crete. ....	87
<b>Figure 4-5:</b> Red lines represent the ensemble of average annual precipitation and temperature of all GCMs for Crete concerning RCP4.5, including 95% confidence limits. The dashed lines represent the annual ensemble precipitation and temperature trends. The green area represents the amplitude of the annual precipitation and temperature (min and max) in terms of the GCMs. ....	88
<b>Figure 4-6:</b> Ensemble of annual precipitation for 3 representative stations for all scenarios. ....	89
<b>Figure 4-7:</b> Time percentage of severe and extreme droughts for all RCPs during 2065-2099 period. ....	91
<b>Figure 4-8:</b> Time percentage of severe and extreme droughts for RCP4.5 during 1973-2005 and 2005-2035 periods. ....	92
<b>Figure 4-9:</b> Time percentage of severe and extreme droughts for RCP4.5 during 2035-2065 and 2065-2099 periods. ....	93
<b>Figure 4-10:</b> SN-SPI for three representative stations concerning all RCPs during the period 1973-2099. ....	94

## List of Tables

---

<b>Table 2-1:</b> Thresholds of SPI for drought characterization.....	27
<b>Table 2-2:</b> Simple and two-variable linear regression for 55 stations, regarding each year of 1974-2005. ....	36
<b>Table 2-3:</b> Simple and two-variable linear regression for Crete and its parts for different years. ....	37
<b>Table 2-4:</b> Characteristics of the stations used.....	39
<b>Table 3-1:</b> Hydrological characteristics of Platis basin. ....	62
<b>Table 3-2:</b> Characteristics of the stations used for Platis basin precipitation extraction.....	62
<b>Table 3-3:</b> Nash-Sutcliffe estimators for calibration and validation periods and drought characteristics concerning observed, HBV-observed and WFD datasets.....	64
<b>Table 3-4:</b> Drought characteristics in different hydrometeorological variables and different datasets for Platis basin for the period 1974-1999.....	69
<b>Table 3-5:</b> Change percentage of drought characteristics for 4 future periods (scenarios A2 and B1) concerning the three-model ensemble.....	77
<b>Table 4-1:</b> Types of representative concentration pathways.....	79
<b>Table 4-2:</b> Origin and grid size of GCMs used (Zunz et al., 2012). ....	85

# 1. Introduction

---

## 1.1 Climate and climate change

Human activity and life on Earth are strongly connected with climate and weather; hence the knowledge of these factors has always been an issue of great concern to society. In the last century it was recognized that human activity is changing the composition of the atmosphere and subsequently that the climate (both global and regional) is also changing. Global climate change is traced in meteorological variables, such as precipitation and temperature. Analysis of historical meteorological observations revealed that the 100-year linear trend (1906-2005) of 0.74 [0.56 to 0.92]°C (IPCC, 2007) is larger than the corresponding trend of 0.6 [0.4 to 0.8]°C (1901-2000) as presented in the Third Assessment Report (IPCC, 2001). Within the last decade the causal link between increasing concentrations of anthropogenic greenhouse gases in the atmosphere and the observed changes in temperature has been scientifically established (Van der Linden and Mitchell, 2009). **Figure 1-1** illustrates the projected changes in annual mean surface air temperature under the A1B scenario, multi-model ensemble mean of RCM simulations for the time period 2071-2100 relative to the 1961-1990 mean (Van der Linden and Mitchell, 2009).

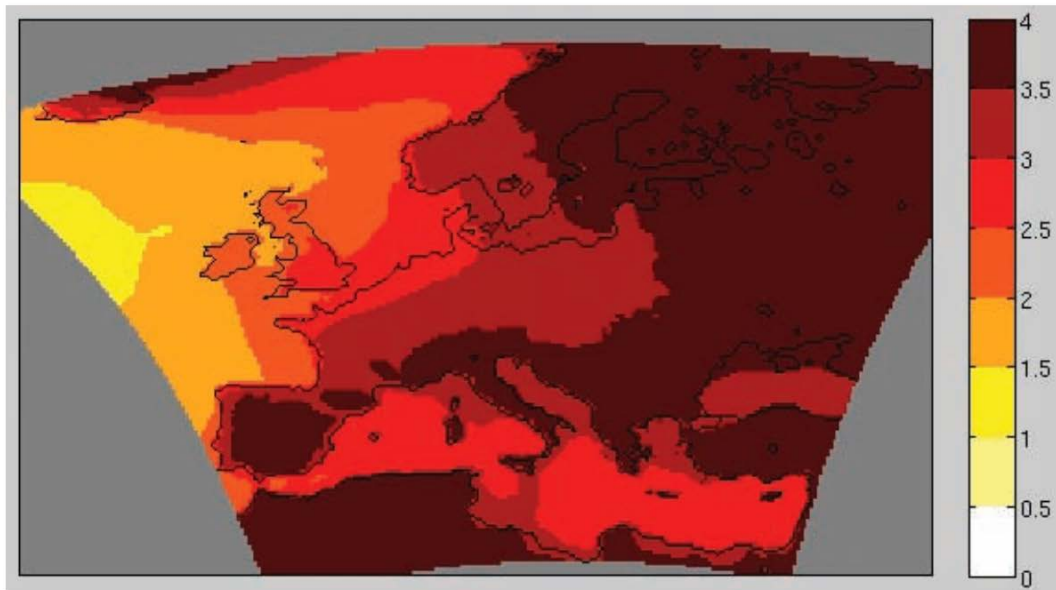


**Figure 1-1:** Projected changes in annual mean surface air temperature (K) under the A1B scenario, multi-model ensemble mean of RCM simulations for the time period 2071-2100 relative to the 1961-1990 mean (Van der Linden and Mitchell, 2009).

As the climate changes, extreme weather events like heat waves, droughts, heavy rain and snow, storms and floods are becoming more frequent or more intense. However, vulnerability to climate change varies widely across regions, due in part to complexities arising from interactions between atmospheric processes, oceans, land surfaces and polar ice masses. Rainfall patterns are also changing; in Europe the Mediterranean area is becoming drier, making it even more vulnerable to drought and wildfires. Northern Europe, meanwhile, is getting significantly wetter, and winter floods could become common. Studies in the Mediterranean region satisfy the evidence of a positive temperature trend in western Mediterranean and a negative trend in the eastern Mediterranean over the 20<sup>th</sup> century (National Observatory of Athens, 2001). Since 1900, precipitation decreased by over 5% concerning the area bordering the Mediterranean Sea, with the exception of central North African coast (Tunisia and Libya), while a precipitation decrease has been well documented in the central-west Mediterranean over the last 50 years (National Observatory of Athens, 2001; Loukas et al., 2007). **Figure 1-2** displays the projected changes in annual and summer precipitation between 1961-1990 and 2071-2100 as simulated by ENSEMBLES Regional Climate Models for the IPCC SRES A1B emission scenario (European Environment Agency, 2012).

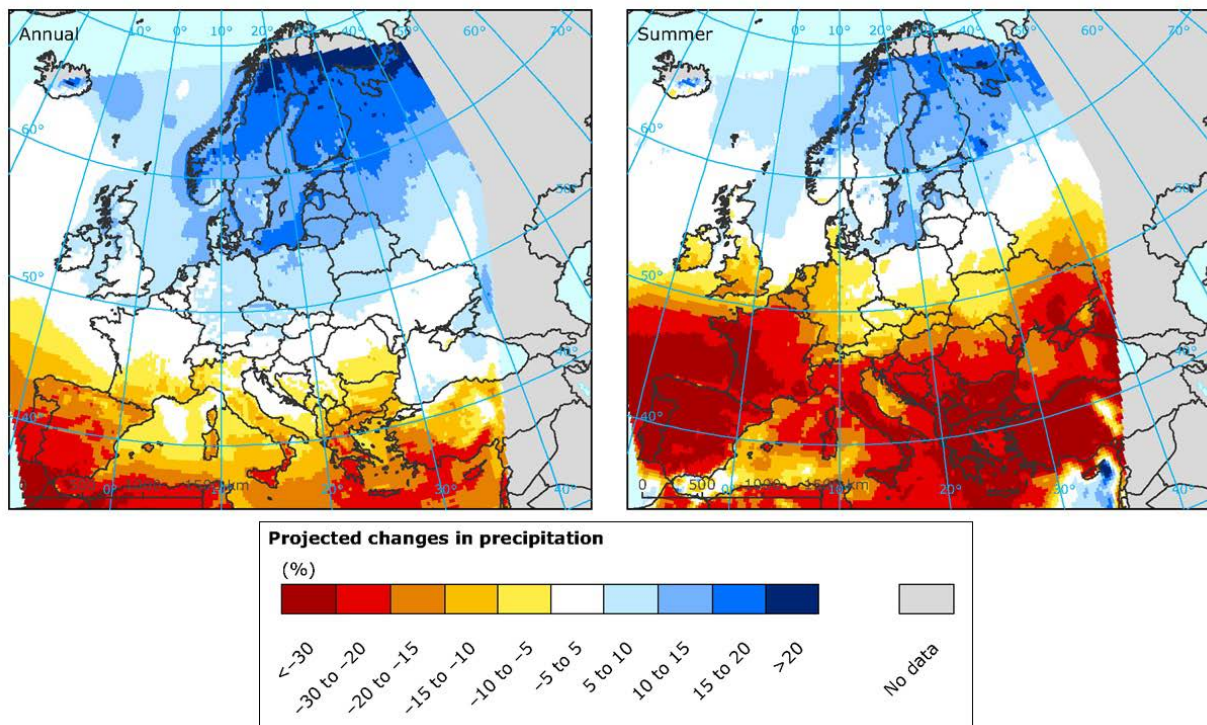


**Figure 1-2:** Projected changes in annual (left) and summer (right) precipitation (%) between 1961-1990 and 2071-2100 as simulated by ENSEMBLES Regional Climate Models for the IPCC SRES A1B emission scenario (European Environment Agency, 2012).

Over the last decade, numerous studies have been published about climate change and drought-related issues, despite the difficulty to distinguish between effects of climate change and multi - decadal climate variability (Berdowski et al., 2001). Especially the Mediterranean region is of particular interest insofar as being characterized as one of the most remarkable “Hot-Spots” in future climate change projections (Vrochidou et al., 2012; Giorgi, 2006). Giorgi and Lionello (2008) describe a picture of climate change over the Mediterranean, involving a decrease in precipitation, especially in the warm season, using global model simulations. Although climate change scenarios of precipitation extremes have been examined in the Mediterranean region via regional climate model simulations (Kyselý et al., 2012), there is still need for further investigation of the drought element connected to hydrological characteristics (Vrochidou et al., 2012).

Climate change is expected to have a range of crucial consequences, some of which will have long-term impacts such as droughts, sea level rise, wind patterns, species distribution and phenology while some will have directly obvious impacts on regional and local levels, such as intense rain and flooding, food production, ecosystem and human health (Wardekker,

2011). However, these impacts are associated with large uncertainties as they add up along the way, resulting to an “uncertainty explosion” or “cascade of uncertainty” (Dessai and Van der Sluijs, 2007).

## **1.2 Droughts**

One of the least understood phenomena connected to the weather which affects environment, society and economy in large areas all over the world is drought (Rossi et al., 1992). In the literature, many definitions of drought are given but the concept of a water deficit is the keynote in every definition of a drought: “Drought is a random condition of severe reduction of water supply availability (compared to normal value) extending along a significant period of time over a large region” (Rossi, 2000). However, all points of view seem to agree that drought is characterized by a significant decrease of water availability caused by a deficit in precipitation during a significant period over a large area. The effects and impacts of drought often accumulate slowly over a considerable period of time and may linger for years after the termination of the event so there are always lags in perceiving these effects and impacts. Drought is an objective phenomenon, so is its onset and end. The main issue is how to describe and how to quantify them. Because of this, drought is often referred to as a “creeping phenomenon” (Tannehill, 1947).

The hydrology of a region is affected by changes in the timing and amount of precipitation, evaporation, transpiration rates, and soil moisture, parameters which in turn affect also the drought characteristics in a region. A typical classification of droughts has been proposed by Dracup et al. (1980) and it has been widely accepted (Wilhite and Glantz, 1985; American Meteorological Society, 2004). According to this classification, meteorological, hydrological, and agricultural droughts, are considered environmental droughts (Wilhite, 2000; Loukas et al., 2007), and they are defined as periods with insufficient amounts of precipitation, river flow or groundwater, and soil moisture, respectively. The social-economic drought comprises the fourth drought type, which is associated to the ineffectiveness of water resources systems to meet the water demands.

Droughts are recognized as an environmental disaster and have raised the concern of various discipline scientists. Climate change and contamination of water supplies have further contributed to the water scarcity (Mishra and Singh, 2010). Lettenmaier et al. (1996) and

Aswathanarayana (2001) have made references to this change in the occurrence of extreme hydrologic events. All points of view seem to merge into the common belief of drought being characterized by a considerable decrease in water availability caused by a deficit in precipitation during a significant period over a large area (Koutroulis et al., 2011; Rossi, 2000; Wilhite, 2000).

### **1.3 Drought indices**

Drought indices are indispensable tools to detect, monitor and evaluate drought events in both time and space. The success of the above depends on the effective definition and quantification of drought characteristics, through which the beginning, end, spatial extent and severity of a drought are identified (Smakhtin and Hughes, 2007).

As a matter of fact, drought indices contain a large amount of data on rainfall, streamflow, snow and other hydrometeorological indicators that transform these huge datasets into a comprehensible picture. Hence, a drought index value is typically tantamount to a single number, more useful than raw data-set for decision making. A large number of drought indices have been suggested, among which including Standardized Precipitation Index (SPI - McKee et al., 1993), Palmer Drought Severity Index (PDSI - Palmer, 1965), Reconnaissance Drought Index (RDI – Tsakiris et al., 2007), deciles (Gibbs and Maher, 1967), Reclamation Drought Index (RDI – Weghorst, 1996), Crop Moisture Index (CMI – Palmer, 1968), Surface Water Supply Index (SWSI - Shafer and Dezman, 1982), and Aggregate Drought Index (ADI – Keyantash and Dracup, 2004).

Various studies are included in the international literature on testing the efficiency and the effectiveness of various drought indices regarding detection and monitoring drought events and regional drought analysis (Palmer, 1965; McKee et al., 1993; Meyer et al., 1993). SPI (Standardized Precipitation Index, McKee et al., 1993) and PDSI (Palmer Drought Severity Index, Palmer, 1965) are the most commonly used amongst the drought indices. This thesis focuses on the SPI application and moreover in the analysis of an SPI variant.

## 1.4 Climate models

General Circulation Models (GCMs) have been used to study the effects of the increasing concentration of carbon dioxide and the other greenhouse gases on the Earth's climate. These models link atmospheric processes with ocean and land surface processes and can be used to provide projections of the changes in temperature, precipitation and other climate variables in response to changes in greenhouse gas emissions. Climate models are systems of differential equations based on the basic laws of physics, fluid motion, and chemistry. To "run" a model, scientists divide the planet into a 3-dimensional grid, apply the basic equations, and evaluate the results (**Figure 1-3**). Atmospheric models calculate winds, heat transfer, radiation, relative humidity, and surface hydrology within each grid and evaluate interactions with neighboring points. Their typical grid size ranges from about 100 to 200 km (Meehl et al., 2007).

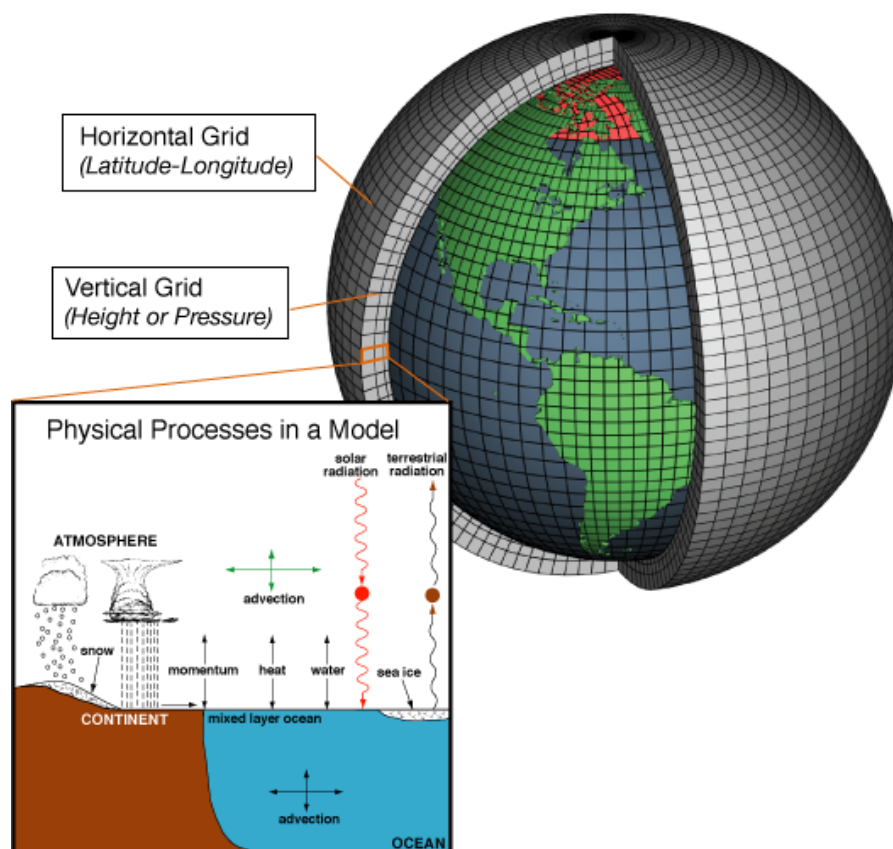


**Figure 1-3:** Schematic representation of a General Circulation Model. The planet is divided into a 3-dimensional grid (horizontal and vertical grid) on which the basic equations are applied ([www.noaa.gov](http://www.noaa.gov)).

In recent years a regional climate modeling technique has been developed at the National Center for Atmospheric Research (NCAR) to produce high resolution regional climate simulations. This consists of increasing the model resolution locally by nesting a high resolution Regional Climate Model (RCM) in a Global Climate Model (GCM) over given areas of interest. In the (one way) nesting technique the meteorological boundary conditions needed to run the RCM are provided by the output of a GCM global climate run.

The climate scenarios extraction includes a three-step process basically consisting of: (1) the development and use of general circulation models (GCMs) to provide future global climate scenarios under the effect of increasing greenhouse gases, (2) the development and use of downscaling techniques (RCMs and statistical methods) for “downscaling” the GCM output to the scales compatible with hydrological models, and (3) the development and use of hydrological, ecological and socioeconomic models to simulate the effects of climate change on hydrological regimes at various scales. The innovative GCM application efforts for climate study have been made by Dickinson et al. (1989) and Giorgi and Mearns (1991); in the following years general reviews of the methodology and progress in simulating hydrometeorological variables from GCM-derived climate change scenarios have been carried out (McGregor, 1997; Giorgi and Mearns; 1999; Varis et al., 2004; Wang et al., 2004; Christensen et al., 2007; Fowler et al., 2007).

## **1.5 Objectives**

With the ultimate aim of improving the understanding of drought mechanisms, the objectives of the present study are focused on the assessment of drought events in the island of Crete and are allocated as follows:

- Combination of methods for drought events analysis in spatial and temporal scale as well as their connection to precipitation variation.
- Hydrological parameters contribution to different drought types.
- Better understanding of drought events appearance.
- Application of a modified drought index for improved relative spatial information between basins.
- Utilization of multiple datasets for climate conditions projection.
- Future scenarios production for drought.

## **1.6 Thesis outline**

Up to this point general information about climate change and droughts has been presented. Furthermore, climate models contribution was developed and the objectives of the thesis were mentioned. The innovative points as well as a brief description of the case study follow the present outline. In Chapter 2 precipitation distribution impacts on droughts are assessed; the connection between spatial precipitation distribution and geographical parameters in the island of Crete is provided with the use of simple and multiple linear regression. Multiple precipitation models are generated for north, south-central and eastern Crete and the respective spatial drought patterns are produced with the application of the SN-SPI drought index. Chapter 3 presents the impact of hydrological and meteorological variables on droughts and moreover, a drought projection using the threshold level method for Platis basin is carried out with the use of three GCMs of CMIP3. In Chapter 4 a drought assessment based on multi-model precipitation projections in Crete is carried out with the use of thirteen GCMs of CMIP5 under the new climatic scenarios RCPs and the application of the SN-SPI leads to an updated drought projection. Finally, Chapter 5 includes the final conclusions and the recommendations for future research.

## **1.7 Innovative points**

The present thesis includes innovative analyses based on drought issue. The innovative points of the present thesis are already presented and published in both greek and international level. These points are focused on the basic and applied research as follows:

Basic research:

- Combination of methods for spatial and temporal drought analysis in the island of Crete.

Applied research:

- Processing of fundamental hydrological and meteorological parameters
- Extraction of climatic trends and drought projection with the aid of Global Climate Models simulation
- Multiple drought type assessment

## 1.8 Case study

The island of Crete is located in the southeastern part of the Mediterranean region and it is well known that comprises an area which has been characterized as one of the most drought prone areas of Greece. The island covers an area of 8336 km<sup>2</sup>, the mean elevation is 460 m and the average slope is 22.8%. Crete is divided into four prefectures, namely from west to east: Chania, Rethymnon, Heraklio and Lassithi. The mean annual precipitation is estimated to be 750 mm, varies from east - 440 mm (southeast - elevation: 10 m) to west - 2118 mm (northwest - elevation: 740 m), decreases in west-east direction by as much as 400mm on average (Vrochidou and Tsanis, 2012) and the potential renewable water resources reach 2650 Mm<sup>3</sup> (Chartzoulakis and Psarras, 2005).

The actual water use is about 485 Mm<sup>3</sup>/year. The main water use in Crete covers irrigation, with a high percentage of 83.3% of the total consumption. The domestic use, including tourism, covers 15.6% and the industrial use 1% of the total consumption (Region of Crete, 2002). The eastern and southern parts are more arid than the west and northern parts, as there is higher precipitation in the Northwestern coastal areas and lower in the Southeastern part of the island, a fact that confirms regional variations in water availability (Chartzoulakis et al., 2005). There are significant effects when the uneven spatial and temporal precipitation distributions of Crete, although common in many Mediterranean areas, are related to intensive agricultural activities and the tourism industry (Tsanis and Naoum, 2003).

Crete has been classified as one of the most drought-prone areas of Greece. The public belief that water resources are inadequate and that some kind of drought is imminent originates from political interests and disputes among the four prefectures and the more than 100 municipalities of the island, as well as poor water management (Manios and Tsanis, 2006). According to evaluations of Region of Crete (2011) the future water demand is expected to reach 550 Mm<sup>3</sup>, taking into account 3% annual tourism growth and 8% increase of irrigated areas.

## **2. Precipitation distribution impacts on droughts**

---

The geographical distribution of precipitation depends on various parameters that include topography, orientation of topography and aspect, direction of wind and continentality (Naoum and Tsanis, 2003). Several studies deal with the variability of precipitation analyzing the relationship between mean annual precipitation and geographical factors (Basist et al., 1994; Guan et al., 2005; Harris et al., 1996; Naoum and Tsanis, 2004), finding significant increasing relations between these characteristics. A common belief that precipitation amounts increase with elevation has then adopted, thereby proving that the mountainous environment is prone to extreme and frequent precipitation events (Allamano et al., 2009). Naoum and Tsanis (2003) studied the spatio-temporal rainfall characteristics in the island of Crete for a range of 12-50 years and found that the rainfall-elevation correlation was significant. In addition, the effect of elevation, longitude and latitude on precipitation distribution was investigated by Naoum and Tsanis (2004) with the generation of second-order models with interaction effects between the variables; however, the island of Crete has no significant latitude range and for the present study it was not considered as an influencing parameter. Drogue et al. (2002) used an operational software called PLUVIA, which distributes point measurements of monthly, annual and climatological rainfall to regularly spaced grid cells through a multiple regression analysis of rainfall versus morpho-topographic parameters derived from a digital elevation model. According to Wotling et al. (2000), a Gumbel rainfall distribution was performed by using a stepwise regression adjusted on rainfall records across Tahiti and an approximation of the pluviometric risk was provided.

The study of weather patterns associated with precipitation events can serve as a reliable early warning system and a non-structural approach for drought mitigation. It is known that storm events are often associated with the development of low-pressure systems (Koutroulis et al., 2010). Over the Mediterranean these systems originate from three main directions which can be roughly distinguished as West (W), Southwest (SW) and Northwest (NW). According to Barry and Chorley (2003), depressions that enter the Mediterranean from the Atlantic Ocean (W source) and baroclinic waves from the Atlas mountain range (SW source) influence by 9% and 17% of the low-pressure systems respectively. The remaining 74% form at the lee of the Alps and Pyrenees (NW source). Each class effects of this weather classification are mentioned in literature (Barry and Chorley, 2003) and being well documented.

The objective of this study is to assess drought events over Crete at both the spatial and temporal scale and connect them with precipitation variability. More specifically, the comprehension of the evolution of this climatic phenomenon and identification of important drought episodes are provided, offering extra reliability to the results via the innovative use of multiple methods. Moreover, the connection between spatial precipitation and weather systems orientation will be of great interest as they comprise a significant clue for the characterization of droughts according to the respective spatial pattern. Determining precipitation variability and its spatial extent and therefore drought risk periods and areas for the island of Crete, can be used as basic but effective drought mitigation and risk management planning. At the same time, this kind of information may be used to support a simplified drought alert system.

## **2.1 Methodology**

### **2.1.1 Multiple linear regression**

Statistical methods can be used to describe the behavior of a set of observations by focusing attention on the observations themselves rather than on the physical processes that produced them. One of those statistical methods is regression. Regression analysis is a technique for analyzing raw data and searching for the messages they contain, hence providing certain insights into how to plan the collection of data when the opportunity arises. In any system in

which variable quantities change, it is of interest to examine the effects that some variables exert or appear to exert on others. There may, in fact, be a simple functional relationship between variables. In most physical processes, however, this is the exception rather than the rule. Often a functional relationship exists that is too complicated to describe in simple terms. In this case we may wish to approximate to this functional relationship by some simple mathematical function, such as a polynomial, which contains the appropriate variables and which graduates or approximates to the true function over some limited ranges of the variables involved. By examining such a graduating function we may be able to learn more about the underlying true relationship and appreciate the separate and joint effects produced by changes in certain important variables. Even where no sensible physical relationship exists between variables, we may wish to relate them by some sort of mathematical equation. While the equation might be physically meaningless, it may, nevertheless, be extremely valuable for predicting the values of some variables from knowledge of other variables, perhaps under certain stated restrictions (Draper and Smith, 1998).

The method of analysis used is the method of least squares (LS), which is simply a minimization of the sum of squares of the deviations of the observed response from the fitted response (Naoum and Tsanis, 2003). This involves the initial assumption that a certain type of relationship, linear in unknown parameters, holds. With precipitation being the dependent (response) variable, the model function is of a specified form that involves both the predictor variables (elevation and longitude) and the parameters. Interaction effects between the variables also can be considered. The unknown parameters are then estimated under certain other assumptions with the help of available data so that a fitted equation is obtained. While the equation might be physically meaningless, it may, nevertheless, be extremely valuable for predicting the values of some variables from knowledge of other variables, perhaps under certain stated restrictions (Draper and Smith, 1998). The general form of the final model is

$$P = b_0 + b_1x_1 + b_2x_2 \quad (2 - 1)$$

where P is precipitation (mm/year),  $x_1$  is elevation (m) and  $x_2$  is longitude (km).

### **2.1.2 Clustering method**

The definition of relationships between factors can be assessed through clustering methodology, which is the process of grouping the data into classes or clusters so that objects

within a cluster have high similarity in comparison to one another, but are very dissimilar to objects in other clusters. Clustering of time series has received considerable attention in recent years as it is a fundamental task in data mining. In the literature, various clustering methods have been used in time series; hierarchical clustering (Oates et al., 1999), K-medoids clustering (Kalpakis et al., 2001), nearest neighbour clustering (Zhang et al., 2004), self-organizing maps (Fu et al., 2001). Amongst all clustering algorithms, K-means clustering has become the most well-known and commonly used partitioning clustering method because it works well for finding spherical-based clusters in small- to medium-sized databases in hydro-meteorological studies (Chavoshi and Soleiman, 2009; Soltani and Modarres, 2006; Ouyang et al., 2010). Hayward and Clarke (1996) made a statistical analysis of mean monthly rainfall in the Freetown Peninsula, performing division of the gauges with clustering, regarding their orientation. Additionally, multiple regression with the parameters of latitude and the distance from the sea was applied providing various results for both groups of rain gauges.

Cluster analysis is a multivariate method which aims to classify a sample of subjects (or objects) on the basis of a set of measured variables into a number of different groups such that similar subjects are placed in the same group. K-means clustering (McQueen, 1967) comprises a prototype-based, partitional clustering technique that attempts to find a user-specified number of clusters (K), which are represented by their centroids. The algorithm first selects initial cluster centers (essentially this is a set of observations that are far apart - each subject forms a cluster of one and its centre is the value of the variables for that subject). Each object is assigned to its “nearest” cluster, defined in terms of the distance to the centroid and after the formation of the centroids of the clusters, the distance from each object to each centroid is re-calculated moving observations to the “nearest” cluster once again. (Tan et al., 2006). This process is repeated until the criterion function converges and the centroids remain relatively stable forming permanent clusters (Struyf et al., 1997). The algorithm aims at minimizing the sum of squared Euclidean distances, for n data points and k centroids, implicitly assuming that each cluster has a spherical normal distribution:

$$F = \sum_{j=1}^k \sum_{i=1}^n |x_i^j - c_j|^2 \quad (2 - 2)$$

where  $|x_i^j - c_j|^2$  (squared Euclidean distance) is a chosen distance measure between a data point  $x_i^j$  and the cluster centre  $c_j$ , and represents an indicator of the distance of the n data points from their respective cluster centres.

The algorithm was applied with the use of MATLAB R2011b package, which also provides a graphical display of the silhouette plot; the silhouette width [s(i)] was recommended by Kaufman and Rousseeuw (1990) as a quality index allowing to select the number of clusters and validate the effectiveness of the analysis. The silhouette width of the  $i^{\text{th}}$  object is defined by

$$s(i) = \frac{b_i - a_i}{\max\{a_i, b_i\}} \quad (2 - 3)$$

where  $a(i)$  is the average distance to other elements in the cluster and  $b(i)$  the smallest average distance to other clusters.  $a(i)$  is interpreted as how well matched  $i$  is to the cluster it is assigned (the smaller the value, the better the matching). An  $s(i)$  close to one means that the data is appropriately clustered. If  $s(i)$  is close to negative one, then the corresponding data is probably in the wrong cluster. An  $s(i)$  near zero means that the elements are on the border of two natural clusters.

### 2.1.3 The SPI

The SPI is used for assessing drought occurrence and offers the advantage of assessing drought conditions over a wide spectrum of time scales, while comparison between dry and wet periods on different locations is possible. Moreover, it is based on precipitation alone, so that a drought could be assessed even if other meteo-hydrological data are not available (Bonaccorso et al., 2003).

The SPI index was developed by McKee et al. (1993). Among others, the Colorado Climate Center, the Western Regional Climate Center and the National Drought Mitigation Center use the SPI to monitor the drought status in the United States. In its original version, precipitation for a long period at a station is fitted to a gamma probability distribution (Thom, 1966). The gamma distribution is defined by its frequency or probability density function:

$$g(x) = \frac{1}{\beta^\alpha \Gamma(\alpha)} x^{\alpha-1} e^{-x/\beta} \quad \text{for } x > 0 \quad (2 - 4)$$

where  $\alpha$  is a shape parameter ( $\alpha > 0$ ),  $\beta$  is a scale parameter ( $\beta > 0$ ),  $x$  is the precipitation amount ( $x > 0$ ) and  $\Gamma(\alpha)$  is the gamma function [ $\Gamma(\alpha) = \int_0^\infty y^{\alpha-1} e^{-y} dy$ ].

Computation of the SPI involves fitting a gamma probability density function to a given frequency distribution of precipitation totals for a station. The alpha and beta parameters of

the gamma probability density function are estimated for each station, for each time scale of interest (3 months, 6 months, 12 months, 24 months, 48 months), and for each month of the year. From Thom (1966), the maximum likelihood solutions are used to optimally estimate  $\alpha$  and  $\beta$  for  $n$  number of precipitation observations:

$$a = \frac{1}{4A} \left( 1 + \sqrt{1 + \frac{4A}{3}} \right) \text{ and } \beta = \frac{x}{a} \quad (2-5)$$

$$\text{where } A = \ln(x) - \frac{\sum \ln(x)}{n} \quad (2-6)$$

The resulting parameters are then used to find the cumulative probability of an observed precipitation event for the given month and time scale for the station under study. The cumulative probability is given by:

$$G(x) = \int_0^x g(x) dx = \frac{1}{\beta^\alpha \Gamma(\alpha)} \int_0^x x^{\alpha-1} e^{-x/\beta} dx \quad (2-7)$$

Gamma function is not defined at  $x=0$  (but there is large number of no rainfall occurrences as we move to shorter time scales); for  $m$  zeros in a precipitation time series, cumulative distribution is therefore modified to include these events:

$$H(x) = (m/n) + [1 - (m/n)G(x)] \quad (2-8)$$

The cumulative probability,  $H(x)$ , is then transformed to the standard normal random variable  $Z$  with mean zero and variance of one, which is the value of the SPI (**Figure 2-1**). This is an equiprobability transformation which is based on the following rational approach of Abramowitz and Stegun (1965) and has the essential feature of transforming a variate from one distribution (ie. gamma) to a variate with a distribution of prescribed form (ie. standard normal) such that the probability of being less than a given value of the variate shall be the same as the probability of being less than the corresponding value of the transformed variate:

$$Z = SPI = - \left( t - \frac{c_0 + c_1 t + c_2 t^2}{1 + d_1 t + d_2 t^2 + d_3 t^3} \right) \text{ when } 0 < H(x) \leq 0.5 \quad (2-9)$$

$$Z = SPI = + \left( t - \frac{c_0 + c_1 t + c_2 t^2}{1 + d_1 t + d_2 t^2 + d_3 t^3} \right) \text{ when } 0.5 < (H(x) < 1 \quad (2-10)$$

where

$$t = \sqrt{\left(\ln\left(\frac{1}{H^2(x)}\right)\right)} \quad \text{when } 0 < H(x) \leq 0.5 \quad (2-11)$$

$$t = \sqrt{\left(\ln\left(\frac{1}{1-H^2(x)}\right)\right)} \quad \text{when } 0.5 < H(x) < 1 \quad (2-12)$$

$$c_0 = 2.515517 \quad (2-13)$$

$$c_1 = 0.802853$$

$$c_2 = 0.010328$$

$$d_1 = 1.432788$$

$$d_2 = 0.189269$$

$$d_3 = 0.001308$$

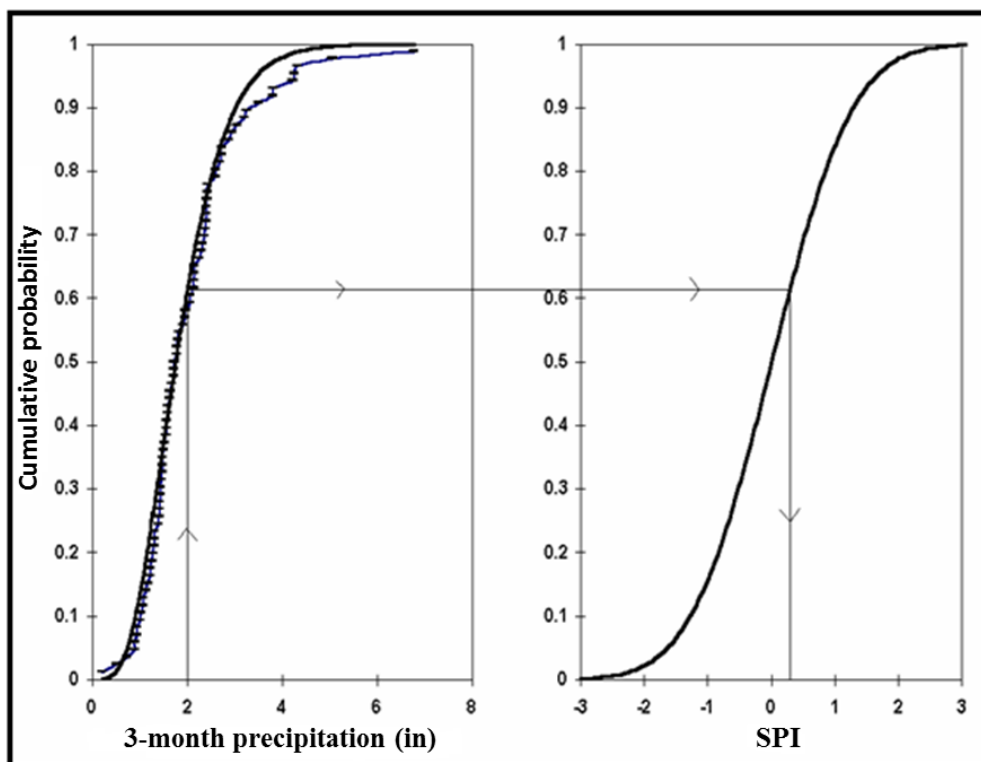


**Figure 2-1:** Example of equiprobability transformation from fitted gamma distribution to the standard normal distribution.

Positive SPI values denote greater than median precipitation whereas negative values denote less than median precipitation. Periods with drought conditions are represented by relatively

high negative deviations. Specifically, the ‘‘drought’’ part of the SPI range is arbitrary divided in four categories; mildly dry ( $0 > \text{SPI} > -0.99$ ), moderately dry ( $-1.0 > \text{SPI} > -1.49$ ), severely dry ( $-1.5 > \text{SPI} > -1.99$ ) and extremely dry conditions ( $\text{SPI} < -2.0$ ). A drought event is considered to start when SPI value reaches -1.0 and ends when SPI becomes positive again (McKee et al., 1993). Thresholds of the SPI for drought characterization are presented in **Table 2-1**.

There is a general agreement about the fact that the SPI computed on shorter time scales (3 or 6 months) describes drought events that affect agricultural activities (soil moisture), whereas on the longer ones (12, 24 or 48 months) describes the effects of precipitation deficit on different water resources components such as streamflow, groundwater and reservoir storage (Bonaccorso et al., 2003; Tsakiris and Vangelis, 2004; Sönmez et al., 2005; Livada and Assimakopoulos, 2007; Bacanli et al., 2008). In this thesis, the longest time scale (48 months) is set in the calculation of the SPI.

***Table 2-1: Thresholds of SPI for drought characterization***

<b>SPI value</b>	<b>Category</b>	<b>Probability (%)</b>
2 or more	Extremely wet	2.3
1.5 to 1.99	Severely wet	4.4
1 to 1.49	Moderately wet	9.2
0 to 0.99	Mildly wet	34.1
0 to - 0.99	Mildly dry	34.1
-1 to -1.49	Moderately dry	9.2
- 1.5 to -1.99	Severely dry	4.4
- 2 or less	Extremely dry	2.3

Kolmogorov-Smirnov test (Chakravarti et al., 1967) has proved that the used datasets follow gamma distribution; **Figure 2-2** illustrates the fitting of a representative dataset to the expected values of gamma distribution.

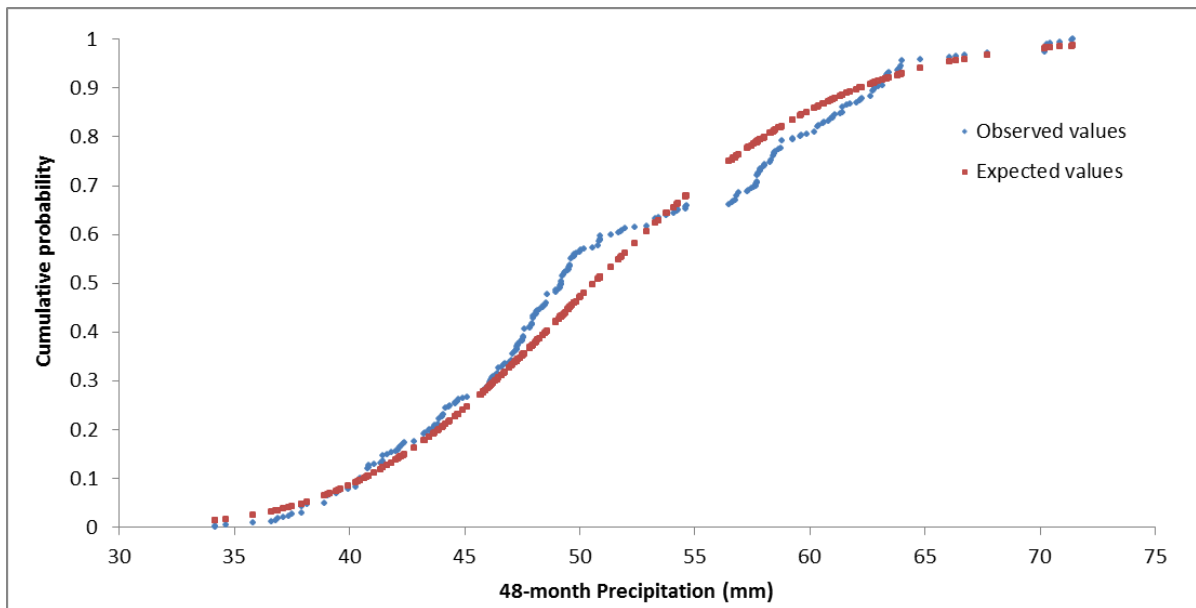


**Figure 2-2:** *Fitting of a representative dataset (observed values) to the expected values of gamma distribution.*

Several studies have been performed for the application of the SPI. Especially in the area of Crete, Tsakiris and Vangelis (2004) concluded that the eastern part of the island suffers more frequently from droughts, according to a method based on the estimation of the SPI and its use for characterizing drought. A digital terrain model, based on spatial distribution utilizing a grid analysis and a simple computer calculating process, was used and it was deduced that the proposed procedure could be easily applied to an area of mesoscale dimensions. It was concluded that a significantly persistent drought occurrence was noted during the period 1987 to 1994, while distinct drought events were observed in the years 1973–1974, 1976–1977, 1985–1986 and 1999–2000. Additionally, Tsakiris et al. (2007) estimated drought areal extent for eastern Crete using the SPI and RDI, and deduced that the driest year during the examined period from 1962–1963 to 1991–1992 is 1989–1990.

The selection of the most appropriate drought index was carried out, according to previous studies. Tsakiris et al. (2007) concluded that SPI and RDI give comparable results. However, discrepancies occur due to the fact that RDI uses an additional meteorological determinant (PET) apart from precipitation. The PDSI, on the other hand, is very complex, spatially variant, difficult to interpret, and temporally fixed. The application of the SPI index covers a significant part of many studies that have been carried out over the last decades (Bonaccorso et al., 2003; Loukas and Vasiliades, 2004; Wu et al., 2007). Nevertheless, Vicente-Serrano and Begueria (2003) point out that drought indices are not as useful in identifying spatial

patterns of drought risk since they are based on standardized or normalized shortages in relation to “average conditions”, which relate to a given station and a given period.

#### 2.1.4 The SN-SPI

Although SPI is widely used for assessing drought occurrence, there are some limitations in providing relative information when applied for different regions (at the river basin scale). In its original form it provides a local measure of drought, which as such is not necessarily suitable for comparisons across space and time. As a result, the frequency of drought spells is about the same for all stations no matter if they lie in extremely arid or extremely rainy regions, even though the rainy sites may receive several times more rain than the arid sites. In this context, Dubrovsky et al. (2009) applied the relative drought indices (rSPI and rPDSI), which are calibrated using a reference weather series as a first step, which is then applied to the tested series.

A similar approach for the creation of a modified index based on the SPI was realized by Koutroulis et al. (2011). The Spatially Normalized-SPI (SN-SPI) is a variant of the SPI and allows the comparison between watersheds with different mean annual precipitations. After the normalization, the index smooths the extreme conditions and makes it possible to compare stations by taking into account the spatial character of precipitation. In this thesis, the SN-SPI was recommended as a drought index for the calculation of drought climatology for the island of Crete in Greece, because it is spatially normalized for improved assessment of drought severity (Koutroulis et al., 2011). The fundamental virtue of this index consists of its capacity for compacting and unifying spatial information, reducing it to a common language.

More specifically, the procedure includes the normalization of SPI values through the incorporation of the precipitation values. The calculation of the SN-SPI is based on a two-step procedure. The first step is the normalization of the SPI index according to the relative average precipitation, based on a set of coefficients ( $a_i, b_i$ ) that satisfy:

$$\frac{\bar{P}_i}{\bar{P}_{all}} = a_i \quad (2 - 14)$$

$$\frac{\bar{P}_{all}}{\bar{P}_i} = b_i \quad (2 - 15)$$

where  $\bar{P}_i$  is the mean monthly precipitation for each watershed  $i$ ,  $\bar{P}_{all}$  the mean monthly precipitation for all watersheds,  $SPI_{max}$  the maximum SPI value of all watersheds. Given  $a_i$  and  $b_i$   $SPI'$  is calculated through:

$$SPI' = SPI \cdot a_i \text{ if } SPI > 0 \quad (2 - 16)$$

$$SPI' = SPI \cdot b_i \text{ if } SPI < 0 \quad (2 - 17)$$

The second step is the rescaling of  $SPI'$  in order to meet the scale of SPI, based on the coefficients  $c$  and  $d$  estimated through:

$$\frac{SPI_{max}}{SPI'_{max}} = c \quad (2 - 18)$$

$$\frac{SPI_{min}}{SPI'_{min}} = d \quad (2 - 19)$$

where  $SPI_{min}$  the minimum SPI value of all watersheds,  $SPI'_{max}$  the maximum corrected SPI value of all watersheds and  $SPI'_{min}$  the minimum corrected SPI value of all watersheds. Given  $c$  and  $d$  the  $SN - SPI$  calculation is defined by

$$SNSPI = SPI' \cdot c, \text{ if } SPI' > 0 \quad (2 - 20)$$

$$SNSPI = SPI' \cdot d, \text{ if } SPI' < 0 \quad (2 - 21)$$

For example, two watersheds are considered, Tavronitis and Petras, with 1347 mm and 723 mm average annual rainfall respectively. Tavronitis watershed can be relatively characterized as wet and Petras watershed as dry. SPI series for both watersheds are almost the same and here lies the limitation of the SPI when used to compare areas of different average precipitation. **Figure 2-3** displays that the severity of the 1990-1995 period is identical for both watersheds, although Tavronitis receives more precipitation than Petras. This period is severely dry for both watersheds when calculating the SPI, whereas it comprises a mildly dry period just for Tavronitis with SN-SPI calculation. In similar manner, the SPI indicates severely wet conditions for Petras during 1981-1984, while after the normalization with SN-SPI it is characterized by mildly wet conditions.

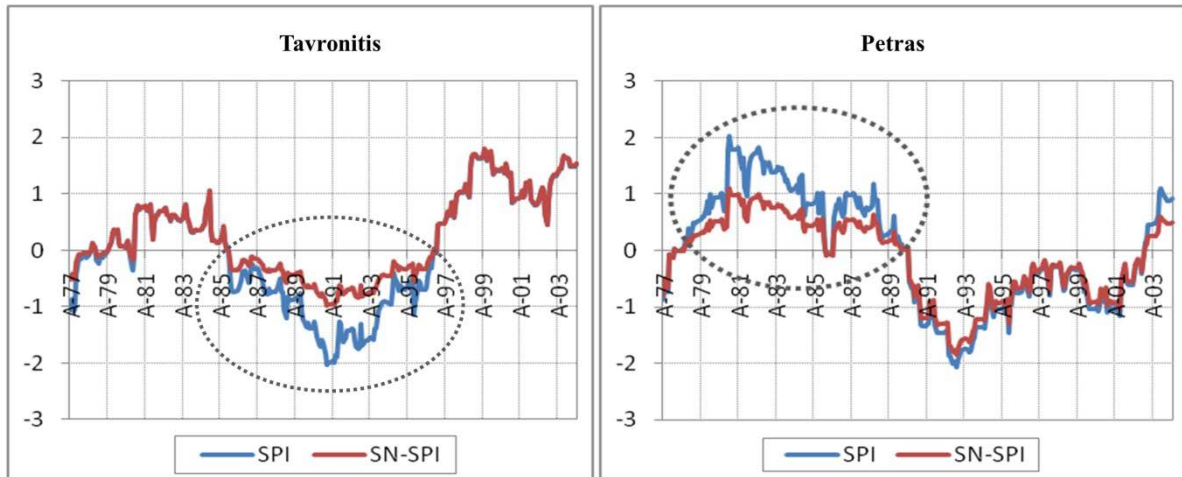


**Figure 2-3:** Monthly SPI and SN-SPI (48-month time scale) time series for 2 representative watersheds.

## 2.2 Data

Monthly precipitation data was compiled by the WRDPC service (Water Resources Department of the Prefecture of Crete) for 56 precipitation stations (**Figure 2-4**). The stations mainly cover the eastern part of the island which has a higher level of agricultural activity than the western part. The gauges were located at elevations that ranged from sea level, in the prefecture of Iraklion (central Crete), to 905m a.s.l, in the prefecture of Lassithi (eastern Crete) (Region of Crete, 2009). These data cover a thirty (30) years' time period for each month of the hydrological year (September to August), from 1974 to 2005.

In order to simplify calculations, a relative coordinate system was defined by locating an origin (0,0) at the lower left corner of the island at latitude 3800000 m and longitude 461000 m. GGRS87-Greek Geodetic Reference System 1987 was the coordinate system used. All  $Y$  coordinates employed in the regression were hence the result of subtracting 3800000 from the original latitudes of the different stations and dividing by 1000 to obtain latitudes in km. Similarly, all  $X$  coordinates were derived by subtracting 461000 from the original longitudes of the different stations and dividing by 1000 to obtain longitude values in km. This manipulation of coordinates is important when performing the regression analysis. Large numbers for latitude and longitude could result in small values for model parameters ( $b_i$ ) and any small error could result in significant changes in the model output. It is then more practical to put all variables into approximately the same order of magnitude to ensure that they receive appropriate weighting in the multiple regression analysis.

Geographic Information System (GIS) technology represented by the commercial package ArcView GIS 10, was used to provide the tools for spatial data management and generate maps including the Digital Elevation Model (DEM). DEM comprises the source of spatially gridded data developed by the Greek Army Geographical Service, with a cell size of 30 m, resulting in a grid of 33.386 cells.

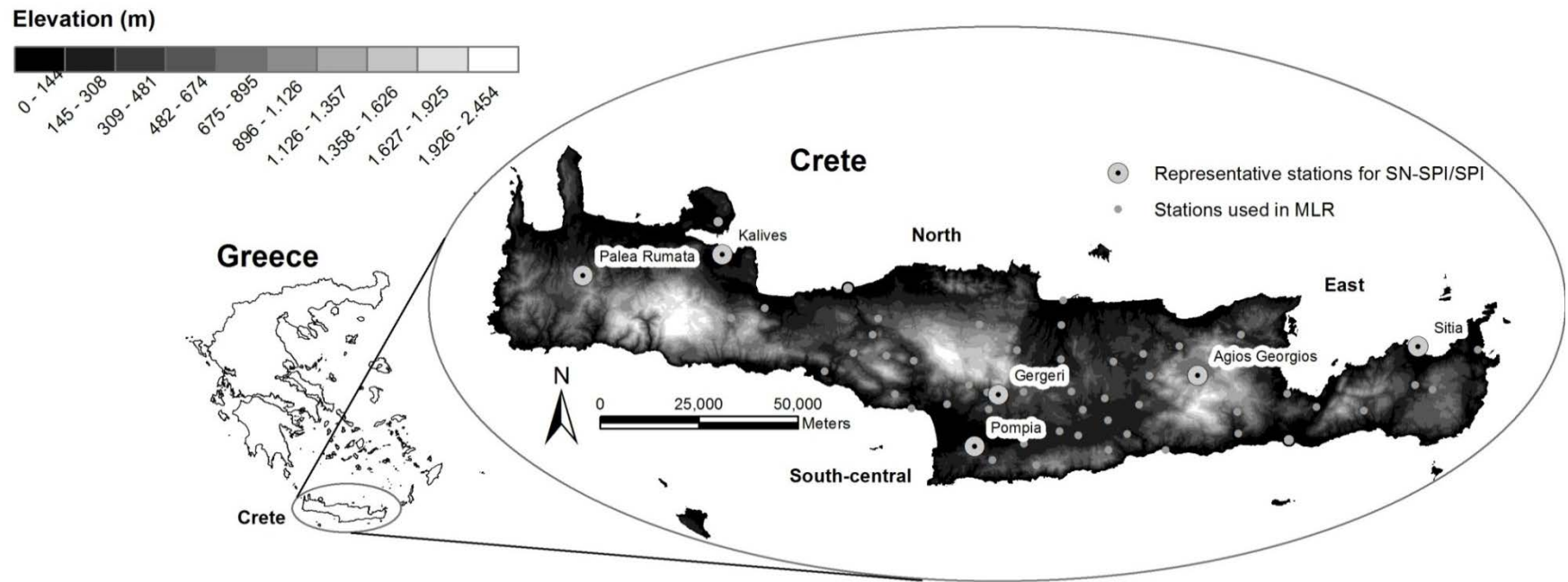


*Figure 2-4: Area of study, 56 stations used in MLR and 18 representative stations for SPI Crete, Greece*

## 2.3 Results

### 2.3.1 Influence of elevation and longitude on precipitation

Two parameters (elevation and longitude) were adopted to perform simple linear regression individually for 55 stations. The station of Askifou was excluded from this method in order to obtain more reasonable results, as Askifou (with elevation 740 m) exemplifies a special case of a region with orographic precipitation. The island was divided into three parts (northern, south-central and eastern), so as orientation of topography factors is taken into account. Upon examining the correlation between precipitation and elevation taking into consideration the three parts, it was found that the regression plot for all stations justifies the positive correlation (**Figure 2-5a**). The plot based on elevation provided a more physically meaningful interpretation of the effect of this variable on precipitation; the presence of the orographic effect at high elevations. On the other hand, further analysis covering the parameter of longitude showed that there is a negative trend between the afore-mentioned parameter and precipitation (**Figure 2-5b**). The noticeable downward gradient of precipitation from one part to another denotes a statistical evidence of the geographical factor. In other words, the decrease of precipitation is responsive to longitude increasing. It is then verified that topographic and geographic factors determine the spatial association in precipitation variations. More specifically, the precipitation magnitude decreases in West-East direction and increases in elevation by as much as 400 mm. Previous studies that tested statistical models relating annual precipitation to elevation or longitude (Naoum and Tsanis, 2004) showed that the best results were obtained were both elevation and longitude.

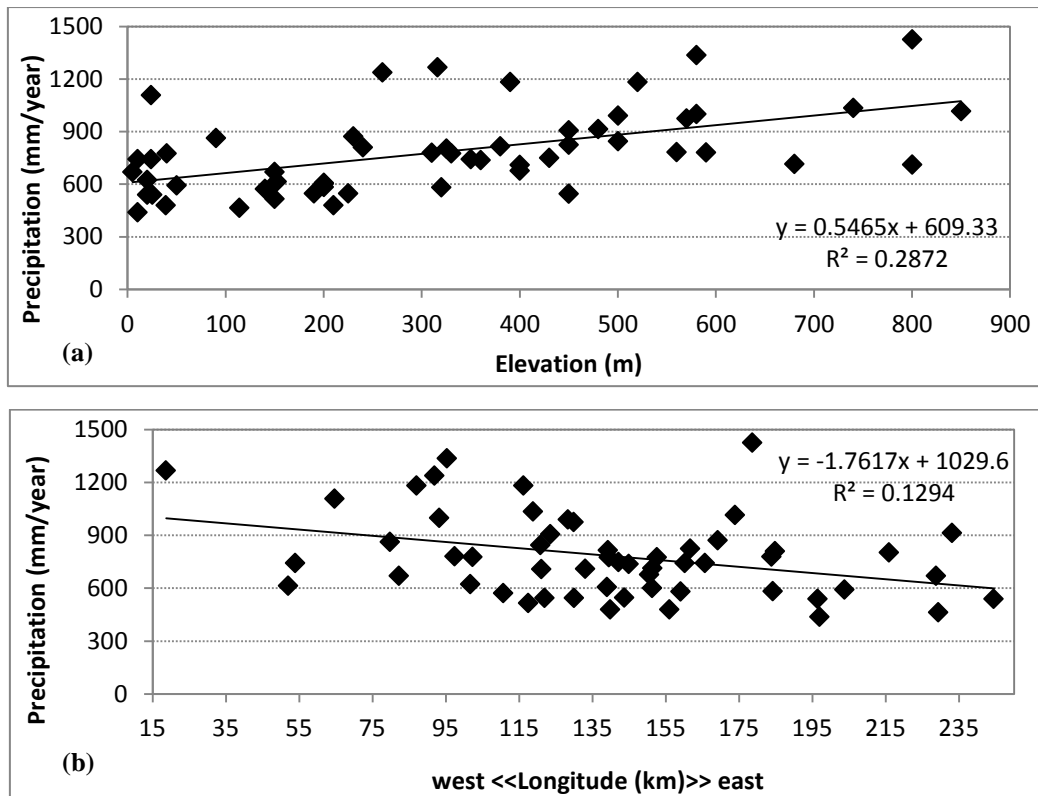


*Figure 2-5: a) Elevation versus mean annual precipitation plot and b) Longitude versus mean annual precipitation plot for Crete*

Therefore, simple and multiple linear regression was used to study the level of association between the two variables for a thirty years' period, from 1974 to 2005 (**Table 2-2**). The database of precipitation was used to generate and apply the regression models. The regression equations were produced for the 55 stations, representing the whole island. Simple linear regression was carried out considering just elevation as explanatory variable and the additional independent variable of longitude was introduced in order to construct a more efficient model. The coefficient of determination ( $R^2$ ) is used to determine the adequacy of the regression equation. The regression analysis shows that 1989-1990 represents the year with the minimum precipitation amount (499 mm) and 2002-2003 is the year with the maximum precipitation amount (1423 mm); moreover, an average year is taken into account (1978-1979, 902 mm). The  $R^2$  varies between 9% and 42% for the one-variable model (maximum in 2004-2005) while a range of  $R^2$  23% to 53% is obtained for the two-variable model (maximum in 1974-1975). The  $R^2$  values were significantly increased, when longitude was added to the model, a fact that comprises a possible sign of model improvement.

**Table 2-2:** Simple and two-variable linear regression for 55 stations, regarding each year of 1974-2005.

<b>Years</b>	<b>b<sub>0</sub></b>	<b>b<sub>1</sub></b>	<b>b<sub>2</sub></b>	<b>R<sup>2</sup></b>	<b>Extracted precipitation (mm)</b>
<b>1974-75</b>	555.39	0.58		38%	834
	795.89	0.57	-1.70	53%	832
<b>1975-76</b>	728.52	0.56		23%	996
	1045.06	0.54	-2.23	39%	995
<b>1976-77</b>	422.99	0.52		21%	672
	652.21	0.51	-1.62	31%	671
<b>1977-78</b>	807.58	0.99		38%	1283
	1196.40	0.97	-2.74	51%	1281
<b>1978-79</b>	572.08	0.68		40%	902
	704.94	0.68	-0.94	43%	901
<b>1979-80</b>	633.64	0.67		27%	958
	797.29	0.67	-1.15	31%	957
<b>1980-81</b>	703.19	0.64		29%	1014
	1073.96	0.63	-2.61	49%	1012
<b>1981-82</b>	680.11	0.58		23%	958
	1091.89	0.56	-2.90	48%	956
<b>1982-83</b>	452.91	0.55		28%	719
	672.12	0.54	-1.55	37%	718
<b>1983-84</b>	627.88	0.59		35%	911
	854.07	0.58	-1.59	46%	910
<b>1984-85</b>	695.33	0.62		34%	993
	901.37	0.61	-1.45	42%	992
<b>1985-86</b>	432.43	0.39		23%	619
	620.85	0.38	-1.33	34%	618
<b>1986-87</b>	778.09	0.48		12%	1012
	918.45	0.48	-0.99	14%	1011
<b>1987-88</b>	525.55	0.73		31%	875
	689.26	0.72	-1.15	35%	875
<b>1988-89</b>	515.68	0.46		21%	736
	750.35	0.45	-1.65	33%	735
<b>1989-90</b>	<b>354.84</b>	<b>0.30</b>		<b>23%</b>	<b>499</b>
	<b>503.14</b>	<b>0.29</b>	<b>-1.05</b>	<b>36%</b>	<b>498</b>
<b>1990-91</b>	521.82	0.36		21%	697
	642.24	0.36	-0.85	25%	696
<b>1991-92</b>	590.59	0.49		16%	828
	847.79	0.48	-1.81	25%	827
<b>1992-93</b>	421.71	0.36		16%	597
	693.86	0.35	-1.92	34%	596
<b>1993-94</b>	504.21	0.58		31%	785
	768.15	0.57	-1.86	44%	784
<b>1994-95</b>	566.77	0.70		31%	903
	601.28	0.70	-0.24	32%	903
<b>1995-96</b>	688.61	0.61		29%	980
	925.34	0.60	-1.67	39%	979
<b>1996-97</b>	635.13	0.64		17%	943
	1077.78	0.62	-3.12	34%	941
<b>1997-98</b>	543.22	0.73		29%	897
	821.98	0.72	-1.96	39%	896
<b>1998-99</b>	648.11	0.43		9%	856
	1099.23	0.42	-3.18	29%	854
<b>1999-00</b>	424.11	0.37		16%	605
	690.94	0.37	-1.88	33%	604
<b>2000-01</b>	578.34	0.62		24%	876
	978.52	0.60	-2.82	46%	875
<b>2001-02</b>	632.34	0.63		17%	934
	843.34	0.62	-1.49	21%	933
<b>2002-03</b>	<b>1050.17</b>	<b>0.77</b>		<b>18%</b>	<b>1423</b>
	<b>1552.64</b>	<b>0.76</b>	<b>-3.54</b>	<b>35%</b>	<b>1421</b>
<b>2003-04</b>	656.62	0.57		23%	933
	714.85	0.57	-0.41	23%	933
<b>2004-05</b>	499.13	0.65		42%	811
	615.34	0.64	-0.82	45%	810

Followingly, the regression analysis was carried out for the three subareas (northern, south central and eastern parts) for the three representative years (**Table 2-3**). The relationship

between precipitation and elevation is not as strong for the whole island (55 stations) as it is for individual parts, especially the eastern part for all years assessed, except 2002-2003. This is attributable to the relatively high elevations of stations in this part, which is likely to result in a higher association than the other parts ( $R^2$  up to 79% for 1989-1990). Developing separate regression equations and still using elevation and longitude as the predictor variables for the three divisions of Crete, the analysis provided even more descriptive models.

**Table 2-3:** Simple and two-variable linear regression for Crete and its parts for different years.

	Spatial extent	Number of stations	$b_0$	$b_1$	$b_2$	$R^2$
<b>Min precipitation year 1989-90</b>	Crete	55	354.84	0.30	–	23%
		55	503.14	0.29	-1.05	<b>36%</b>
	north	17	609.29	0.26	-1.36	26%
	south-central	20	555.68	0.26	-2.03	35%
	eastern	18	231.35	0.49	0.23	79%
<b>Max precipitation year 2002-03</b>	Crete	55	1050.17	0.77	–	18%
		55	1552.64	0.76	-3.54	<b>35%</b>
	north	17	1656.06	0.72	-3.98	17%
	south-central	20	2034.33	0.85	-8.20	51%
	eastern	18	1012.87	0.96	-0.86	39%
<b>Average precipitation year 1978-79</b>	Crete	55	572.08	0.68	–	40%
		55	704.94	0.68	-0.93	<b>43%</b>
	north	17	982.88	0.81	-3.23	64%
	south-central	20	733.76	0.50	-1.78	49%
	eastern	18	323.59	1.00	0.94	70%
<b>Long-term 1974-2005</b>	Crete	55	609.33	0.55	–	29%
		55	850.16	0.54	-1.70	<b>41%</b>
	north	17	1040.35	0.68	-3.30	49%
	south-central	20	1030.50	0.48	-3.90	42%
	eastern	18	599.00	0.72	-0.35	67%

Results reported by Naoum and Tsanis (2003) demonstrated that, for a typical dry year, the island of Crete would receive up to 800 mm of precipitation, for an average year, precipitation has a range between 800 and 1100 mm and finally for a wet year, the island would receive precipitation greater than 1100 mm. Based on these values, the range of elevation–precipitation gradient ( $b_1$ ) is 0.26-0.49, 0.72-0.96 and 0.5-1 mm/m for minimum, maximum and average precipitation years, respectively. The range of longitude-precipitation

gradient ( $b_2$ ) for a minimum precipitation year is -2.03 to 0.23 mm/ km, -8.20 to -0.86 mm/km for a maximum precipitation year and -3.23-0.93 mm/km for an average year. In brief, the results show that there is a general increase in the coefficient of determination from the one-variable equation to the two-variable equation for all years under study.

Following the multiple linear regression method, **Table 2-4** summarizes the precipitation characteristics of 55 stations. There is clear indication that in terms of average values, the south-central part experiences 5% less mean annual precipitation than the eastern part and 23% less than the northern part. During the year 1989-1990, the south-central part is characterized by 7% and 29% less precipitation than the eastern and northern part respectively. It is also confirmed that during 2002-2003 the eastern part received 13% and 24% less precipitation than the south-central part and northern part. After merging both south-central and eastern parts considering the low difference percentages, there is obvious statistical evidence of the decreasing longitude-precipitation gradient. However, differences between stations with different elevations lie on the orographic effect, so stations with high elevation represent higher precipitation values.

*Table 2-4: Characteristics of the stations used.*

Part of Crete	Stations	Mean annual precipitation (mm)	Elevation (m)	Longitude (km)	Min prec. year 89-90 Mean Precipitation	Max prec. year 02-03 Mean Precipitation	Average year 78-79 Mean Precipitation
North	Palea Rumata	1267	316	18.7	640	1738	1282
	Suda	614	152	52	356	930	608
	Kalives	742	24	53.9	519	1411	720
	Mouri	1108	24	64.7	695	1985	969
	Rethimno	670	5	82.2	493	1058	786
	Kavousi	1000	580	93.2	498	2189	1062
	Voleones	1238	260	91.9	716	1869	1149
	Spili	1182	390	87	807	1811	1087
	Vizari	778	310	102.3	519	841	773
	Gerakari	1336	580	95.3	602	2330	1235
	Anogia	1035	740	118.8	629	955	1220
	Krussonas	990	500	128.3	688	1448	965
	Iraklio	480	39	139.9	289	728	455
	Finikia	775	40	139.5	475	1555	655
	Metaksochori	749	430	142.1	486	1392	1130
	South-central	Voni	775	330	152.6	439	1256
Profitis Ilias		816	380	139.3	518	1579	717
Average		915	300	100	551	1475	902
Agios Kirillos		545	450	122	251	1224	602
Kapetaniana		711	800	133.1	352	1442	785
Lefkogia		863	90	79.8	458	1524	654
Melabes		782	560	97.4	541	1359	783
Agia Galini		623	20	101.7	365	1210	554
Vorizia		1183	520	116.2	588	2162	1058
Lagolia		573	140	110.7	345	1210	565
Zaros		844	500	120.8	417	1603	795
Agia Varvara		975	570	129.9	552	1500	937
Gergeri		907	450	123.5	465	1700	772
Partira		677	400	150.5	391	1156	633
Asimi		607	200	139	350	972	718
Vagionia		546	190	130	311	874	647
Tefeli		737	360	144.9	487	1333	744
Achentrias		715	680	151.4	459	1234	712
Kalivia		601	200	151.3	357	1055	603
Demati		480	210	156	196	987	537
Moroni	709	400	121.1	363	1340	710	
Pompia	516	150	117.5	255	1135	414	
Pretoria	547	225	143.7	325	919	511	
Average	707	356	127	391	1297	687	
Eastern	Kasteli	743	350	160.2	421	1200	873
	Armacha	824	450	161.7	514	1290	898
	Avdu	872	230	169.2	491	1739	1030
	Kassanoi	582	320	159.1	380	893	576
	Agios Georgios	1016	850	173.9	700	1137	1058
	Kalo Chorio	540	20	196.5	389	911	482
	Malles	780	590	183.9	430	1234	920
	Kapsaloi	743	10	165.7	208	780	574
	Neapolis	810	240	184.8	477	933	890
	Exo Potamoi	1425	800	178.6	731	2406	1592
	Mithoi	584	200	184.2	311	945	594
	Ierapetra	439	10	197	235	705	445
	Pachia Ammos	592	50	203.8	301	1161	597
	Stavrochori	803	325	215.9	435	907	936
	Sitia	464	114	229.4	283	657	440
	Maronia	670	150	228.8	425	1075	713
	Katsidoni	914	480	233.1	510	1319	1173
	Paleokastro	540	25	244.5	290	940	556
Average	741	290	193	418	1124	795	

### 2.3.2 Precipitation shortage and excess

Multiple linear regression results are graphically demonstrated with the generation of maps in GIS. Each cell of the grid represents a precipitation value according to the produced regression models and the DEM. **Figure 2-6a** indicates the spatial distribution of precipitation for a long-term 30-year average, obtained by multiple linear regression method. Taking into account the minimum precipitation year 1989-90, the precipitation shortage is derived from the difference between the precipitation of a 30-year average at each cell and the precipitation of the year 1992-1993 at each cell as well (**Figure 2-6b**). Considering the maximum precipitation year 2002-03, the precipitation excess is the result of the difference between the precipitation of a 30-year average at each cell and the precipitation of the year 2002-03 (**Figure 2-6c**). Both spatial distribution of precipitation shortage and excess follow the spatial distribution of precipitation via a long-term average. This is in line with our expectations, since at high elevations as well as at the western part of Crete high-amount precipitation events occur. The eastern part has the lowest mean elevation and low average precipitation, so the precipitation excess in this part is found to be the less than the western part.

More specifically, during 1989-90, the mean annual precipitation is affected by elevation less than the mean annual precipitation of 30-year average, as shown in **Table 2-3** ( $b_1^{\min} < b_1^{\text{long-term}}$ ). This explains the fact that the precipitation shortage for the “dry” year is greater at high elevations. Contrarily, for the “wet” year, elevation affects more the mean annual precipitation ( $b_1^{\max} > b_1^{\text{long-term}}$ ). The downward gradient of precipitation from west to east is weaker for the “dry” year when compared to the 30-year average ( $|b_2^{\min}| < |b_2^{\text{long-term}}|$ ). On the other hand, during the “wet” year precipitation decreases in a higher rate from west to east ( $|b_2^{\max}| > |b_2^{\text{long-term}}| > |b_2^{\min}|$ ) and as a result the precipitation excess is higher in the western part. This denotes that the orographic effect is stronger during the wet year in the western part of Crete.

Regarding the spatial distribution of flood events over Crete (1990-2007), 66% of them were reported for western Crete region, while the rest 34% were reported for eastern Crete (Koutroulis et al., 2010). The East to West precipitation gradient can be attributed to the regional NW to SE dominant meteorological atmospheric patterns and the higher elevation and steepest slope morphology of the western Crete in comparison to the eastern region of the island.

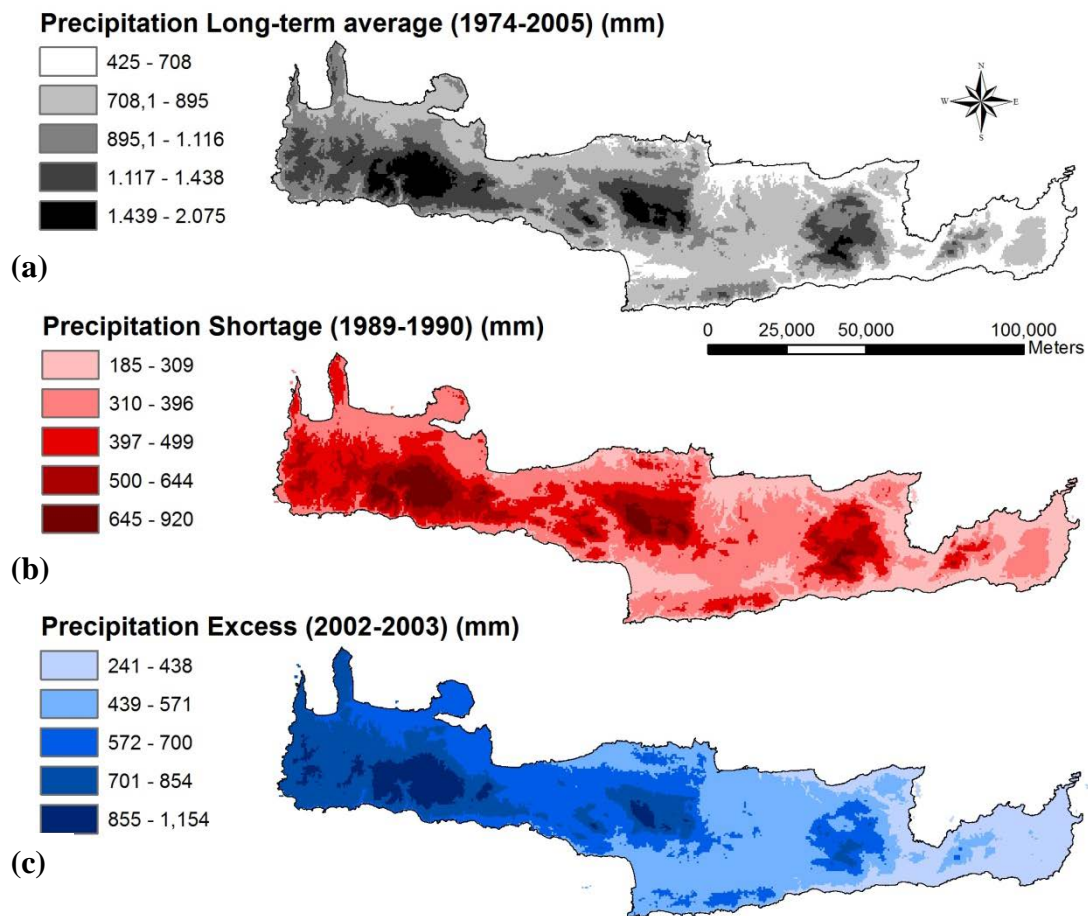


*Figure 2-6: Spatial distribution of a) precipitation for a long-term average of the period 1974-2005, b) precipitation shortage concerning the year 1989-1990 and c) precipitation excess concerning the year 2002-2003.*

### 2.3.3 Spatiotemporal drought analysis

Long period characteristics represented by 48-month time scale values of SN-SPI, were calculated for six (6) representative stations, in order to provide an overview of prolonged drought occurrences in relation to the factor of elevation and longitude during the period 1974-2005. The results of drought analysis in the island of Crete during this period show a definite tendency towards prolongation and greater severity of drought episodes. **Figure 2-7** illustrates the drought conditions of two representative stations in the north-western part of Crete. The period 1988-1997 was recorded to be a period of drought for both stations, with a greater intensity in Kalives. It is rather obvious that the sensitivity of precipitation variability is depicted in the index results. The SN-SPI behaves in a similar way to the SPI; however, a significant difference lies on the fact that the SPI is temporally comparable, but the SN-SPI is spatio-temporally comparable among different areas with different mean total annual precipitation.

Obviously, the difference between the indices appears mainly at the peaks of the time series. The SN-SPI presents Palea Rumata as less dry during 1988-97, Kalives as less wet during 1980-85 and 1999-04. In the case of Palea Rumata (1267 mm) normalization takes place during dry conditions (1988-97) whereas in Kalives (742 mm) normalization is obvious during wet conditions (1980-85, 1999-04). SN-SPI values present Palea Rumata with mildly dry conditions and Petras with mildly wet conditions during the aforementioned periods. Stated in the simplest terms, the same SPI value occurs for different precipitation levels and, therefore, these stations cannot be compared via SPI. On the other hand, different SN-SPI values occur for different precipitation levels. The spatial pattern of precipitation of Kalives indicates the correlation between the low precipitation values of 1987-1989 and the SN-SPI negative peaks during 1991-1993 (as the 48-month index utilizes the precipitation total for 48 months).

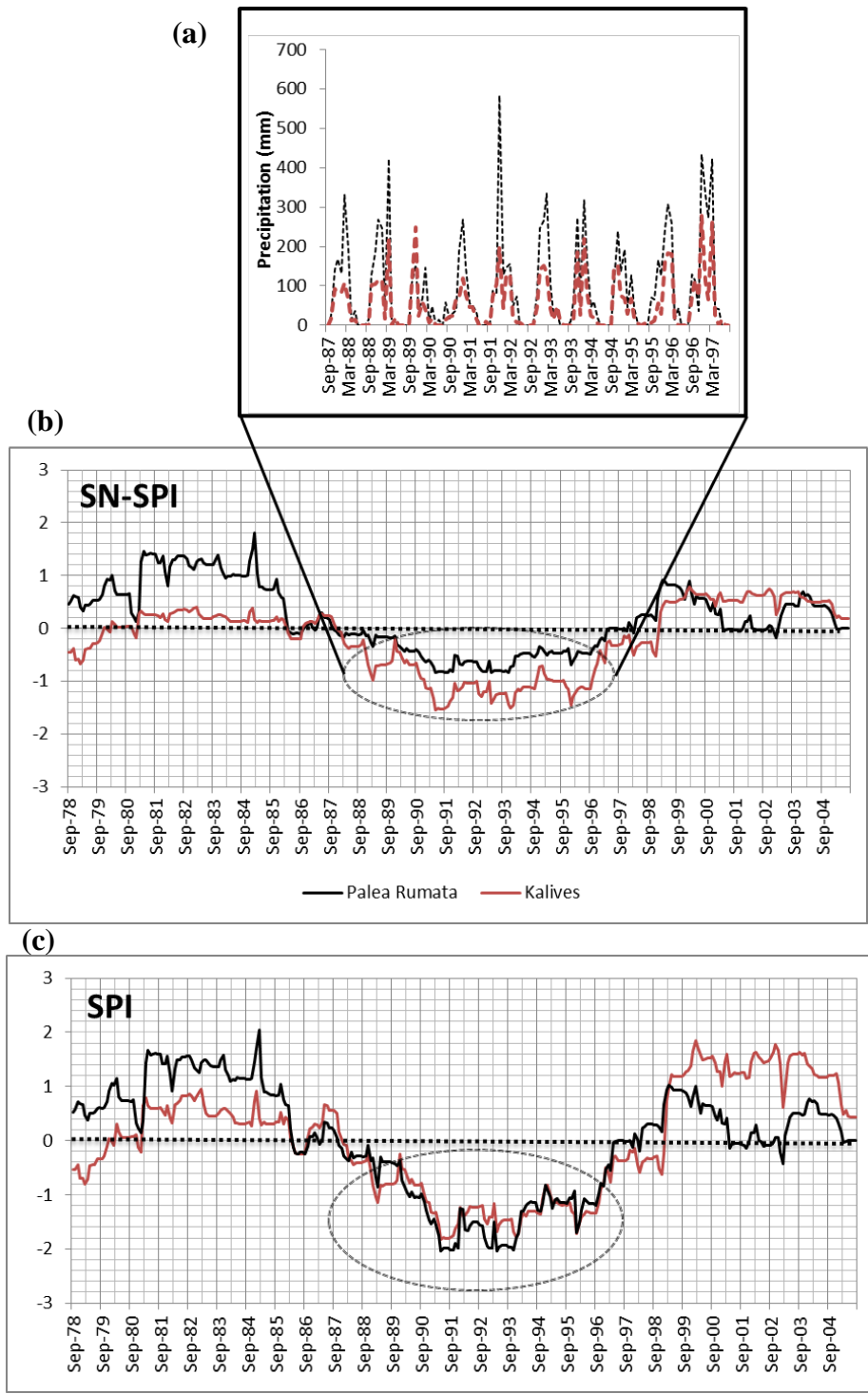


**Figure 2-7:** a) Monthly precipitation time series for drought events b) 48-month time scale SN-SPI and c) SPI for two representative stations of north-western Crete based on the period 1974-2005

The south-central stations experience a drought period during 1988-95, while Pompia is characterized by a mildly dry period during 1999-02 (**Figure 2-8**). Normalization took place

for Gergeri during dry conditions and for Pompia during wet conditions. The severe drought spell of Pompia is a result of the low recorded precipitation during 1989-90.

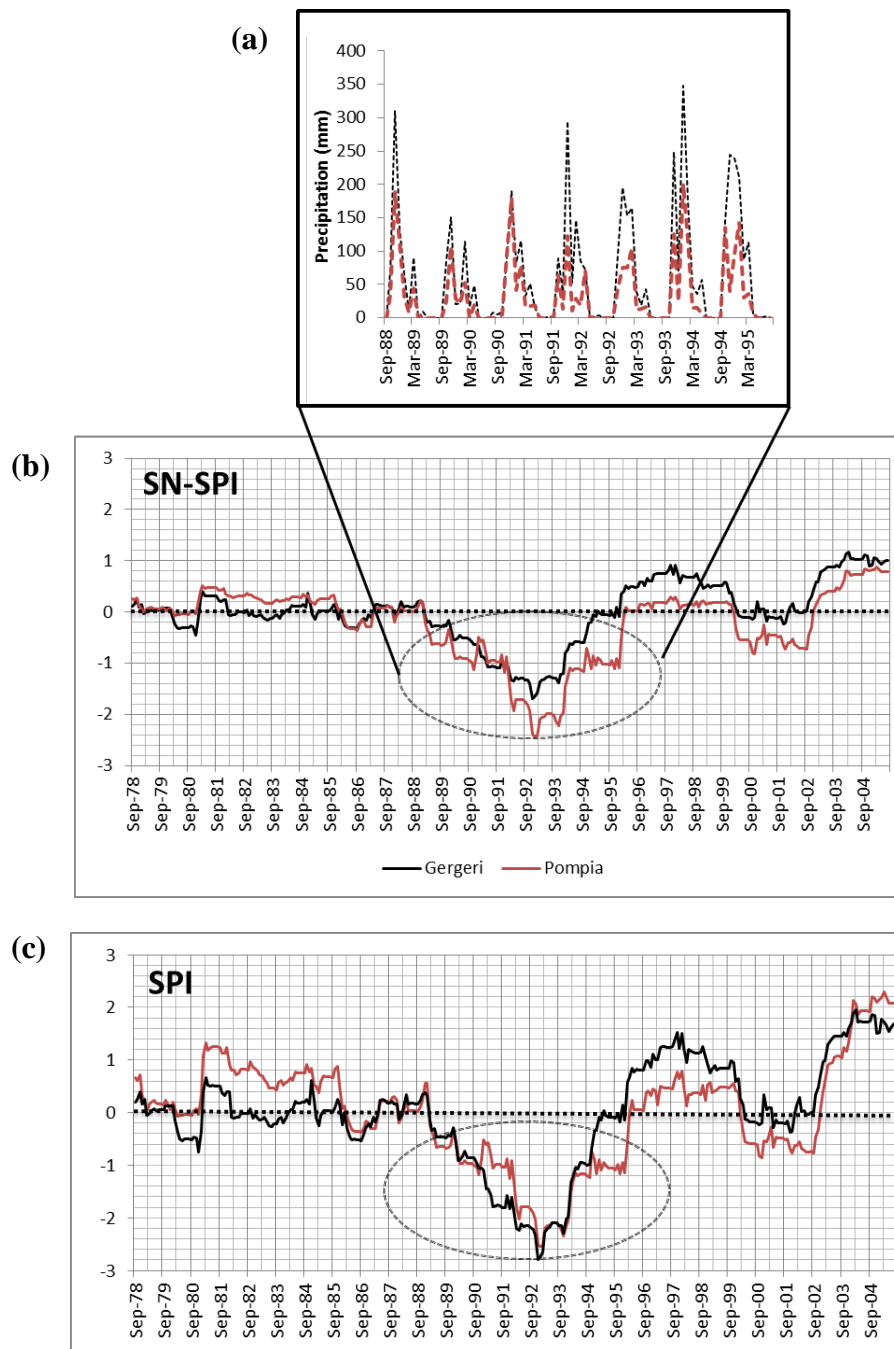


**Figure 2-8:** a) Monthly precipitation time series for drought events b) 48-month time scale SN-SPI and c) SPI for two representative stations of south-central Crete based on the period 1974-2005

Finally, as **Figure 2-9** shows, the eastern part of Crete experiences the most long-term drought period (Sitia, 464 mm), that signs its beginning in 1990 and ends in 2003 with no intervals. It is important to stress that Agios Georgios (1016 mm) has three drought periods

and appears the afore-mentioned drought period 8 years earlier (1982). There is also a significant normalization for the wet periods for both stations. The precipitation variability reveals very low values for Sitia during the referring periods and a correspondence between the lowest peak of the index and the precipitation amount 48 months before. As a result, the additional drought period at the southern and eastern part is justified by the combination of the regional atmospheric patterns and the morphological variability among different parts of the island as stated by Koutroulis et al. (2010). Graphical examination of spatial evolution of drought confirms that the eastern part suffers more than the rest of the island from dry conditions. Generally speaking, for the 30-year period, there are 26 stations with downward precipitation trend, 24 follow upward precipitation trend while 6 remain stable.

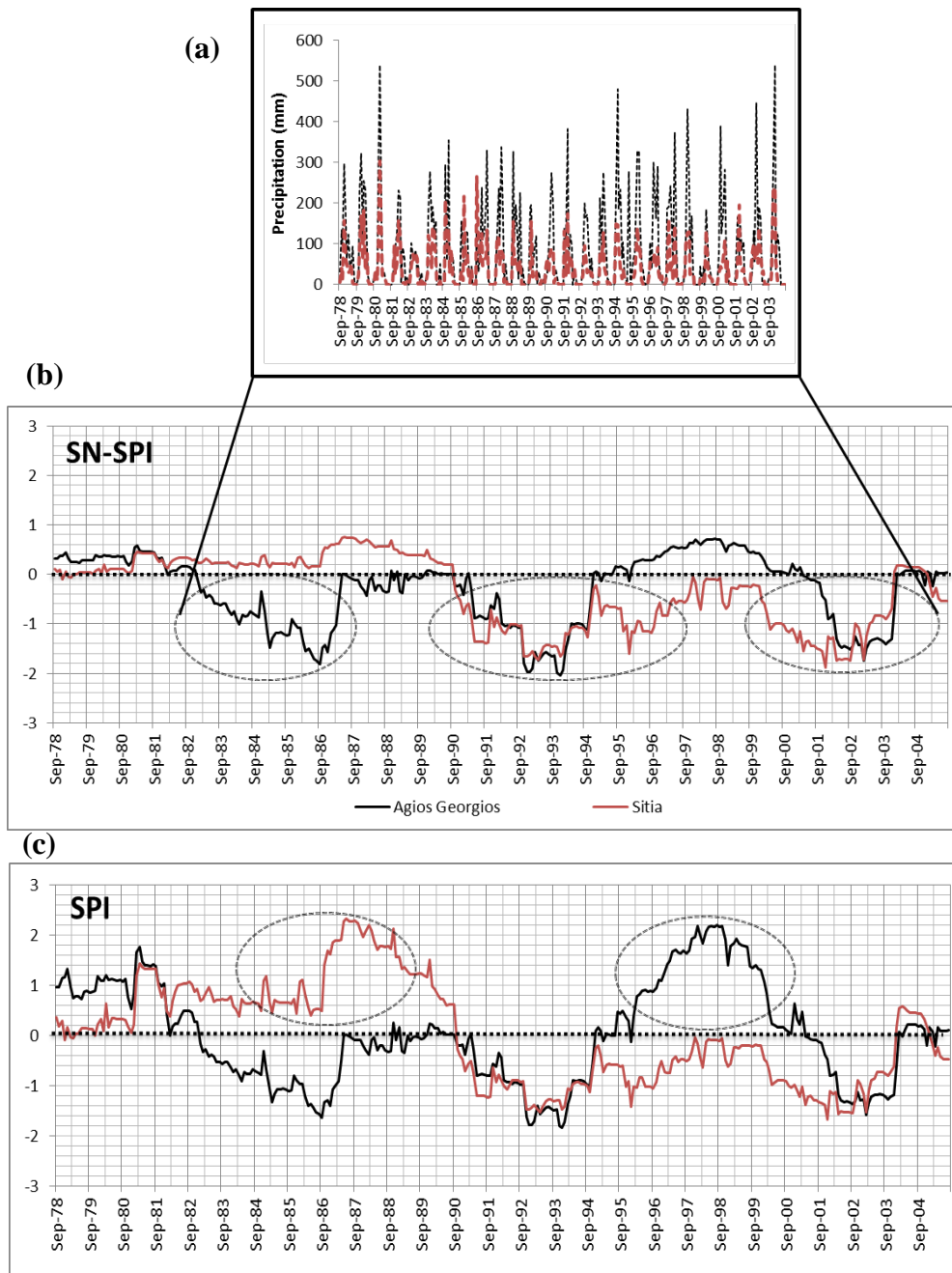


**Figure 2-9:** a) Monthly precipitation time series for drought events b) 48-month time scale SN-SPI and c) SPI for two representative stations of eastern Crete based on the period 1974-2005

Similarities in time series of the SN-SPI across stations have been identified through SN-SPI drought months (SN-SPI<0); this calculation comprised the main component for k-means cluster analysis with the use of MATLAB R2011b. The multiple correlation carried out including the parameters of elevation and longitude for 55 stations resulted to the generation of 2 optimum clusters (**Figure 2-10a**). The definition of the number of the clusters a priori is a process that follows the minimization of the average silhouette width after several hypotheses (**Figure 2-10b**). Then, the performance of multiple runs, each with a different set of randomly chosen initial centroids, led to the selection of the optimum set of clusters. The cluster (1) which includes low elevations (31 stations) corresponds to a higher value of drought months (162) in comparison with stations of high elevations (24 stations, 157 months, cluster 2) a fact that confirms the downward gradient of drought appearance as the elevation increases. The average silhouette width (0.72) indicates that a reasonable structure has been found. There is clear indication that cluster analysis results are connected to MLR results and justify the negative correlation between drought events and the most important factor in the bi-variate model of the precipitation distribution, elevation.

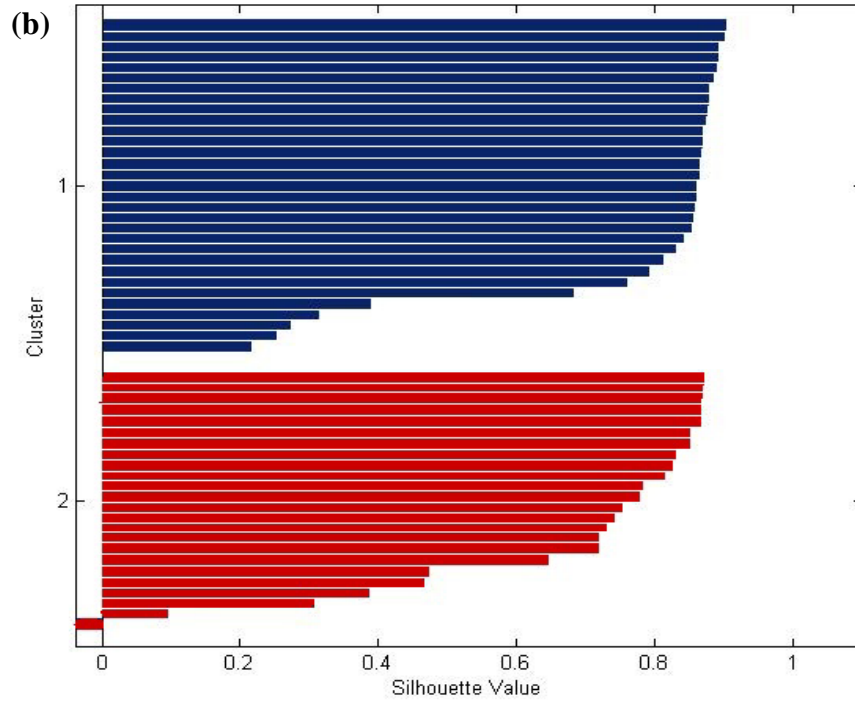
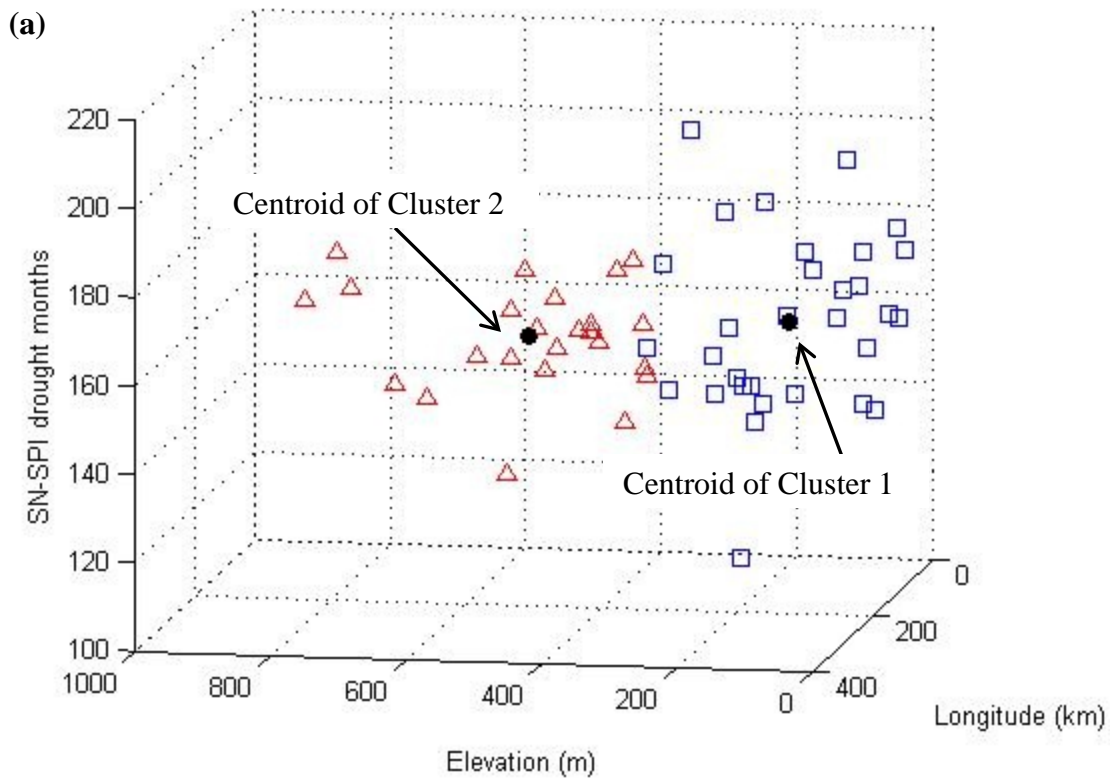


**Figure 2-10:** Spatial separation of 55 stations using cluster analysis. a) Stations plot illustrating drought months as the dependent variable and b) silhouette plot of the clusters.

### **3. The impact of hydrometeorological parameters on droughts**

---

There can be significant variations of drought impacts between regions due to the different characteristics of the economy, society and the environment. Hence, different types of droughts are identified (AMS, 2004). Meteorological drought is defined usually by the departure of precipitation from the “normal” or average amount and the duration of the dry period while agricultural drought refers to situations in which the soil moisture is no longer sufficient to meet the needs of the crops growing in the area, focusing on properties such as precipitation shortage, differences between potential and actual evapotranspiration and soil moisture deficits. Finally, hydrological drought associates the effect of periods of precipitation shortfalls on surface or subsurface water supply (Wilhite, 2000). In spite of the fact that precipitation is the primary factor that controls drought, other factors such as high temperature or dry winds contribute to the amplification of its intensity. The severity of drought depends on the moisture deficit degree, the duration of the phenomenon and its spatial extent. Drought impacts first appear on agriculture which is prone to be affected by soil moisture decrease and high evapotranspiration. During extended dry periods, soil water depletes fairly rapidly. On the other hand, the last to be affected from an extended dry period are usually surface water and subsurface water resources (Sönmez et al., 2005).

A drought variable can be defined as a prime variable responsible for assessing drought effects, and is considered a key element in defining drought and deciding on the techniques for its analysis. Therefore, droughts are commonly classified into four categories, which are mostly

based on different parts of the hydrological cycle (Peters, 2003). At first, a meteorological drought is caused by lack of precipitation possibly in combination with high evapotranspiration. The meteorological drought causes a lack of soil moisture, which is called a soil moisture or agricultural drought and which affects agricultural crops and/or the natural vegetation. Precipitation deficit may also cause the streamflow drought which is defined by low streamflow values. The soil moisture drought results to a recharge decrease, which in turn causes lower groundwater levels and decreasing groundwater discharge to the surface water system, which is a groundwater drought. It is noted that the impact of drought on agriculture is slower than on streamflows or reservoir levels (Panu and Sharma, 2002). Vrochidou and Tsanis (2012) identified meteorological drought events over the island of Crete at spatial and temporal scale by assessing precipitation variability and using Spatially-Normalized Standardized Precipitation Index (SN-SPI).

In order to simulate the afore-mentioned parameters and study the potential impacts of future climate change and urban development on basin water quantity and quality, many researchers are increasingly using hydrological models. Although modelling is a probabilistic process with the risk of uncertainty, it is a useful methodology for experimenting with the dynamics that govern complex environmental systems and for projecting possible ranges of impacts. Hydrological models are often divided into three categories; lumped, distributed and stochastic models. Distributed models require a detailed hydrologic description of the area, while stochastic models are used for dimensioning purposes and have little forecasting use (Silberstein, 2006). In the present study, HBV model is suggested to be used as it comprises a modern, well-tested and operational tool. Despite its simplicity, its simulation performance is commendable, and the original use for hydrological forecasting has expanded to applications such as filling gaps in measured time-series, simulation of stream-flow in ungauged rivers, design flood calculations and water quality studies input data. The flexible structure of the HBV system allows the model to make necessary sub-divisions with respect to different climate zones, land-use, density of the hydrometeorological network etc. (SMHI, 2006). Grillakis et al. (2011) deduced that the HBV model simulates the streamflow more efficiently and several papers have been carried out with its application (Booij et al., 2011; Love et al., 2011; Normand et al., 2010).

Various climate change impact studies dealing with Global Climate Models (GCMs) data have been conducted (Koutroulis et al., 2011); Kerkhoven and Gan (2011) examined the uncertainty of observed streamflows and simulated past and future streamflows from a hydrologic model, driven by GCM data, concerning two watersheds in Western Canada, using multifractal analysis. Dibike and Coulibaly (2005) studied the hydrologic impact of climate change in the Saguenay watershed in northern Quebec, Canada by comparing two downscaling methods and two hydrologic models.

Under the World Climate Research Programme (WCRP), the Working Group on Coupled Modeling (WGCM) established the Coupled Model Intercomparison Project (CMIP) as a standard experimental protocol for studying the output of coupled atmosphere-ocean general circulation models (AOGCMs). The GCMs CNRM, ECHAM5 and IPSL used in this study comprise part of the phase 3 of the CMIP. A set of emission scenarios, called the Special Report on Emissions Scenarios (SRES) was published by the Intergovernmental Panel on Climate Change (IPCC). The analysis of different possible future development directions of the principal economic, demographic and technological drivers of future greenhouse gas and sulphur emissions, resulted to four scenario storylines, labeled A1, A2, B1 and B2, two of which are chosen for the present study (Parry et al., 2004; Nakićenović et al., 2000). In brief, A2 scenario is characterized by a heterogeneous world of slow technological development with emphasis in self-reliance and preservation of local identities and continuous population increase. In general, the A2 is at the higher end of the gas emission scenarios and it was selected to reflect the impact of a large potential climate change even though it is not the upper limit in terms of projected temperature increase. The B1 scenario describes a convergent world with the same global population that declines after midcentury, as in the A1, but with rapid changes in economic structures, reductions in material intensity and the introduction of resource-efficient technologies (Parry et al., 2004). This scenario was selected as the lower limit scenario. Nevertheless, there will be a new generation of scenarios for climate change research (Moss et al., 2008, 2010) that may better represent future conditions and produce new results.

The aim of this study is to examine the ability of large scale forcing datasets (WATCH Forcing Data-WFD) to reproduce drought characteristics and to study drought events taking into account hydrometeorological variables using the threshold level method in Platis basin, in the island of

Crete. The main objective is to clarify the contribution of decreasing hydrological resources as a driver of drought appearance within the context of climate change. The study also elaborates on the future projection analysis of these variables for identifying potentially induced severe drought phenomena from two gas emission scenarios aspects.

## 3.1 Methodology

### 3.1.1 Blaney-Criddle method

Evapotranspiration (ET) comprises an important parameter needed by water managers for the design and management of irrigation systems as well as hydrological modeling (Mohan and Arumugam, 1995). In the literature (Xu and Singh, 2002; McMahan et al., 2012) there is a great number of methods used for calculating potential evapotranspiration (PET). Xystrakis and Matzarakis (2011), who compared 13 reference PET models to find the best model for cropland ET in the island of Crete, found that the FAO equation was complicated enough because of data unavailability, and thus more empirical methods were appropriate. Although the Penman–Monteith equation has been tested efficiently in different climates, the need for full meteorological data such as minimum and maximum air temperature, minimum and maximum relative humidity, solar radiation and wind speed limits the widespread use of this equation (Monteith, 1965; Pereira and Pruitt, 2004).

The annual potential evapotranspiration in Crete is about 1400mm-1550mm (Region of Crete, 2002). The Blaney–Criddle equation is a relatively simplistic method for calculating evapotranspiration and ideal when only air temperature data is available for a site. Measured evapotranspiration for Platis test area is available only in monthly time-step. WFD provided daily potential evapotranspiration (PET) calculated with the Blaney-Criddle equation (Blaney and Criddle, 1950):

$$PET_i = p_i \cdot (0.46 \cdot T_i + 8)N_i \quad (3-1)$$

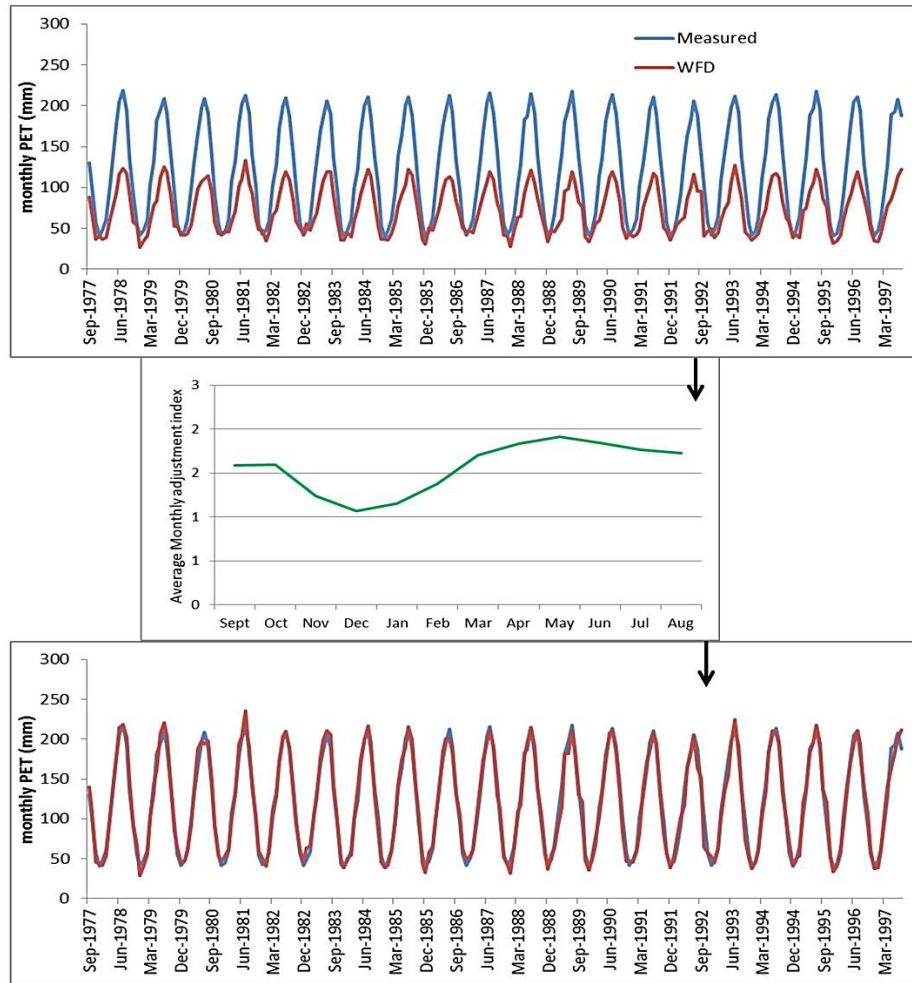


*Figure 3-1: Adjustment of WFD PET to measured values.*

### 3.1.2 The hydrological model HBV

The HBV model (Bergström, 1995; Lindström et al., 1997; Bergström et al., 1997) is a conceptual model of catchment hydrology which simulates discharge using rainfall, temperature and estimates of potential evaporation. In the present thesis, the model is used as lumped, representing the basin as a single entity, considering that the input data are evenly distributed. The model consists of four subroutines, a subroutine for snow accumulation and snowmelt based on the degree-day approach, a soil moisture accounting procedure to update the soil water, the runoff generation routine and a flow-routing procedure consisting of a simple filter with triangular distribution of weights (SMHI, 2006). The soil moisture accounting routine, which is

controlled by three parameters, computes an index of the wetness and soil moisture storage in a catchment. Parameter FC is the maximum soil storage capacity in the basin and parameter  $\beta$  determines the relative contribution to runoff from a millimeter of rain or snowmelt at a given soil moisture deficit while parameter LP controls the shape of the reduction curve for potential evapotranspiration. The runoff generation routine transforms excess water from the soil moisture routine to discharge to each sub-basin and it consists of one upper, non-linear and one lower, linear reservoirs connected in series by constant percolation rate (PERC). These are the origin of the quick and slow runoff components of the hydrograph. Flow of water from these reservoirs into runoff is governed by the linear storage coefficient ( $K_0, K_1, K_2$ ) and overflow from the upper storage ( $Q_0$ ) based upon exceedance of the threshold storage volume UZ. Computed outflow from a catchment is transformed using a triangular weighting function, the base width of which is the calibration parameter MAXBAS. The version of HBV used in this study is an Integrated Hydrological Modelling System (IHMS 5.10.1) HBV 7.1 developed by Swedish Meteorological and Hydrological Institute (SMHI) (SMHI, 2006).

Input data are observations of precipitation, air temperature, vapour pressure, wind speed and estimates of potential evaporation. The efficiency of the model simulations as expressed by the closeness between observed and simulated flows was evaluated using the Nash–Sutcliffe (NS) coefficient (Nash and Sutcliffe, 1970) equation:

$$NS = 1 - \frac{\sum (QC - QR)^2}{\sum (QR - QR_{mean})^2} \quad (3-2)$$

where QR is the observed flow and QC the computed flow,  $QR_{mean}$  is the average observed flow over the calibration period. The range of NS lies between  $-\infty$  and 1.0 (perfect fit). A result lower than zero indicates that the mean value of the observed time series would have been a better predictor than the model. This model will provide the necessary results of the hydrological parameters (simulated flow, soil moisture and groundwater reservoir level) for further use in drought assessment. In order to reduce the problem of the squared differences and the resulting sensitivity to extreme values the NS is often calculated with logarithmic values of QC and QR. The logarithmic transformation of the flow values leads to the flattening of peaks and the low flows are kept more or less at the same level. As a result the influence of the low flow values is

increased in comparison to the flood peaks resulting in an increase in sensitivity of  $\ln NS$  (Krause et al., 2005).

The model was calibrated manually, for the period 1974-1988, based on the efficiency criteria of  $NS$ ,  $\ln NS$  and coefficient of determination  $R^2$ . More weight was given to  $\ln NS$ , to focus on a better performance of low flows (SMHI, 2006). Moreover, the model was validated against observed flow for the period 1989-1999 in order to establish calibration reliability. A schematic sketch of the HBV model -with the following characteristics- is shown in **Figure 3-**.

$$RF = \text{rainfall} = p_{corr} \cdot r_{fcf} \cdot P \quad \text{if } T > tt$$

$$SF = \text{snowfall} = p_{corr} \cdot s_{fcf} \cdot P \quad \text{if } T < tt$$

SM = soil moisture

P = observed precipitation (mm)

T = observed temperature ( $^{\circ}\text{C}$ )

$tt$  = threshold temperature ( $^{\circ}\text{C}$ )

$r_{fcf}$  = rainfall correction factor

$s_{fcf}$  = snowfall correction factor

$p_{corr}$  = general precipitation correction factor

EA = actual evapotranspiration

CF = capillary transport

EL = evapotranspiration from interception

$\Delta Q$  = contribution to the response function

$Q_0$  = reservoir outflow upper reservoir

$Q_1$  = reservoir outflow lower reservoir

UZ = reservoir content upper reservoir

LZ = reservoir content lower reservoir

FC = maximum soil moisture storage

LP = limit for potential evapotranspiration

PERC = percolation rate

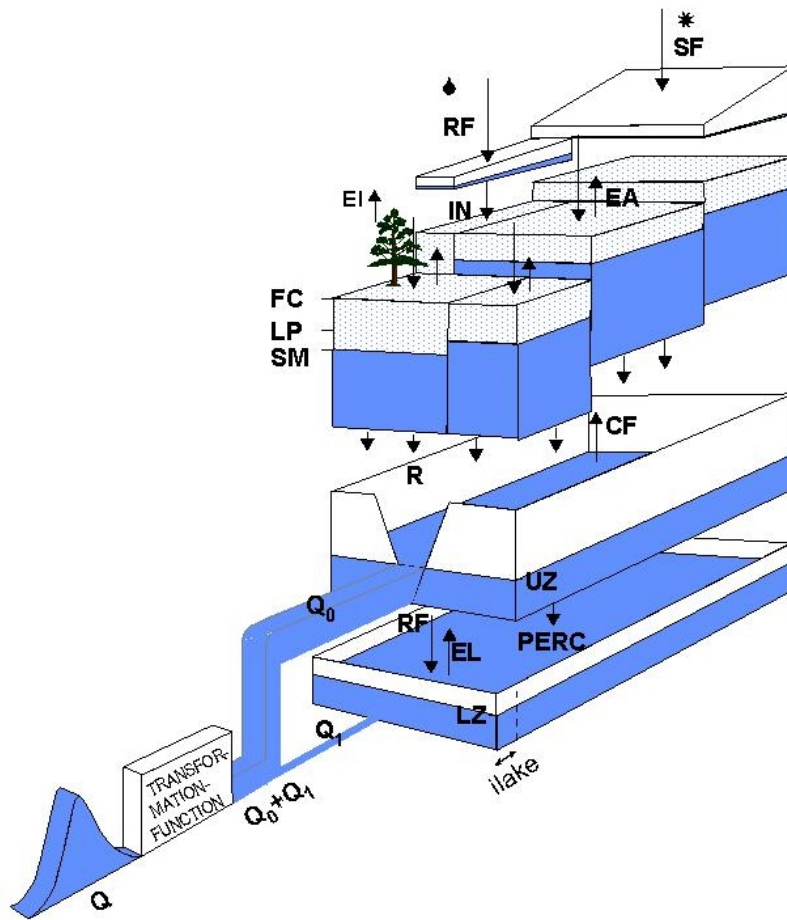


*Figure 3-2: Schematic presentation of the HBV model for one subbasin (SMHI, 2006).*

### 3.1.3 Threshold level method

The threshold level approach originates from the runs of crossing theory, which was first developed by Rice (1954) and further developed by Cramer and Leadbetter (1967) according to Bras and Rodriguez-Iturbe (1985). The method was first applied to droughts by Yevjevich (1967). The drought severity can usually be defined by the drought deficit, the drought duration or drought intensity (Peters, 2003). In this study, the threshold level approach will be applied to flow (observed and simulated), soil moisture and groundwater reservoir. Drought duration, deficit as well as the number of drought events will be used as the main identifiers for drought severity.

Yevjevich (1967) originally defined droughts as periods during which the current water demand exceeds the water supply. Both the water supply,  $S(t)$ , as well as the water demand,  $D(t)$ , are expressed as time series, and a drought event is defined as an uninterrupted sequence of negative values in the supply-minus-demand series,  $Y(t)=S(t)-D(t)$ . Later, Yevjevich (1983) simplified the concept by representing the demand as a threshold level in view of droughts being defined as periods during which the discharge is below the threshold level (Yahiaoui et al., 2009).

A stepwise illustration of the flow duration curve calculation is seen in **Figure 3-3**. Derivation of daily, monthly and seasonal period of record flow duration curves are illustrated in **Figure 3-3a** and the exceedance percentiles for each day of the year are calculated from a L-day moving window as demonstrated in **Figure 3-3b**.

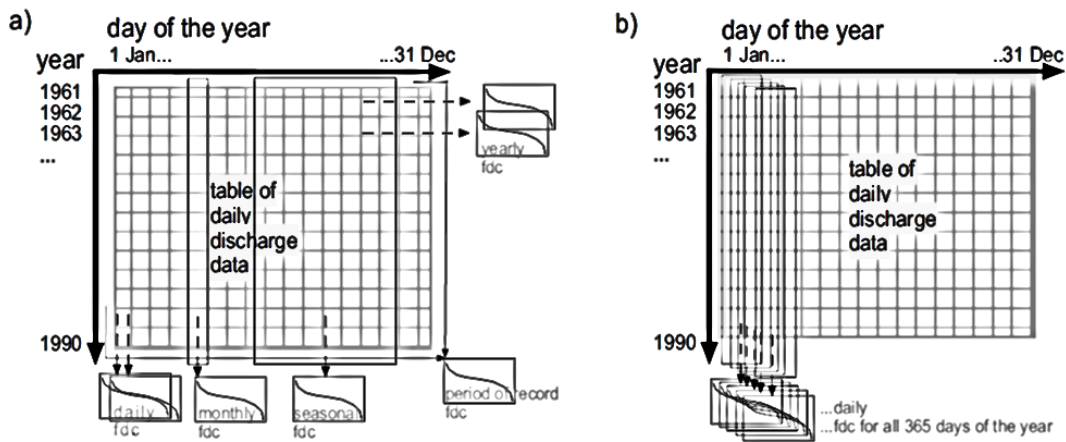


**Figure 3-3:** Determination of different flow curves for the threshold level definitions a) calendar units (day, month, season) and b) moving window (daily)(Hisdal and Tallaksen, 2000)

Unusual low flows during high flow seasons might be important for later drought development. However, periods with relatively low flow either during the high flow season or for instance due to a delayed onset of a snowmelt flood, are commonly not considered a drought. Therefore, the events defined with the varying threshold should be called streamflow deficiency or streamflow anomaly rather than streamflow drought. For example applying a 31- day window, the flow exceedance on 1 June would be calculated from all discharges recorded between 17 May and 16 June in each year of the period of record.

The afore-mentioned threshold represents physical parameters which occur or are exceeded on a specific percent of the period (Hisdal and Tallaksen, 2000). A sequence of drought events is obtained from the hydrograph by considering situations where hydrometeorological parameters are below a certain threshold level. Each drought event is characterized by its duration, deficit volume and time of occurrence. The time of drought occurrence is defined as the date of minimum flow in the drought. An event is counted when it starts during a specific hydrological year, even if it continues to the next hydrological year. Drought events of duration less than three days are ignored. During a prolonged dry period it is often observed that the flow exceeds the threshold level in a short period of time and thereby dividing a large drought into a number of minor droughts that are mutually dependent. The parameters values exceeded 80% of the time (Q80: 20<sup>th</sup> percentile) were used as the threshold (Oosterwijk et al., 2009).

### 3.2 Study area and data

The Platis catchment is located in the south-central part of the island of Crete in Greece and covers an area of 210 km<sup>2</sup> (**Figure 3-4**). The mean annual precipitation is estimated to be 923 mm with 87 wet days on average (a wet day is defined by precipitation over 0.1 mm) over the period 1974-1999 (**Table 3-1**) and its mean elevation is 698 m a.m.s.l. with a maximum of 2453.5 m. **Figure 3-5** illustrates the monthly and annual plot of precipitation time series. The climate ranges between sub-humid Mediterranean and semi-arid with long hot and dry summer and relatively humid and cold winter with a mean annual temperature 15 °C (Pavlakis, 2004). The mean annual flow reaches 272 Mm<sup>3</sup> and it is estimated that about 46% (126 Mm<sup>3</sup>) evapotranspires, 19% (51 Mm<sup>3</sup>) flows to the sea and 35% (95 Mm<sup>3</sup>) recharges the groundwater (Pavlakis, 2004). The land cover consists predominantly of agricultural areas (46.5%), artificial surfaces (0.1%) and forest and semi-natural areas (53.5%). The hydrogeological base of the area consists of impermeable quartzites and phyllites, as well as permeable carboniferous, limestone formations, neogene and quaternary deposits (Pavlakis, 2004).

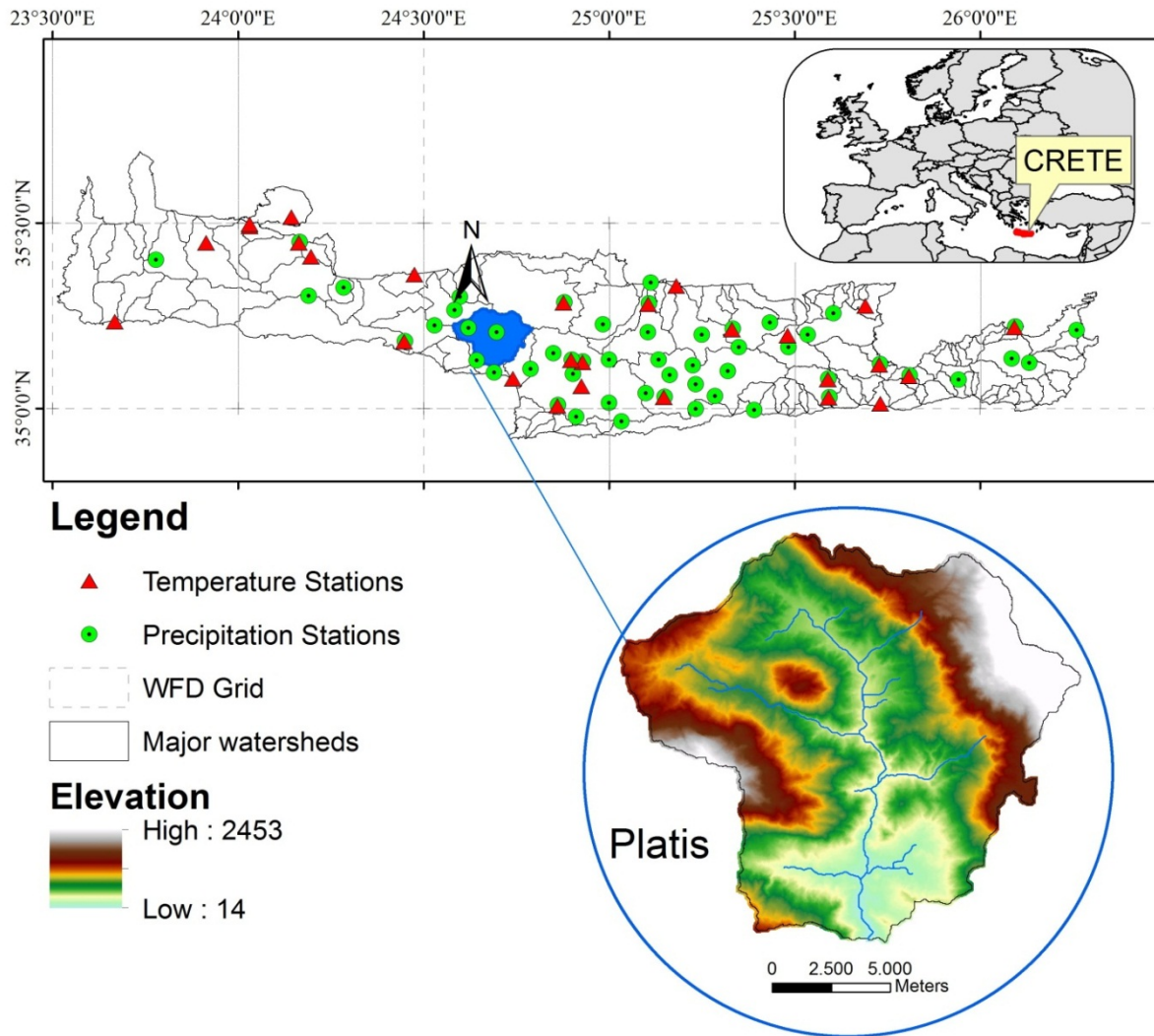


*Figure 3-4: Platis basin location and relief.*

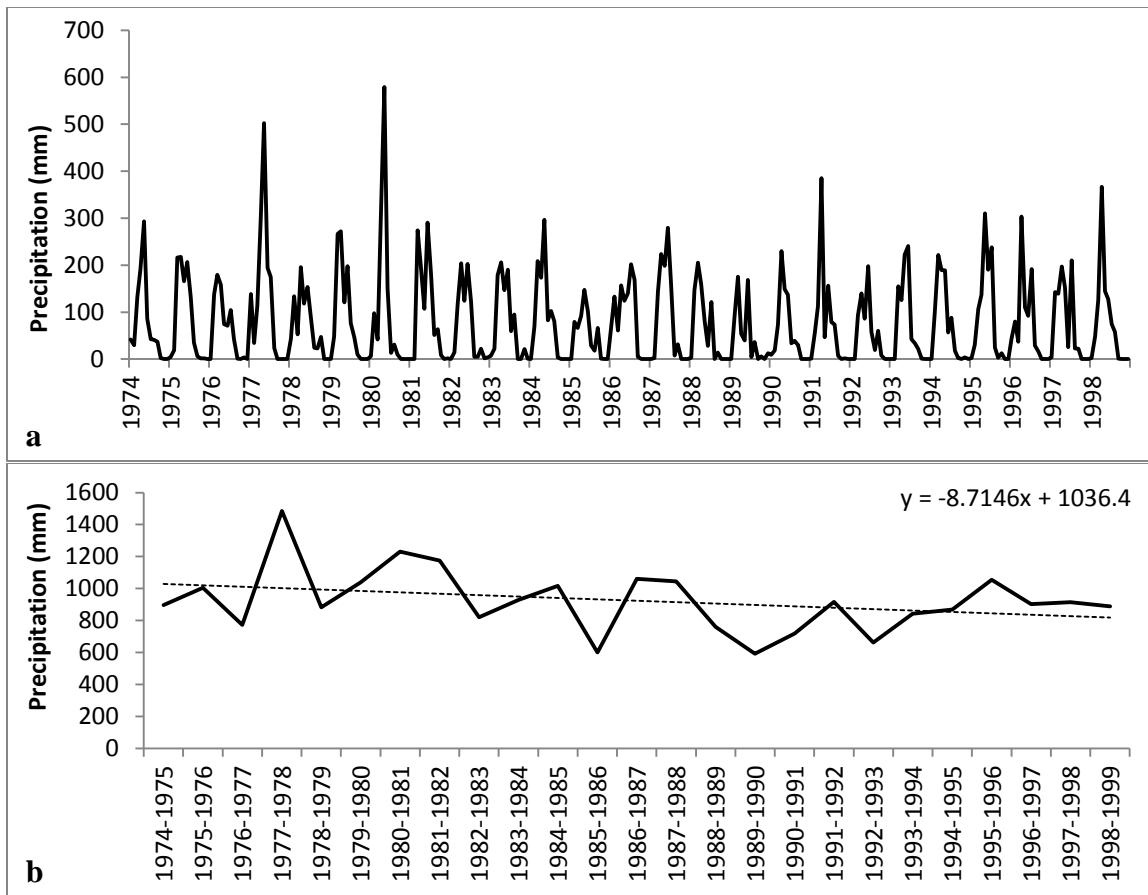


**Figure 3-5:** a) Monthly and b) annual precipitation time series for Platis basin for the period 1974-1999.

The local meteorological data used for the HBV model were obtained from four meteorological stations located in the Platis catchment (**Table 3-2**). Average daily temperature data of the nearby meteorological stations were provided by the Hellenic National Meteorological Service. Time-series of measured evapotranspiration for Platis test basin were available from one nearby meteorological station, at monthly time-step. Mean daily precipitation was derived from four stations using Thiessen method and daily average temperature was calculated from multiple linear regression for the period 1974-1999. Daily potential evaporation (PET) values were estimated through a combination of a locally calibrated Blaney-Criddle equation (Allen and Pruitt, 1986) and adjustment indices from generic daily WFD PET data, as described in the part of methodology. Daily discharge time-series were used for model calibration.

The methodology is tested using the available global dataset of observed forcing data (WATCH Forcing Data - WFD) of the period 1974-1999 from the EU project WATCH (WATER and global Change) in combination with local observational data (precipitation and temperature) (Weedon et al., 2011). The WFD have been derived from the ERA-40 reanalysis product of the European Centre for Medium Range Weather Forecasting (ECMWF) as described by Uppala et al. (2005). However, the one-degree ERA-40 data require adjustment based on half-degree monthly observational data in the form of the August 2008 version of CRU-TS2.1 from the Climatic Research Unit, in order to remove model biases (Hagemann et al., 2005).

Furthermore, WATCH Driving Data (WDD), which are used for projection purposes, are constructed from three GCMs output (precipitation and temperature), CNRM (Royer et al., 2002), ECHAM5 (Roeckner et al., 2003) and IPSL (Hourdin et al., 2006), interpolated at half-degree resolution concerning the period 1974-2100 and corrected for biases based on the WFD with the statistical bias correction method described in Piani et al. (2010). According to this method, statistical relationships between cumulative density functions (CDFs) of a common period between observed and simulated precipitation are established and applied to the projected precipitation. The transfer function derives from mapping a theoretical distribution (such as the gamma distribution) on GCM and observed precipitation CDFs. Two climate scenarios, A2 and B1 comprise the runs from the three GCMs used in this study. The half-degree GCM outputs are then interpolated in order to get the GCM precipitation at Platis basin level by using the Nearest Neighbor Interpolation (NN) (Gutin et al., 2002).

**Table 3-1: Hydrological characteristics of Platis basin.**

Year	Dry days/year	Wet days/year	Annual precipitation (mm)
1974-1975	271	94	897.5
1975-1976	269	97	1004.8
1976-1977	289	76	771.8
1977-1978	270	95	1484.7
1978-1979	277	88	882.7
1979-1980	266	100	1038.8
1980-1981	277	88	1230.4
1981-1982	263	102	1174.5
1982-1983	287	78	820.2
1983-1984	259	107	927.8
1984-1985	283	82	1017.5
1985-1986	280	85	601.1
1986-1987	256	109	1060.1
1987-1988	278	88	1045.6
1988-1989	297	68	759.5
<b>1989-1990</b>	305	60	<b>592.3</b>
1990-1991	270	95	718.0
1991-1992	270	96	916.5
1992-1993	290	75	662.4
1993-1994	291	74	841.8
1994-1995	274	91	868.2
1995-1996	255	111	1054.9
1996-1997	293	72	902.3
1997-1998	273	92	914.9
1998-1999	310	55	889.4
<b>AVERAGE</b>	<b>278</b>	<b>87</b>	<b>923.1</b>
<b>STDEV</b>	<b>14.4</b>	<b>14.6</b>	<b>199.0</b>

**Table 3-2: Characteristics of the stations used for Platis basin precipitation extraction.**

	Annual Precipitation (mm)	Area percentage
<b>Gerakari</b>	1336	24%
<b>Vizari</b>	778	52%
<b>Melabes</b>	782	14%
<b>Agia Galini</b>	623	9%

### 3.3 Results

#### 3.3.1 Hydrological model calibration and validation results and regime

The hydrological model was successfully calibrated using a 15-year period of daily observed data (precipitation, temperature and flow). The first year of calibration 1/9/1973–31/8/1974, was used to initialize the model. According to Nash-Sutcliffe (NS) criterion over the flow calibration, the performance of the IHMS-HBV model delivered satisfactory calibration results for the simulated flow; the NS for the calibration period was 0.81 (the same for  $R^2$ ), while the lnNS for low flow periods was 0.78 (**Table 3-3**). The HBV model was also calibrated using WFD precipitation and temperature as well as observed flow as input data, thereby producing WFD simulated parameters (simulated flow, soil moisture and lower groundwater reservoir). The simulation with observed data better reproduces observed flow than the calibration using WFD (NS = 0.53, lnNS = 0.68 and  $R^2 = 0.47$ ).

In order to establish calibration reliability, the model was validated for a 10-year period (1989-1999) for both datasets. Model performance was further evaluated through the identification of flow droughts for Platis basin using the threshold method over the calibration and validation periods (**Table 3-3**). For drought calculation, flow deficit more than 1 mm was taken into account. It is noted that Nash values for WFD are lower than the observed dataset.

**Table 3-3:** Nash-Sutcliffe estimators for calibration and validation periods and drought characteristics concerning observed, HBV-observed and WFD datasets.

	Calibration (1974-1988)			Validation (1989-1999)			Total historical period (1974-1999)		
	Observed	HBV-observed	WFD	Observed	HBV-observed	WFD	Observed	HBV-observed	WFD
<b>NS</b>	-	0.81	0.53	-	0.59	0.42	-	0.77	0.51
<b>lnNS</b>	-	0.78	0.68	-	0.7	0.67	-	0.76	0.68
<b>R<sup>2</sup></b>	-	0.81	0.47	-	0.61	0.39	-	0.77	0.45
<b>Number of droughts</b>	9	7	8	14	13	15	23	20	23
<b>Drought duration (days)</b>	13	20	21	15	18	23	14	20	23
<b>Deficit amount (mm)</b>	0.2	0.27	0.26	0.24	0.28	0.3	0.22	0.27	0.29

The hydrological regime of Platis basin is presented via long-term daily averages concerning five parameters for the period 1974-1999 in **Figure 3-6**. Analyzing the results of the hydrological model on an average daily basis for both local and WFD datasets, it was found that the hydrograph (observed and simulated) shows a clear seasonal pattern: high flows occur during January and February, while there is no flow during summer and autumn period (end of May to end of October). HBV simulates this pattern quite well, while some underestimation in winter is visible. The coefficient of determination for local simulated and WFD time series is  $R^2=0.89$ .

The negative relation between soil moisture and temperature indicates the effect of evapotranspiration on the soil moisture content. It is also obvious from **Figure 3-6** that soil moisture is at its maximum during winter months. Local and WFD simulated soil moisture datasets conclude to  $R^2=0.99$ . When temperature starts to reach about 20 °C (June) soil moisture falls under 50 mm. At that moment also groundwater storage reaches zero ( $R^2=0.98$  concerning local and WFD simulated groundwater time series). Soil moisture rises following the increase of precipitation (November to April). In general, besides precipitation ( $R^2=0.7$ ), temperature is an important factor for the hydrological regime in Platis.

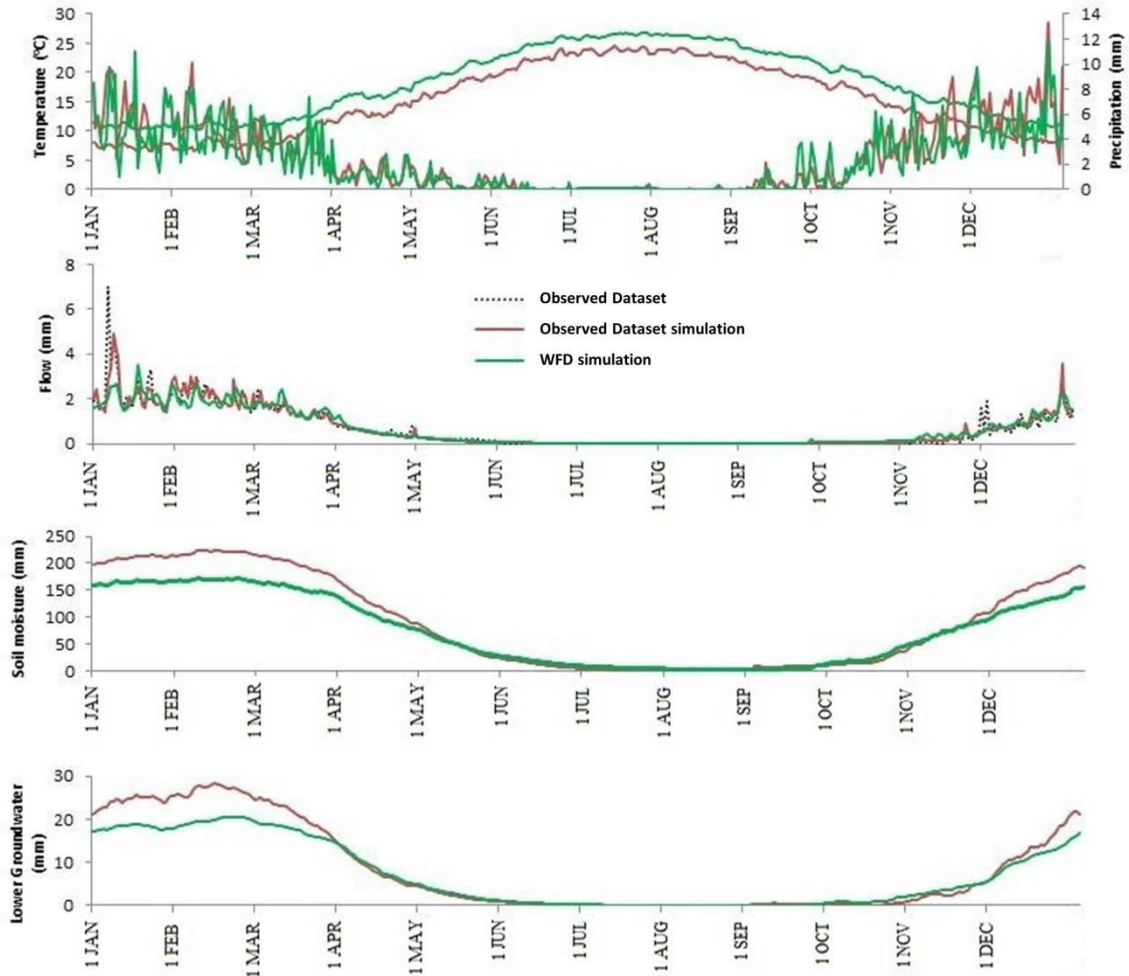


**Figure 3-6:** Long-term daily averages derived from local and WFD datasets for Platis basin for the period 1974-1999. Top panel: temperature and precipitation; second panel: observed and simulated flow; third panel: soil moisture; lower panel: lower groundwater storage.

Moreover, the hydrological status for the past period (observed and model ensemble) is illustrated with long-term monthly averages in **Figure 3-7**. The forcing of the WFD calibrated HBV model with the bias corrected GCM output from 2001 to 2100 (WDD) offered an overall projected representation of the parameters. The three (3) GCMs past data were standardized to a single model average, with -10% error in precipitation and +2.2°C in temperature comparing to the observed dataset. The GCMs future results concerning both scenarios can be compared via four 25-year future period curves from 2001 to 2100. It is worth mentioning that both scenarios exhibit a decrease in precipitation and an increase in temperature averages compared to the past

climate data. In A2 scenario, the GCM ensemble change (compared to past WFD) was -30% for precipitation and +4.5°C for temperature for the last 25-year period; B1 scenario represents “milder” results, giving -8% change in precipitation and +2.5°C change in temperature from 2001 onwards.

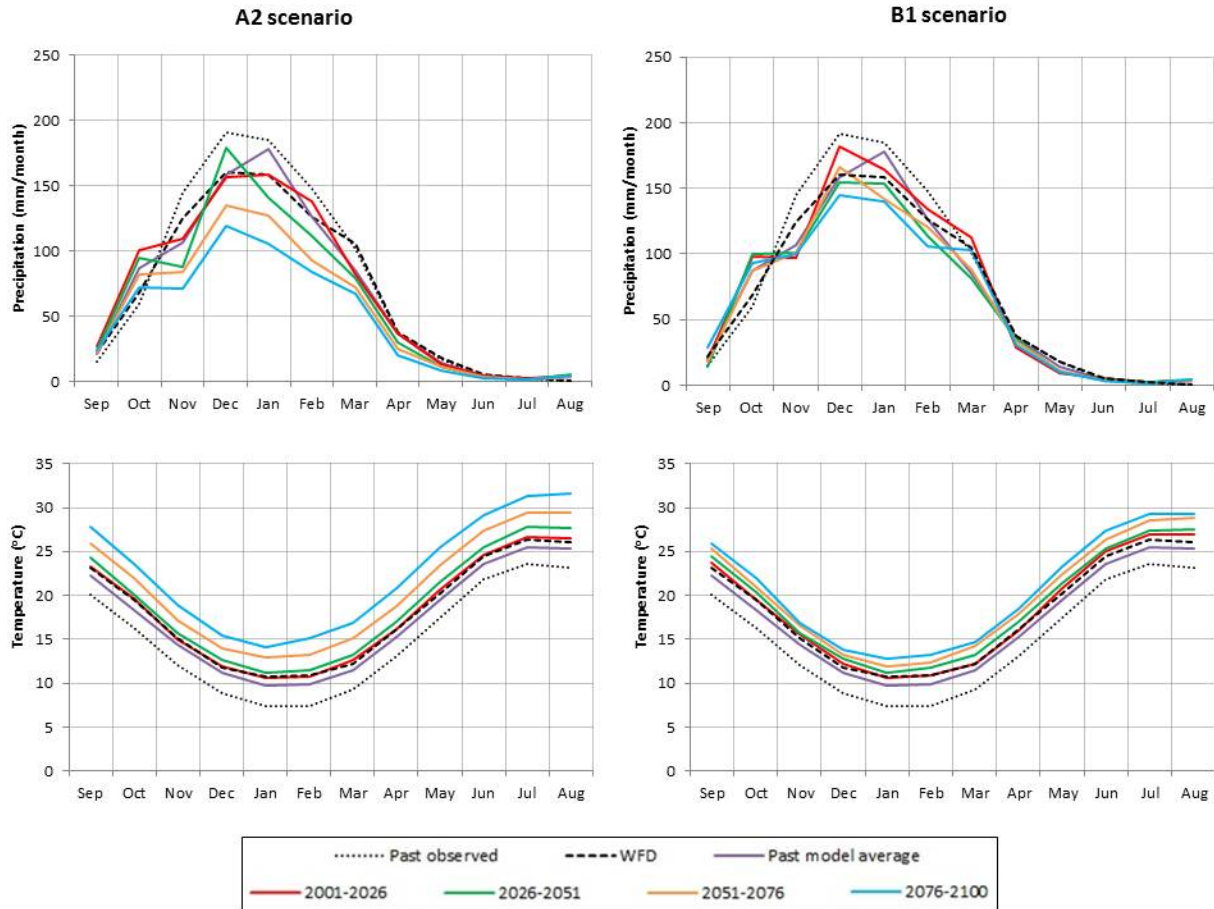


**Figure 3-7:** Seasonal variability between the past (observed and 3-model average) and future periods for precipitation and temperature climatic variables concerning A2 and B1 scenarios.

The seasonal variability of the hydrological parameters (flow, soil moisture, lower groundwater) from the three model simulations are demonstrated for the past and future periods in **Figure 3-8**. It was found that in past time series the simulated flow corresponds well to the observed (+3% difference), while soil moisture and lower groundwater are underestimated by 17% and 31% respectively. The GCMs projections of both scenarios indicate a significant decrease in flow, soil moisture and groundwater reservoir. Comparing to the WFD averages, A2 scenario provides -56% decrease for flow, -34% for soil moisture and -65% for groundwater over 2076-2100,

whereas B1 scenario exemplifies more conservative predictions with a -18% change for flow, -15% for soil moisture and -22% for groundwater.

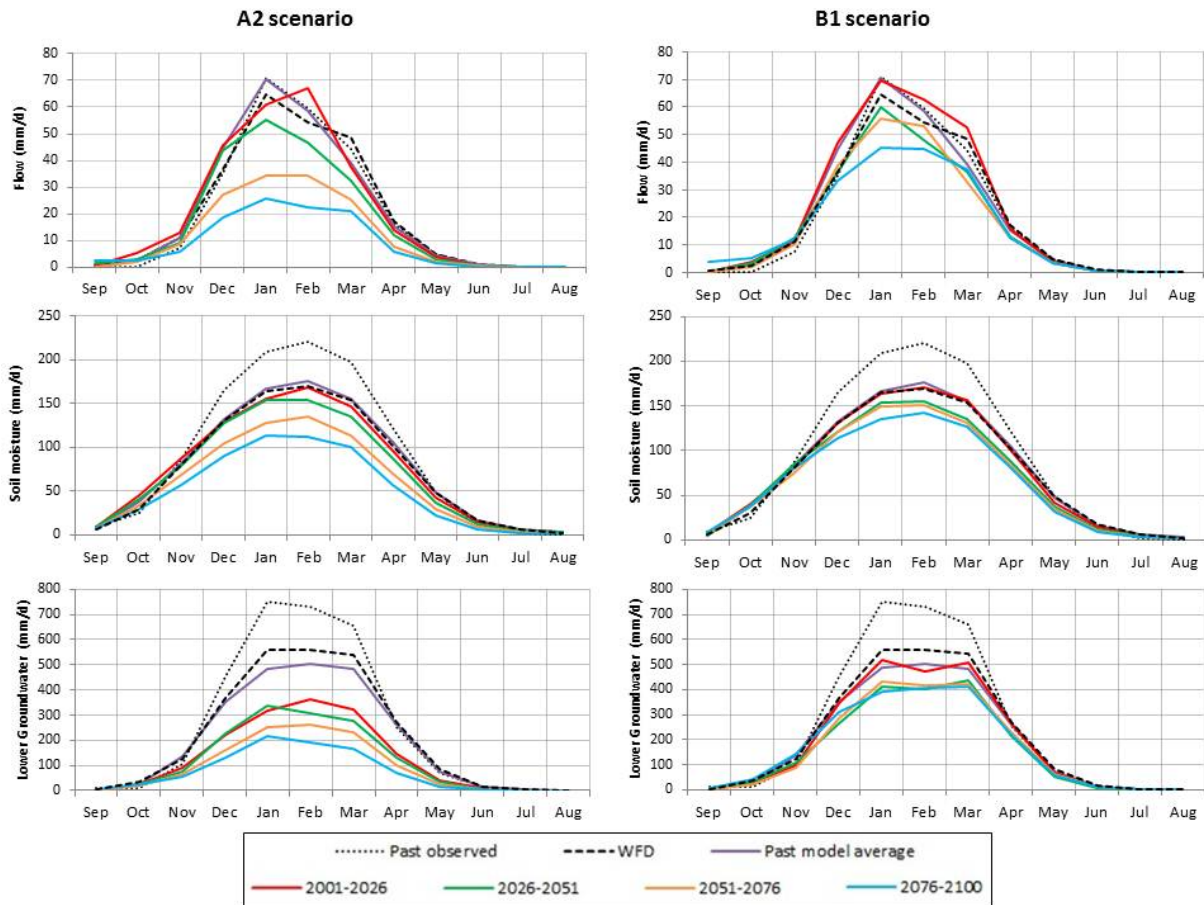


**Figure 3-8:** Seasonal variability between the past (observed and three-model average) and future periods for flow, soil moisture and lower groundwater climatic variables concerning A2 and B1 scenarios.

### 3.3.2 Drought in different hydrometeorological variables

Droughts for Platis basin were identified using the threshold level method over the period 1974-1999. The 20<sup>th</sup> percentile of each parameter and each dataset was calculated thereby extracting the corresponding “threshold” time series. For drought calculation, at least three consecutive days that do not reach the “threshold” values, are considered as a drought event and the

difference between the threshold values and the original time series is defined as deficit amount; soil moisture deficit more than 1 mm, flow and lower groundwater deficit exceeded by 0.1 mm were taken into account. From the observed, simulated flow, soil moisture and lower groundwater time series, several drought characteristics were determined with the threshold level method, i.e. number, mean duration, and mean deficit amount of droughts (**Table 3-4**).

**Table 3-4:** Drought characteristics in different hydrometeorological variables and different datasets for Platis basin for the period 1974-1999.

Dataset	Variable	Number of droughts	Drought duration (days)	Deficit amount (mm)
			Mean	Mean
Observed	Observed flow	23	14	0.22
	Simulated flow	20	20	0.27
	Soil moisture	45	17	16
	Lower groundwater	32	21	3.08
WFD	Simulated flow	23	23	0.29
	Soil moisture	43	18	13.9
	Lower groundwater	38	19	2.53
CNCM	Simulated flow	20	20	0.24
	Soil moisture	42	20	14.57
	Lower groundwater	31	24	2.47
ECHAM5	Simulated flow	22	21	0.23
	Soil moisture	37	21	18.25
	Lower groundwater	31	27	2.25
IPSL	Simulated flow	17	22	0.36
	Soil moisture	40	23	19.79
	Lower groundwater	29	35	3

The relative difference between results from simulated and observed flow for each characteristic was also examined. Notwithstanding the Nash-Sutcliffe values for both forcing datasets (NS for WFD is lower than NS for HBV-observed), the simulation with WFD seems to produce better fit for threshold level method results regarding the number of droughts. According to **Table 3-4**, the number of droughts in the simulated time series (20) correspond well to the droughts of the observed dataset (23), mean drought duration is overestimated by the simulation (20 drought days), and the simulation of mean deficit is again quite close to observations (0.27 mm).

Generally, soil moisture and lower groundwater droughts are the most frequent; the number of droughts in the soil moisture is higher than in lower groundwater. The models results underestimate the number of flow, soil moisture and groundwater drought events (up to 20, 42, 31 for CNCM, 22, 37, 31 for ECHAM5 and 17, 40, 29 for IPSL respectively) while mean drought duration is overestimated (up to 20, 20, 24 days for CNCM, 21, 21, 27 days for ECHAM5 and 22, 23, 35 days for IPSL respectively) as shown in **Table 3-4**.

In order to investigate drought events and perform a correlation analysis between the events and precipitation data, a focus on a specific year with the minimum precipitation amount which represents dry conditions would serve for such examination. 1989-1990 represents the year with the minimum precipitation amount (592 mm) with 99 rainy days; drought propagation through soil moisture, observed, simulated flow and lower groundwater reservoir for the dry hydrological year 1989-1990 is shown in **Figure 3-9**. Lower groundwater was selected for graphical examination as it represents the groundwater storage of the basin contributing to the base flow and the origin of slow runoff. Flow (observed and simulated) drought begins to develop together with lower groundwater (December 1989). Two flow and groundwater drought periods are followed until the high precipitation of February 1990 recharged soil moisture and groundwater to the maximum of the year. The following low precipitation values lead to another drought event for all parameters. It is obvious that soil moisture and groundwater droughts develop together. It is therefore reasonable to assume that precipitation causes equal temporal evolution of deficits to all parameters. Furthermore, there is lack of precipitation, flow and groundwater during summer months, whereas winter months comprise the period during which recharge takes place. Meteorological drought through precipitation was not analyzed, since the threshold level method gave zero values for the threshold Q80 and close to zero values concerning the threshold of Q60.

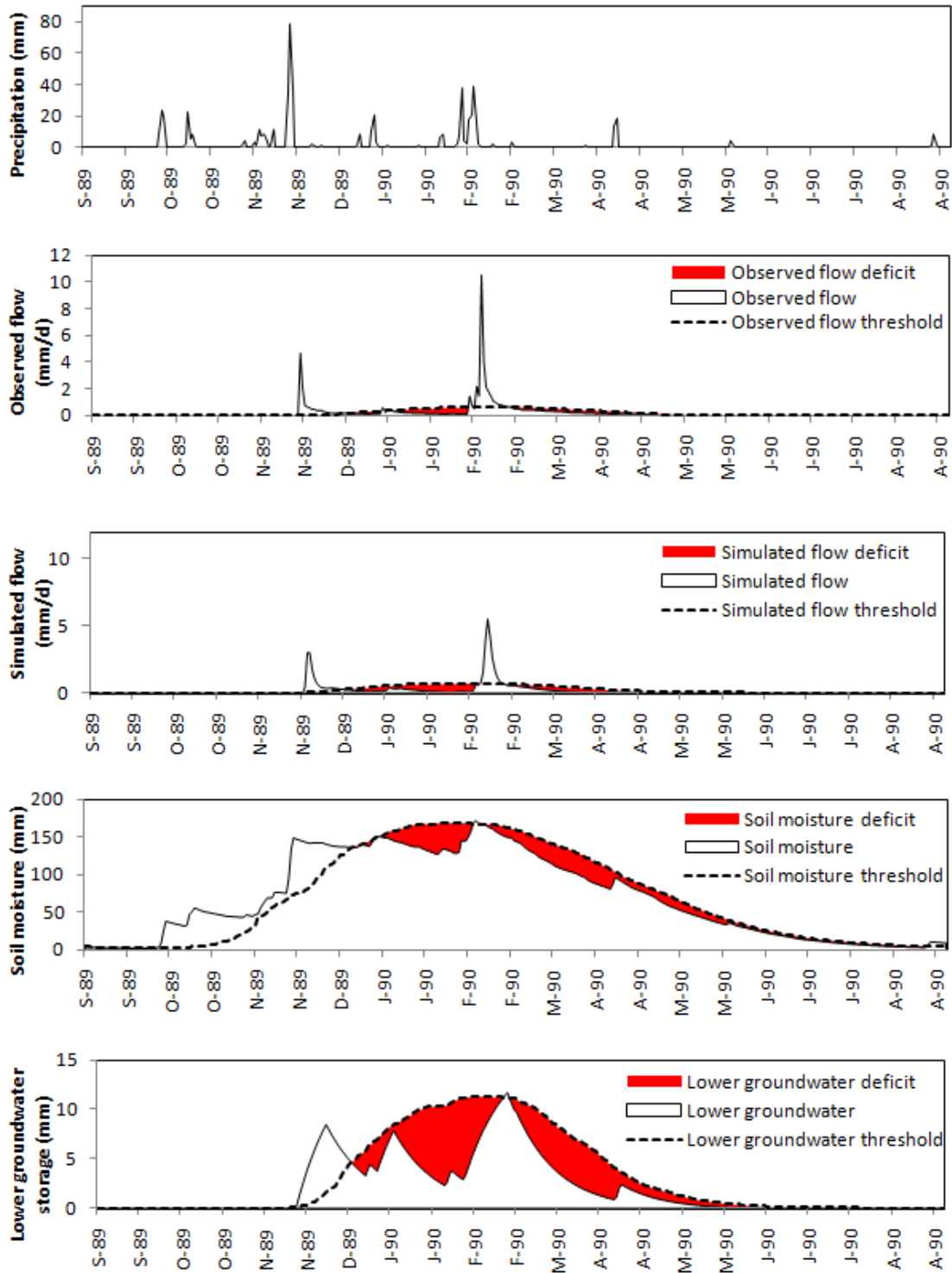


**Figure 3-9:** Example of drought propagation in Platis catchment for the hydrological year 1989-1990. Top panel: Mean annual precipitation; second panel: observed flow, dashed line = daily observed flow threshold; third panel: simulated flow, dashed line = daily simulated flow threshold; fourth panel: soil moisture storage, dashed line = daily soil moisture threshold; lower panel: lower groundwater storage, dashed line = daily lower groundwater threshold.

### 3.3.3 Frequency distributions

Taking into account the projected decreases in all parameters, a frequency distribution analysis was performed to obtain insight into how the afore-mentioned changes are connected to drought appearance.

Cumulative frequency distributions of drought duration for observed dataset and WFD regarding simulated flow, soil moisture and lower groundwater during the past period 1974-1999, are displayed in **Figure 3-10**. For all parameters, the results provided high correlation for both datasets. Many short duration droughts are evident in the plots; nearly 50% of the flow (both observed and simulated) drought events last over 5 days. Soil moisture and groundwater discharge both show a similar distribution in duration as was expected. Simulated flow and groundwater plots display some marked gaps at 80% of probability.

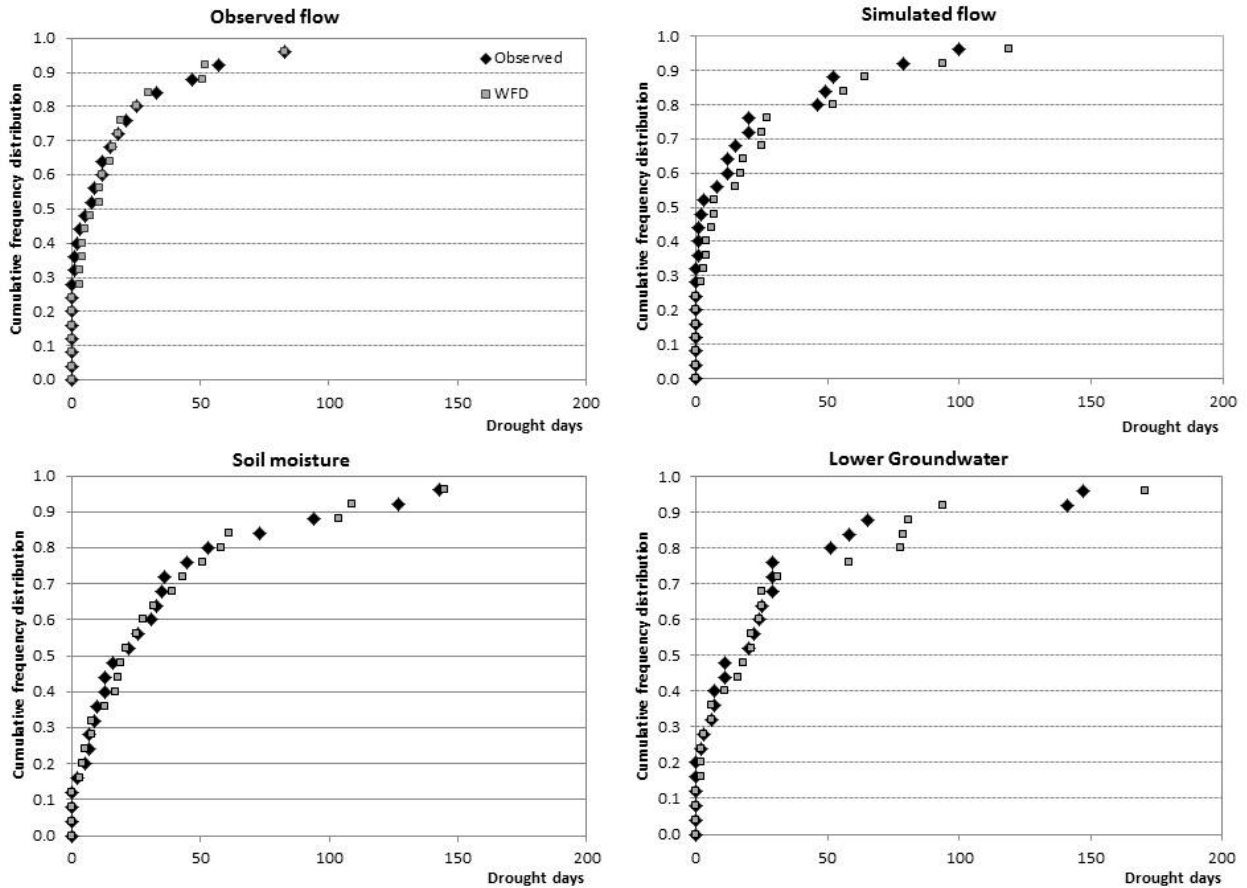


**Figure 3-10:** Cumulative frequency distribution of drought duration (in days) for observed dataset and WFD regarding simulated flow (top), soil moisture (middle) and lower groundwater (bottom) during the past period 1974-1999.

Frequency distributions for drought duration regarding the past period 1974-2001 and the future period 2001-2100 (scenario A2) of three models (**Figure 3-11**) show a clear tendency towards severe drought conditions. From 2001 onwards, drought duration is significantly increased; soil moisture droughts are characterized by a longer duration in comparison with the other parameters. The probabilities for greater drought duration are increased from one period to another; this shift on the curves indicates a robust signal in terms of the drought propagation. Regarding the simulated flow, the soil moisture and the lower groundwater, 50% of the events lasted over 10, 30 and 20 days in the past period and 50, 200 and 110 days on average in the last future period respectively. The parameters with a less continuous distribution may be related to the rather low number of events or the given model structure.

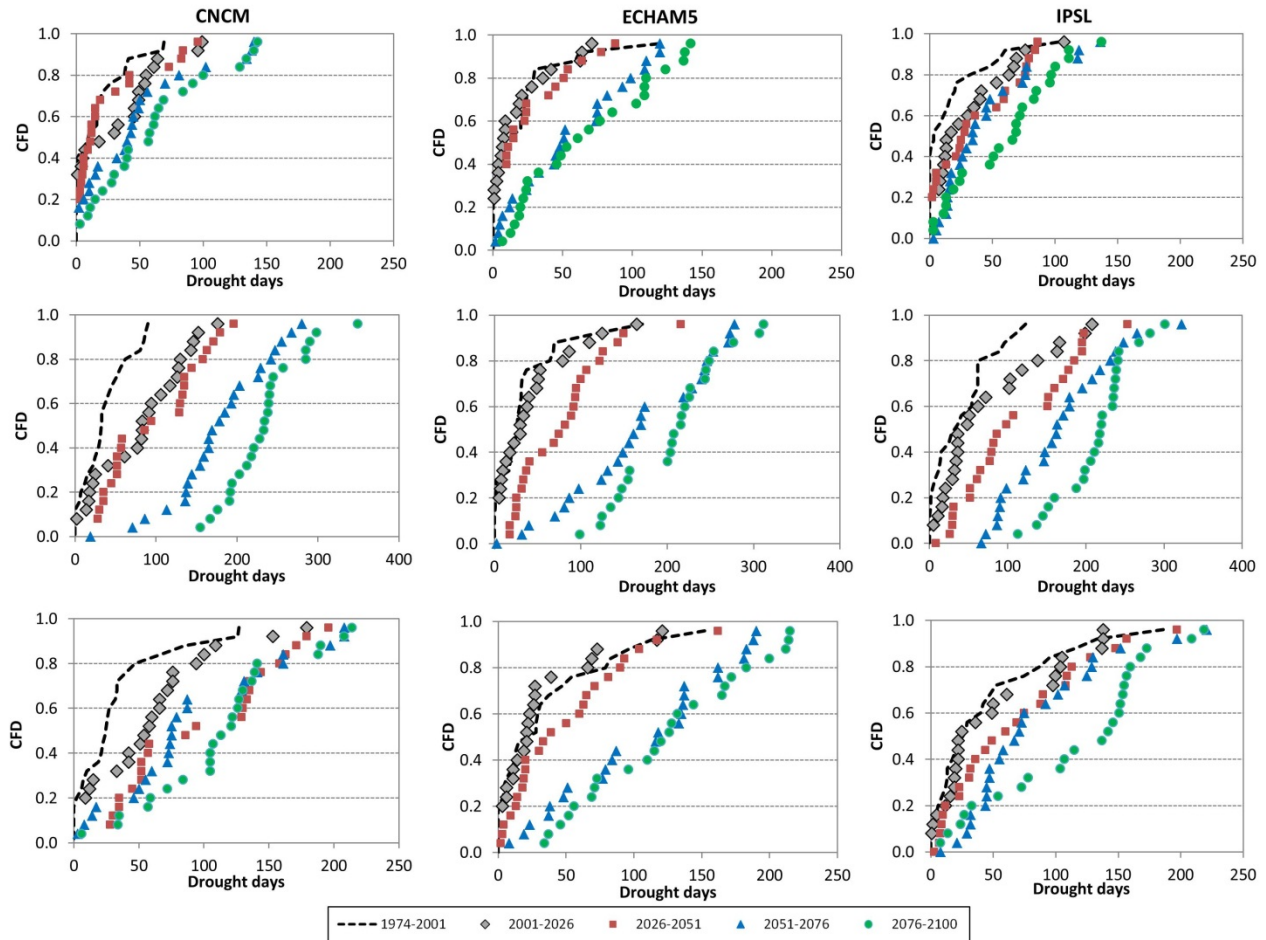


**Figure 3-11:** Cumulative frequency distribution of drought duration (in days) for three models (CNCM, ECHAM5 and IPSL) regarding simulated flow (top), soil moisture (middle) and lower groundwater (bottom) during the past period 1974-2001 and future period 2001-2100 (Scenario A2), divided into four 25-year sub-periods.

Visual comparison of **Figures 3-11** and **3-12** indicate that B1 scenario results demonstrate more uniform distributions which are close to linear structures and milder climate conditions for all parameters with similar results among the sub-periods. Increased drought duration probabilities in the future periods for both scenarios are illustrated; soil moisture droughts last longer than the other parameters. According to expectations, B1 scenario offers a more optimistic view of drought status. Regarding the simulated flow, the soil moisture and the lower groundwater, 50% of the events lasted 20, 100 and 50 days on average in the last future period respectively. Uniformity in the curves indicates the corresponding structure of dataset. For example, soil moisture drought days of ECHAM5 model in **Figure 3-11** appear a noticeable gap in the range

160-200 implying that there are no such values derived by this dataset. The modeling chain encompasses three different processes, beginning from the GCMs output data, the HBV model simulation and the threshold level method and thus, the origination of these discontinuities is indefinite. It is obvious that soil moisture resembles closely the properties of groundwater discharge (duration and deficit volume). This further supports the use of either parameter when information on the spatial aspects of drought is required.

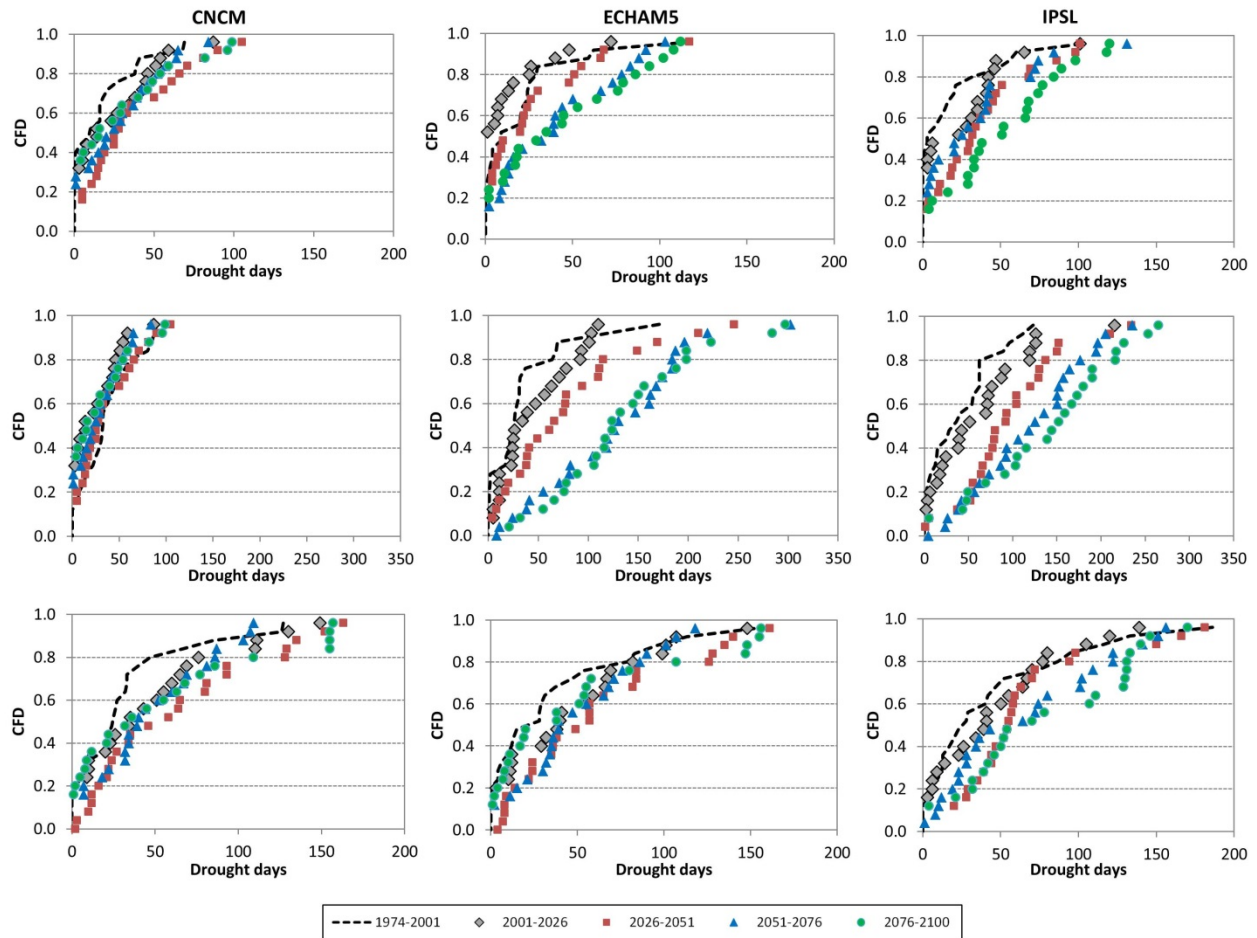


**Figure 3-12:** Cumulative frequency distribution of drought duration (in days) for three models (CNCM, ECHAM5 and IPSL) regarding simulated flow (top), soil moisture (middle) and lower groundwater (bottom) during the past period 1974-2001 and future period 2001-2100 (Scenario B1), divided into four 25-year sub-periods.

The percentage change of drought characteristics for the future periods in terms of the three-model ensemble past status provides a meaningful interpretation of the parameters decrease effect on drought propagation (**Table 3-5**). For A2 scenario, it was found that drought events

number increases up to 98%, 109% and 81% for flow, soil moisture and groundwater respectively. B1 scenario provided more conservative estimates, with a drought events number increase of 56%, 92% and 34% for flow, soil moisture and groundwater respectively. The drought duration difference between scenarios reaches up to 33%, 89% and 34% for simulated flow, soil moisture and groundwater respectively till 2100. Moderate changes can be noticed in drought deficit volume with an estimated maximum increase of 19%, 33% and 22% in flow, soil moisture and groundwater involving A2 scenario, whereas B1 scenario predicted 10%, 2% and 26% maximum increase for the former parameters. The projected precipitation (30% and 7% decrease for A2 and B1 respectively) and temperature (5.3°C and 3.4°C increase for A2 and B1 respectively) follows in accordance with the evolution of the hydrological parameters.

**Table 3-5: Change percentage of drought characteristics for 4 future periods (scenarios A2 and B1) concerning the three-model ensemble.**

Period	Variable	Precipitation (mm)		Temperature (°C)		Number of drought events		Drought duration (days)		Deficit amount (mm)	
		A2	B1	A2	B1	A2	B1	A2	B1	A2	B1
2001-2026	Simulated flow					+17% (+3)	0%	+24% (+5)	+10% (+2)	+5%	+1%
	Soil moisture	+1%	+4%	+1.1	+1.2	+33% (+13)	+37% (+15)	+33% (+7)	+20% (+4)	-6%	-16%
	Lower groundwater					+13% (+4)	+25% (+8)	+9% (+3)	0%	+11%	+13%
2026-2051	Simulated flow					+14% (+3)	+42% (+8)	+35% (+7)	+27% (+6)	+5%	+1%
	Soil moisture	-7%	-6%	+1.9	+1.9	+68% (+27)	+70% (+28)	+52% (+11)	+52% (+11)	-16%	-6%
	Lower groundwater					+46% (+14)	+34% (+10)	+9% (+3)	+26% (+7)	-7%	+20%
2051-2076	Simulated flow					+88% (+17)	+27% (+5)	+51% (+11)	+48% (+10)	+13%	+6%
	Soil moisture	-20%	-6%	+3.6	+2.7	+125% (+50)	+84% (+33)	+116% (+25)	+78% (+17)	+11%	-7%
	Lower groundwater					+75% (+23)	+23% (+7)	+47% (+13)	+19% (+5)	+16%	+18%
2076-2100	Simulated flow					+98% (+19)	+56% (+11)	+81% (+17)	+48% (+10)	+19%	+10%
	Soil moisture	-30%	-7%	+5.3	+3.4	+109% (+43)	+92% (+36)	+194% (+41)	+105% (+22)	+33%	+2%
	Lower groundwater					+81% (+25)	+14% (+4)	+77% (+22)	+43% (+12)	+22%	+26%

## **4. Drought assessment based on multi-model precipitation projections**

---

The potential impacts of climate change and global warming must be considered by water resource managers and the corresponding scientific communities, as water availability is increasingly being stressed (Qi et al., 2009). Many studies have adopted various climate change scenarios to evaluate effects on meteorological parameters. The scenarios presented in the Special Report on Emission Scenarios (SRES) in the Intergovernmental Panel on Climate Change (IPCC) Fourth Assessment Report (AR4) (IPCC, 2007) have been widely applied both for the investigation of hydrological responses to climate change and its projection globally and regionally (Boyer et al., 2010; Crossman et al., 2013; Ficklin et al., 2009; Matondo et al., 2004). The WCRP's (World Climate Research Programme) Working Group on Coupled Modelling (WGCM) has initiated a new set of coordinated climate model experiments that comprise the fifth phase of the Coupled Model Intercomparison Project (CMIP5). Following CMIP3 datasets that were used in the previous Chapter, CMIP5 datasets will notably provide a multi-model context for assessing the mechanisms responsible for model differences in poorly understood feedbacks associated with the carbon cycle and with clouds, examining climate predictability and exploring the ability of models to predict climate on decadal time scales (Taylor et al., 2012). Higher resolution of the new models will offer more complete and reliable results concerning the translation of both climate and drought status.

General Circulation Models (GCMs), which describe the atmospheric process by mathematical equations, are the most adapted tools for studying the impact of climate change at regional scale.

The scenarios emerging from the new set of GCM experiments, are called Representative Concentration Pathways (RCPs) (**Table 4-1**) and constitute a set of greenhouse gas concentration and emissions pathways served to support research on the impacts climate change (Riahi et al., 2011; Kim et al., 2013). The Representative Concentration Pathway (RCP) 8.5 corresponds to a high greenhouse gas emissions pathway compared to the scenario literature (Jevrejeva et al., 2012; Kim et al., 2013; IPCC, 2007), and hence also to the upper bound of the RCPs. The greenhouse gas emissions and concentrations in this scenario increase considerably over time, leading to a radiative forcing of  $8.5 \text{ W/m}^2$  at the end of the century (Riahi et al., 2007). The rest pathways represent milder conditions and can be considered as moderate mitigation scenarios.

**Table 4-1:** Types of representative concentration pathways

<b>Name</b>	<b>Radiative Forcing</b>	<b>Concentration</b>
RCP8.5	$> 8.5 \text{ W/m}^2$ in 2100	$> 1370 \text{ CO}^2\text{-eq}$
RCP6	$6 \text{ W/m}^2$ at stabilization after 2100	$850 \text{ CO}^2\text{-eq}$ at stabilization after 2100
RCP4.5	$4.5 \text{ W/m}^2$ at stabilization after 2100	$650 \text{ CO}^2\text{-eq}$ at stabilization after 2100
RCP3-PD (RCP2.6)	peak at $3 \text{ W/m}^2$ before 2100 and then decline to $2.6 \text{ W/m}^2$	peak at $490 \text{ CO}^2\text{-eq}$ before 2100 and then decline

A large number of studies dealing with changes in precipitation and temperature are included in the international literature (Ramirez-Villegas and Challinor, 2012; Jiang et al., 2007; Goodess, 2013). Kim et al. (2013) examined the combined impacts of future changes in climate and land cover on streamflow using the RCPs 4.5 and 8.5. Additionally, Vidal and Wade (2008) used two emissions scenarios, six global climate models and four downscaling methods in order to build climate change scenarios for three catchment case studies in the UK.

Climate change is expected to affect precipitation, temperature and potential evapotranspiration, and, thus, is likely to affect the occurrence and severity of meteorological droughts. Drought is defined as a sustained and regionally extensive occurrence of below average natural water availability (van Lanen et al., 2007). It is a phenomenon that can be characterized as a deviation from normal conditions in the physical system (climate and hydrology), which is reflected in variables such as precipitation, soil water, groundwater and streamflow. Drought is a recurring and worldwide phenomenon having spatial and temporal characteristics that vary significantly from one region to another (Tallaksen and van Lanen, 2007).

The Mediterranean region lying in a transition zone between the arid climate of northern Africa and the temperate and wet climate of central Europe, is one of the most responsive regions to global warming. A number of studies have reported regional climate change simulations with different generations of global model projections over Europe, including the Mediterranean region (Giorgi and Lionello, 2008; Giorgi et al., 2004; Deque et al., 1998; Christensen and Christensen, 2003; Semmler and Jacob, 2004). More specifically, the projection of precipitation changes and drought evolution in the island of Crete has received considerable attention from the scientific community (Koutroulis et al., 2011; Vrochidou et al., 2012; Deng et al., 2013). Kirono et al. (2011) presented characteristics of droughts simulated by global climate models under enhanced greenhouse conditions with the aid of the Reconnaissance Drought Index (RDI). Drought detection and monitoring is feasible with the use of drought indices. The selection of the most appropriate index has been discussed by Vrochidou and Tsanis (2012) concluding that the Standardized Precipitation Index (SPI) is the most widely used; nevertheless, due to some limitations in providing relative information when applied for different areas, the Spatially-Normalized SPI (SN-SPI), a variant of SPI introduced by Koutroulis et al. (2011), will be applied so as to take advantage of an improved spatial comparison in terms of drought conditions.

The simulation of climate from a single GCM is insufficient to provide the appropriate information for a comprehensive assessment of potential climate change and its impacts (Jacob et al., 2007). Ideally, by using the average of an ensemble of GCMs, the individual model errors are cancelled out and the ensemble uncertainty decreases as increasingly more models are used, even though some realism is sacrificed (Sperna et al., 2012). When compared with each other, different climate models agree qualitatively or semi-quantitatively on several aspects of climate change. In reality, the use of similar parameterization, numerical methods and coarse grid resolutions cause some biases depriving part of independency to the models. Therefore, biases will remain in the multi-model ensemble and the ensemble might not cover the full uncertainty range (Räisänen et al., 2007). Notwithstanding this fact, various studies concluded that a multi-model mean tends to give more robust predictions for future change than single model simulations (Sperna et al., 2012; Giorgi and Mearns, 2002; Murphy et al., 2004; Boorman and Sefton, 1997). It is also stated that deriving model weights from performance for precipitation and or temperature may not be the best solution in hydrological impact studies (Sperna et al., 2012).

In this study, 13 GCM simulations are used in order to produce precipitation patterns and clarify their “character” both spatially and temporally. This multimodel approach hence enhances the reliability of the results. The projections of future precipitation changes will be examined over the island of Crete; moreover, the assessment of drought evolution under the RCP 2.6, 4.5 and 8.5 scenarios both spatially and temporally will serve for addressing alert systems and risk management planning.

## 4.1 Methodology

### 4.1.1 Bias correction

It is well known that the modeled processes that offer precipitation simulations need some form of preprocessing in order to remove the existing biases. Imperfections due to the coarse spatial resolution of GCMs compose the main cause of these biases and are often found in the mean precipitation, the number of drizzle days, and the underestimation of high precipitation values (Grillakis et al., 2013). Often, statistical bias correction methodologies are applied in order to correct the statistical properties on model outputs in order to match those of the observations (Sharma et al., 2007; Christensen et al., 2008; Haerter et al., 2011; Grillakis et al., 2013).

To varying extent, all numerical models suffer from systematic error, i.e. the difference between the simulated value and the observed. Bias is defined as the time independent component of the error. To construct a mapping between the observed and the modeled data, a transfer function is derived (Haerter et al., 2011). The corrected mean  $\mu_{mod}^{cor}$  and variance  $\sigma_{mod}^{cor}$  are:

$$\mu_{mod,sc}^{cor} = \mu_{obs} + \frac{\sigma_{obs}}{\sigma_{mod,con}} (\mu_{mod,sc} - \mu_{mod,con}) \quad (4 - 1)$$

$$\sigma_{mod,sc}^{cor} = \frac{\sigma_{obs}}{\sigma_{mod,con}} \sigma_{mod,sc} \quad (4 - 2)$$

where

$\mu_{mod,sc}^{cor}$  : corrected mean of modeled data of scenario period

$\mu_{obs}$  : mean value of observed data

$\sigma_{obs}$  : variance of observed data

$\mu_{mod,sc}$  : mean value of modeled data of scenario period

$\mu_{mod,con}$  : mean value of modeled data of control period

$\sigma_{mod,con}$  : variance of modeled data of control period

$\sigma_{mod,sc}^{cor}$  : corrected variance of modeled data of scenario period

$\sigma_{mod,sc}$  : variance of modeled data of scenario period

### 4.1.2 The SN-SPI

The drought index used in this study was described in Chapter 2.

## 4.2 Study area and data

Monthly precipitation data was compiled by the WRDPC service (Water Resources Department of the Prefecture of Crete) for 50 precipitation stations (**Figure 4-1**) which mainly cover the central part of the island of Crete, characterized by a higher level of agricultural activity than the western part. These data cover a thirty (30) years' time period for each month of the hydrological year (September to August), from 1973 to 2005, which is set as the control period. **Figure 4-2** illustrates three representative stations evenly distributed over Crete with the corresponding observed mean annual precipitation for the period 1973-2005.

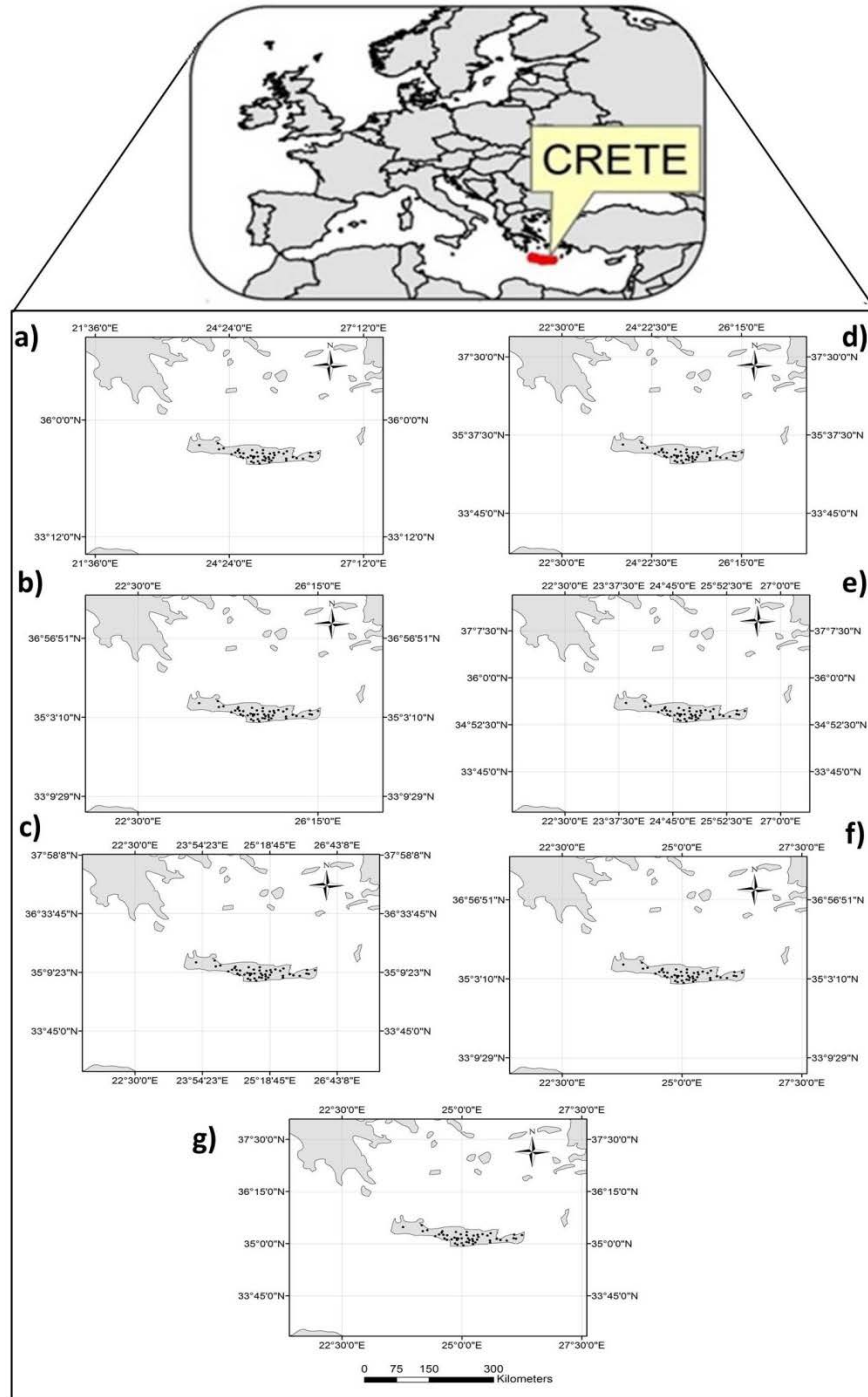


**Figure 4-1:** The models grids and 50 stations over Crete a)  $2.8^{\circ} \times 2.8^{\circ}$ : BCC-CSM1, CanEsm2, MIROC-ESM, MIROC-ESM-CHEM, FGOALS-g2, BNU-ESM, b)  $3.75^{\circ} \times 1.89474^{\circ}$ : IPSL-CM5A-LR c)  $1.40625^{\circ} \times 1.40625^{\circ}$ : MIROC5, d)  $1.875^{\circ} \times 1.875^{\circ}$ : MPI-ESM-LR, MPI-ESM-MR, e)  $1.125^{\circ} \times 1.125^{\circ}$ : MRI-CGCM3, f)  $2.5^{\circ} \times 1.89474^{\circ}$ : NorESM1-M, g)  $2.5^{\circ} \times 1.26^{\circ}$ : IPSL-CM5A-MR.

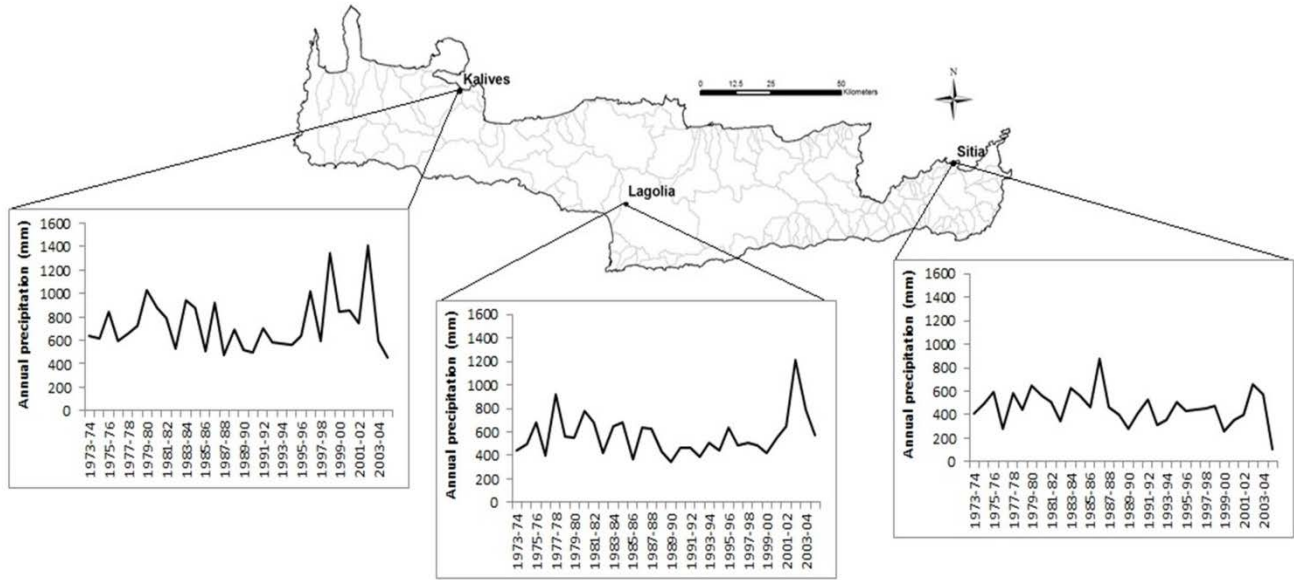


**Figure 4-2:** Observed mean annual precipitation of three representative stations over Crete for the period 1973-2005.

Simulated precipitation and temperature data were provided from 13 GCMs for the period 1973-2099, including 7 different grids and the number of vertical layers concerning both the atmospheric and oceanic component (**Table 4-2**).

*Table 4-2: Origin and grid size of GCMs used (Zunz et al., 2012).*

Model Name	Modeling Center/Institute	Grid size	Vertical layers	
			Atmospheric component	Oceanic component
<b>BCC-CSM1</b>	Beijing Climate Center, China Meteorological Administration	2.8° x 2.8°	26	40
<b>MPI-ESM-LR</b>	Max Planck Institute for Meteorology	1.875° x 1.875°	47	40
<b>MPI-ESM-MR</b>	Max Planck Institute for Meteorology	1.875° x 1.875°	95	40
<b>IPSL-CM5A-LR</b>	Institut Pierre-Simon Laplace	3.75° x 1.89474°	39	31
<b>IPSL-CM5A-MR</b>	Institut Pierre-Simon Laplace	2.5° x 1.26°	39	31
<b>MIROC-ESM</b>	Japan Agency for Marine-Earth Science and Technology, Atmosphere and Ocean Research Institute (The University of Tokyo), and National Institute for Environmental Studies	2.8° x 2.8°	80	44
<b>MIROC-ESM-CHEM</b>	Japan Agency for Marine-Earth Science and Technology, Atmosphere and Ocean Research Institute (The University of Tokyo), and National Institute for Environmental Studies	2.8° x 2.8°	80	44
<b>MIROC5</b>	Atmosphere and Ocean Research Institute (The University of Tokyo), National Institute for Environmental Studies, and Japan Agency for Marine-Earth Science and Technology	1.40625° x 1.40625°	40	49
<b>MRI-CGCM3</b>	Meteorological Research Institute, Japan	1.125° x 1.125°	48	51
<b>NorESM1-M</b>	Norwegian Climate Center	2.5° x 1.89474°	26	53
<b>FGOALS-g2</b>	LASG, Institute of Atmospheric Physics, Chinese Academy of Sciences and CESS, Tsinghua University	2.8° x 2.8°	26	30
<b>BNU-ESM</b>	College of Global Change and Earth System Science, Beijing Normal University	2.8° x 2.8°	26	50
<b>CanESM2</b>	Canadian Centre for Climate Modeling and Analysis	2.8° x 2.8°	35	40

Given the coordinates of the stations and the different grids, the GCM outputs were interpolated in order to get the GCM precipitation at each station location by using the Nearest Neighbor Interpolation (NN) (Gutin et al., 2002). The NN method was selected among the various interpolation methods that are offered in the literature for a number of reasons (Sluiter, 2009). The major reason is that we intended to preserve the original climate signal of the GCMs even though the large grid spacing. By involving more GCM grid cell data on the interpolation procedure (as in Inverse Distance Weighting – IDW) may result to significant information dilution, or signal cancellation between two or more grid cell data from GCM outputs. The GCMs data were corrected for biases using the observed precipitation data of Prefecture of Crete (**Figure 4-3**). A representative station (Kalives, RCP4.5) was used to show the level of association between raw and bias corrected data. It is reasonable to assume that GCMs overestimate precipitation data.

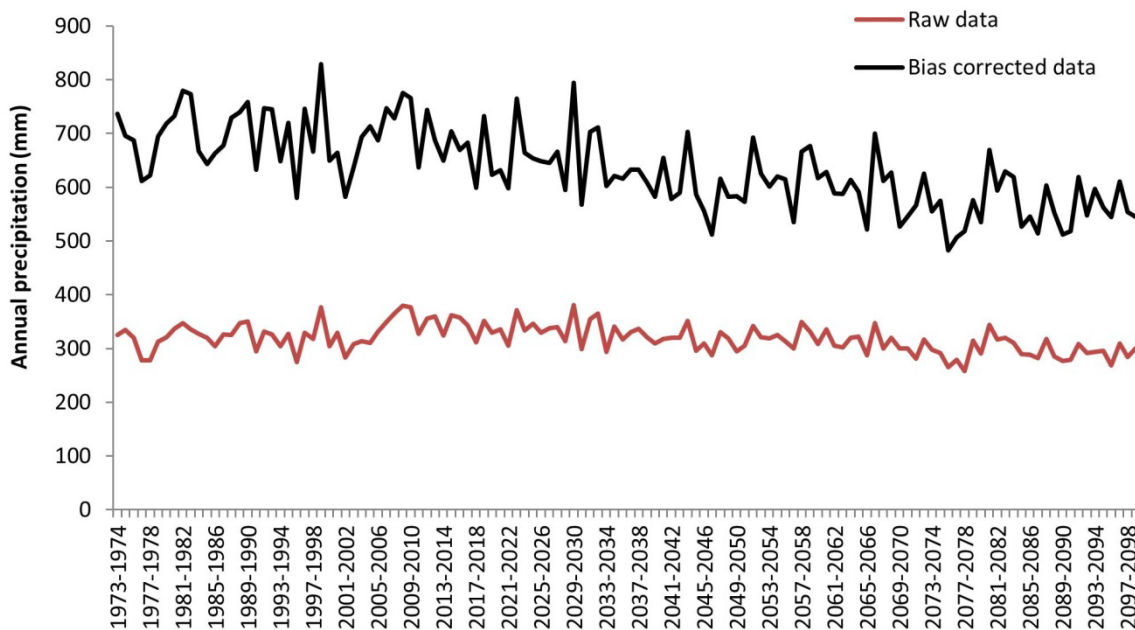


**Figure 4-3:** a) Raw precipitation data versus bias corrected time series for a representative station (Kalives) for RCP4.5.

### 4.3 Results and discussion

The monthly global precipitation and temperature output of 13 GCMs, between 1973 and 2099 for all scenarios is presented as an ensemble of annual averages in **Figure 4-4**. It is obvious that annual precipitation over Crete follows a negative trend, especially when applying RCP8.5; the last 34-year period (2065-2099) the average precipitation will decrease by 6%, 17% and 26% concerning RCP2.6, 4.5 and 8.5 respectively. Temperature analysis revealed that it will increase by 1, 2 and 3°C up to 2099 for RCP2.6, 4.5 and 8.5 respectively.

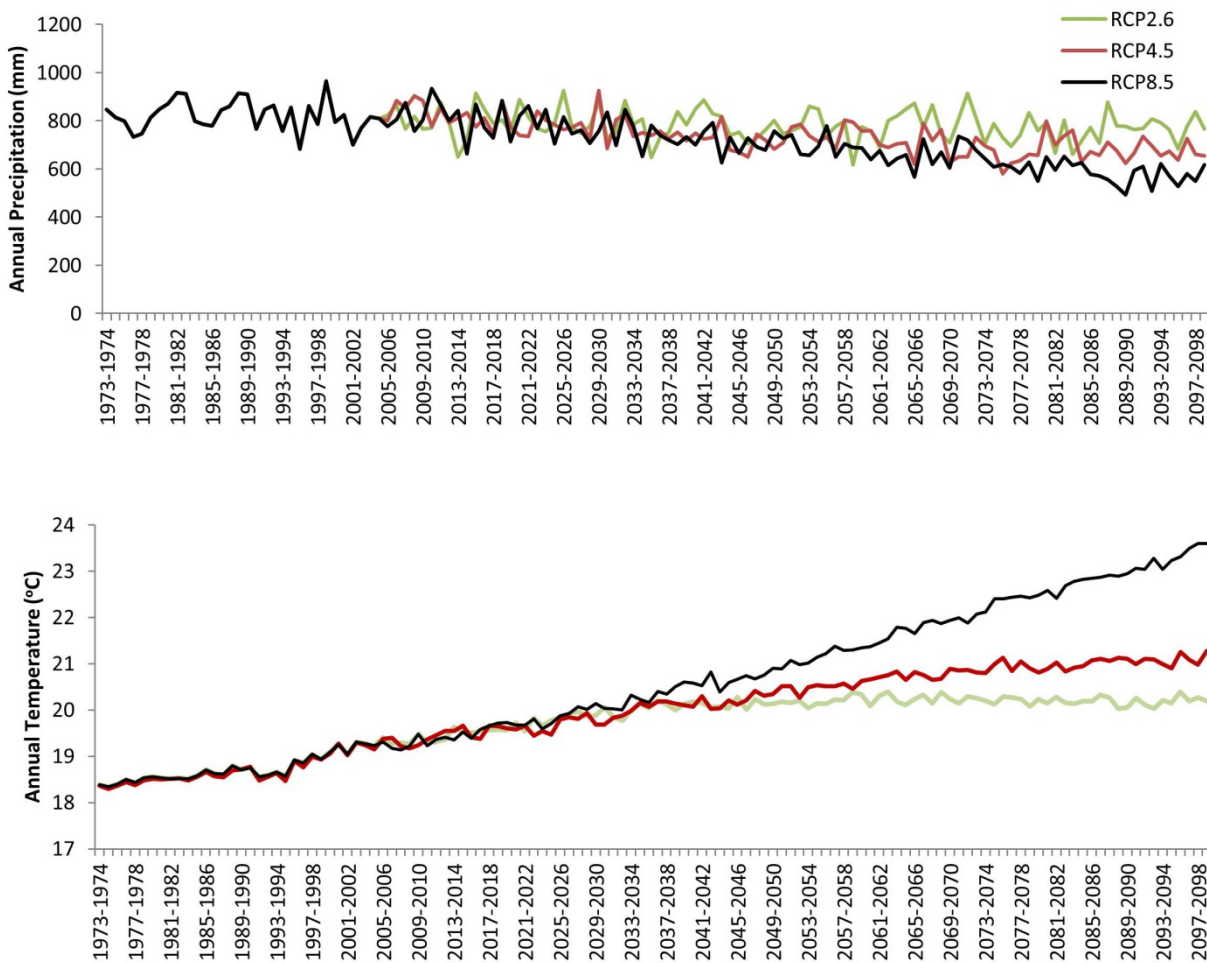


**Figure 4-4:** Ensemble of annual precipitation and temperature of all GCMs and scenarios for Crete.

A presentation of precipitation and temperature trends of RCP4.5 with maximum and minimum time series, including 95% upper and lower confidence limits, is shown in **Figure 4-5**. In order

to get a better insight on the spatial distribution and evolution of precipitation, three representative stations were chosen across the island.

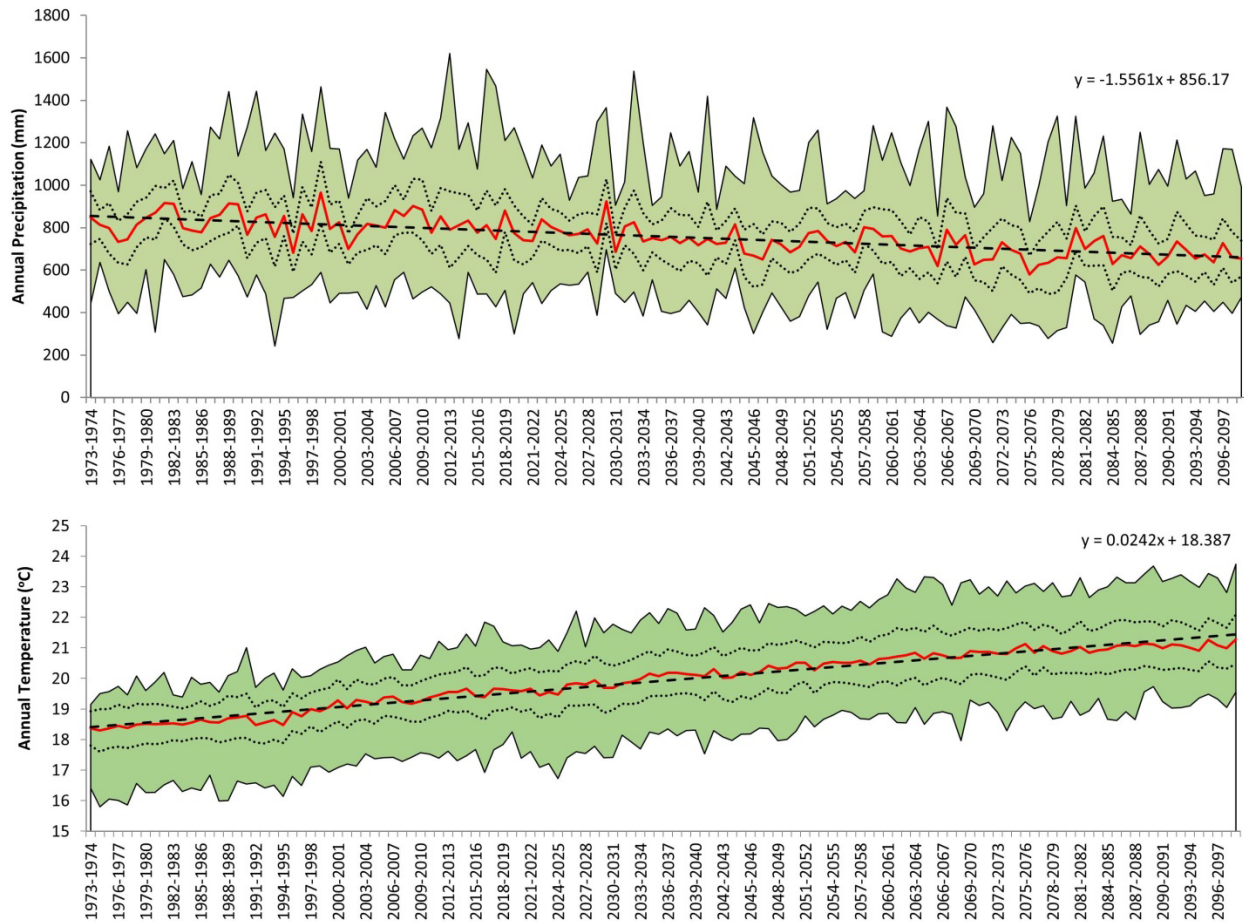


**Figure 4-5:** Red lines represent the ensemble of average annual precipitation and temperature of all GCMs for Crete concerning RCP4.5, including 95% confidence limits. The dashed lines represent the annual ensemble precipitation and temperature trends. The green area represents the amplitude of the annual precipitation and temperature (min and max) in terms of the GCMs.

As for RCP2.6, during the upcoming 2005-2035 period, less mean precipitation is expected (2%, 3% and 3% for Kalives, Lagolia and Sitia respectively), while during the next two time periods of 2035-2065 and 2065-2099, the average precipitation will decrease by 6% and 7% respectively (**Figure 4-6**). RCP4.5 indicated a more significant precipitation decrease (2% and 3% and 3% for Kalives, Lagolia and Sitia respectively) reaching 20% for Sitia station concerning the last future period. The projections denoted the most critical precipitation decrease when analyzing RCP8.5; there is a 5% of decrease during the 2005-2035 period, whereas a continuous decrease takes

place during the next period reaching 15%, 15% and 18%. The last period is characterized as the driest with a precipitation decrease of 29%, 26% and 30% respectively (**Figure 4-6**).

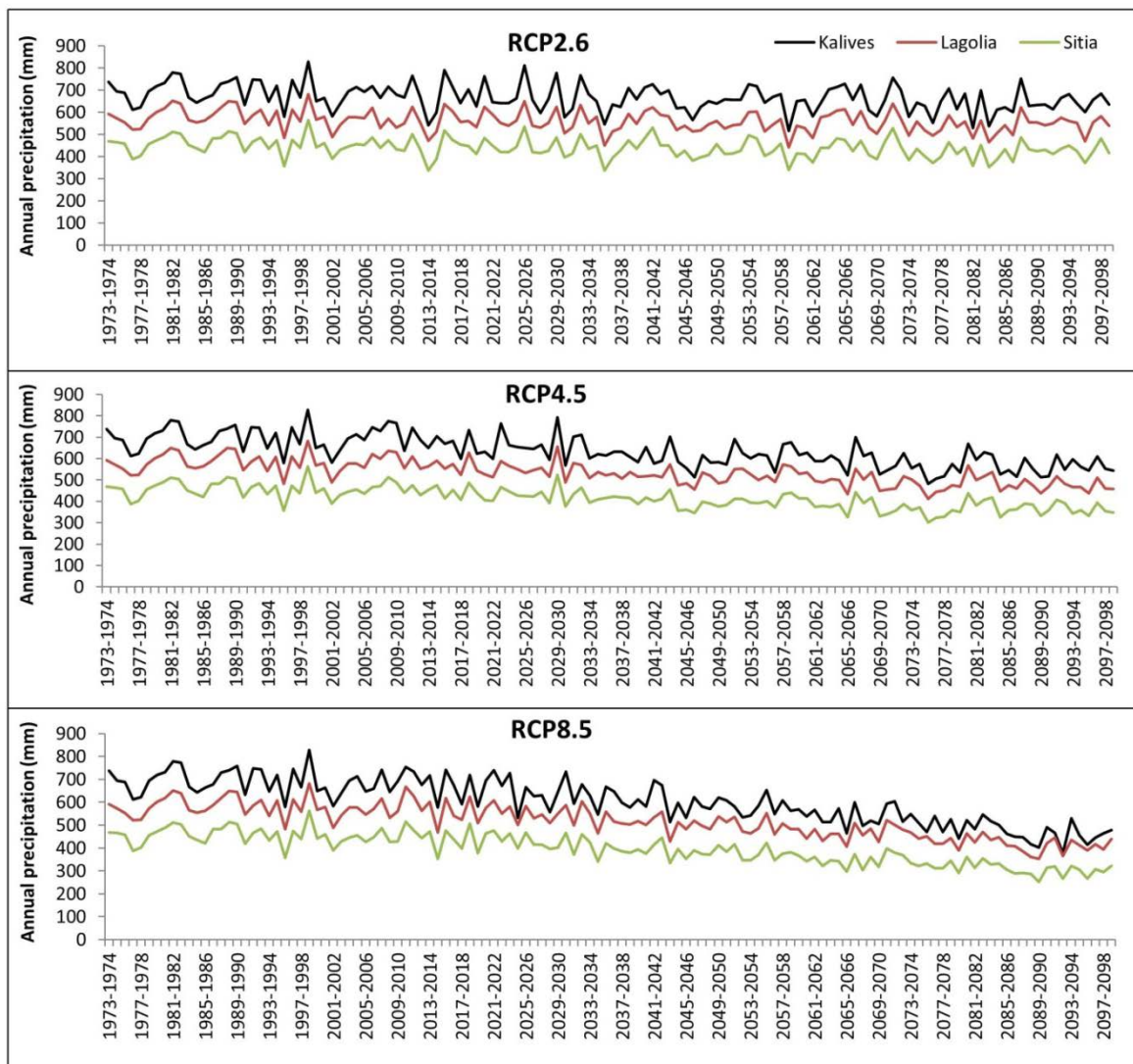


**Figure 4-6:** Ensemble of annual precipitation for 3 representative stations for all scenarios.

Following the precipitation analysis, drought scenarios were formulated by adopting the corresponding precipitation data of the thirteen GCMs. 48-month time scale values of SN-SPI were calculated for 50 stations, in order to provide an overview of prolonged drought occurrences for the periods 1973-2005, 2005-2035, 2035-2065 and 2065-2099, taking into account the scenarios RCP2.6, RCP4.5 and RCP8.5. According to the SN-SPI classification scale, the stations were then classified in terms of severely and extremely dry conditions (SN-

SPI<-1.5) as an average time percentage, which was defined as the temporal part of extreme dryness out of each 30-year period under study.

The model ensemble of the time percentages of the models of severe and extreme droughts for each station was adopted in order to present an overall picture of drought duration both spatially and temporally. The time percentage of severe and extreme droughts for the period 2065-2099 for all scenarios is illustrated in **Figure 4-7**. According to our expectations, RCP2.6 scenario represents milder conditions in comparison with RCP4.5 and the RCP8.5 indicates the most intense drought conditions in terms of duration; 28% of the stations suffer from severe and extreme drought conditions for up to 32% of time, while the same duration was a result for RCP2.6 and 4.5 for 2 % and 16% of the stations respectively.

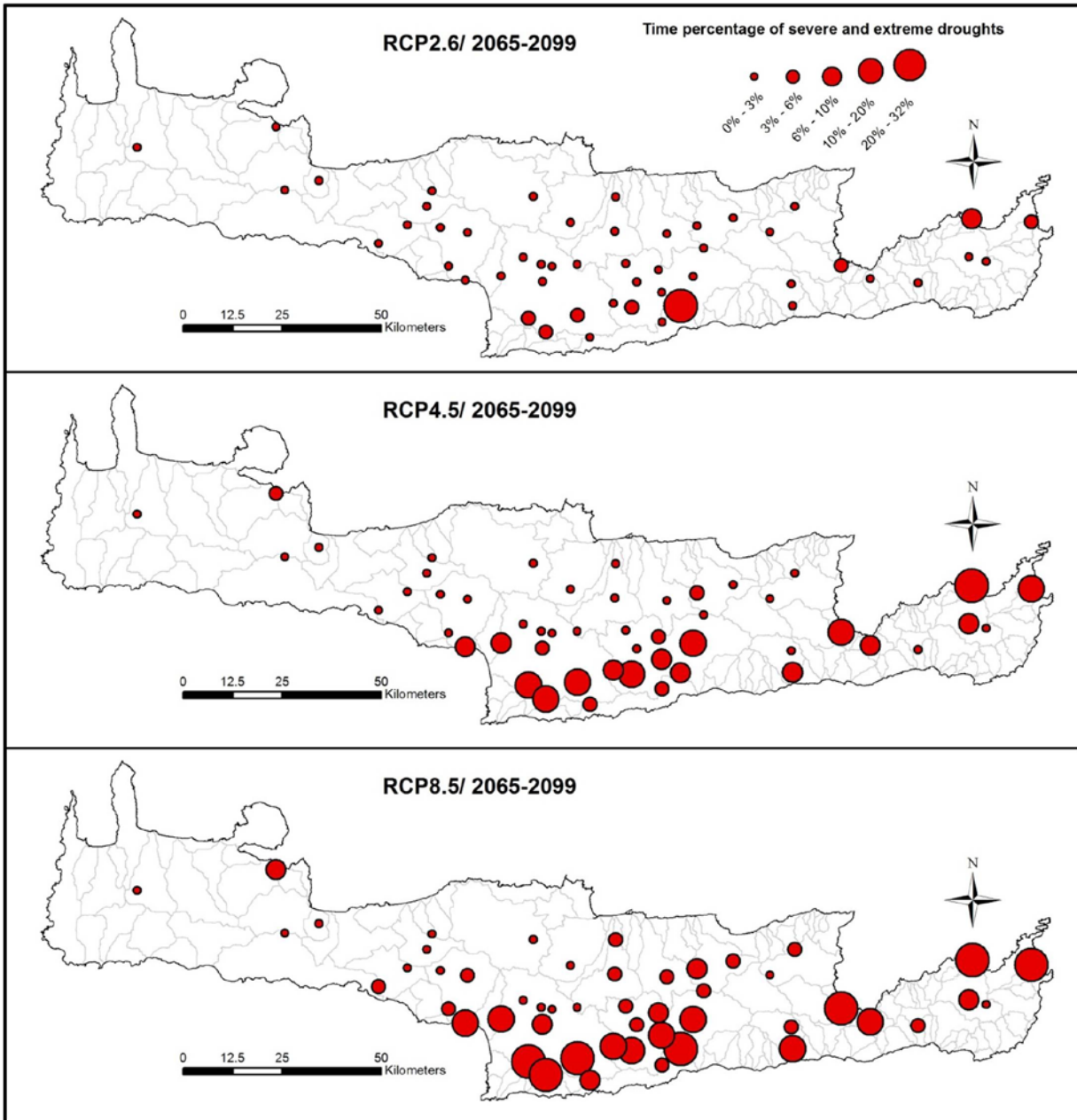


**Figure 4-7:** Time percentage of severe and extreme droughts for all RCPs during 2065-2099 period.

Upon examining the temporal evolution of drought duration just for RCP4.5, it was found that the past period is mostly characterized by a 3% of time extreme drought duration (**Figure 4-8**). Passing to the next period, just a station is under drought conditions for up to 10% of time.

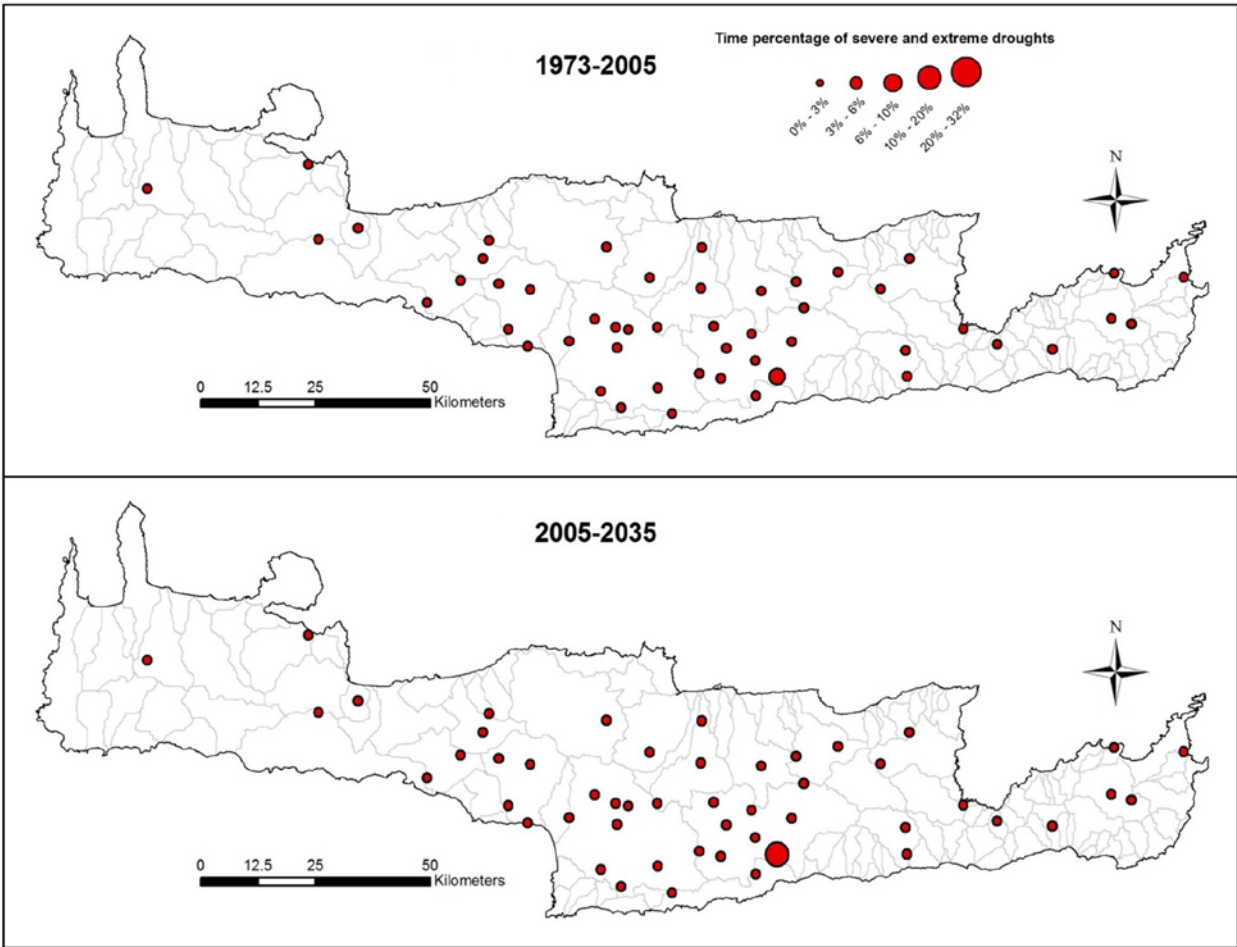


**Figure 4-8:** Time percentage of severe and extreme droughts for RCP4.5 during 1973-2005 and 2005-2035 periods.

Visual comparison of stations under RCP4.5 displayed in **Figure 4-9** shows a clear tendency towards greater drought conditions in the southern and eastern part from one period to the next. As a matter of fact, during the period 2035-2065, 18% of stations undergo extreme droughts for 6% of time against the last period during which drought phenomena are getting intensified as mentioned before.

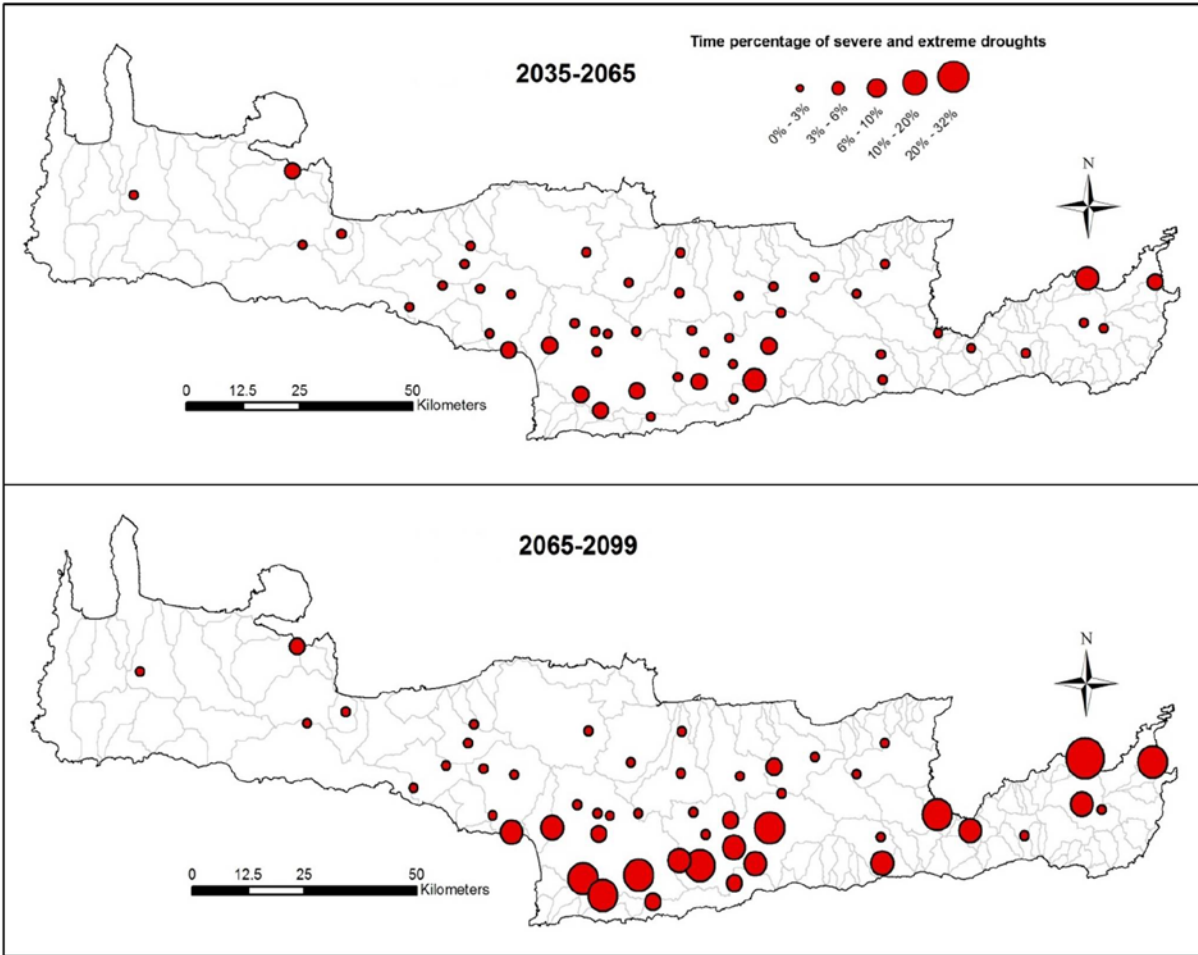


**Figure 4-9:** Time percentage of severe and extreme droughts for RCP4.5 during 2035-2065 and 2065-2099 periods.

The SN-SPI for Kalives, Lagolia and Sitia is presented for all scenarios regarding the period 1973-2099 (**Figure 4-10**). It is important to note that the SN-SPI plots followed the corresponding precipitation patterns as presented in **Figure 4-6**. As for the first plot, moderate dryness with various fluctuations is observed till 2035; a fluctuated pattern including five periods of extreme drought conditions characterize the period 2035-2099 with a greater intensity in Sitia. In SN-SPI plots for RCP4.5, a moderate drought is observed in 2047-2055 and is followed by a 30-year drought occurrence interrupted in 2083. As expected, RCP8.5 offers a picture of a continuous drought development after 2060; extreme drought spells will be recorded in Lagolia and Sitia after 2090.

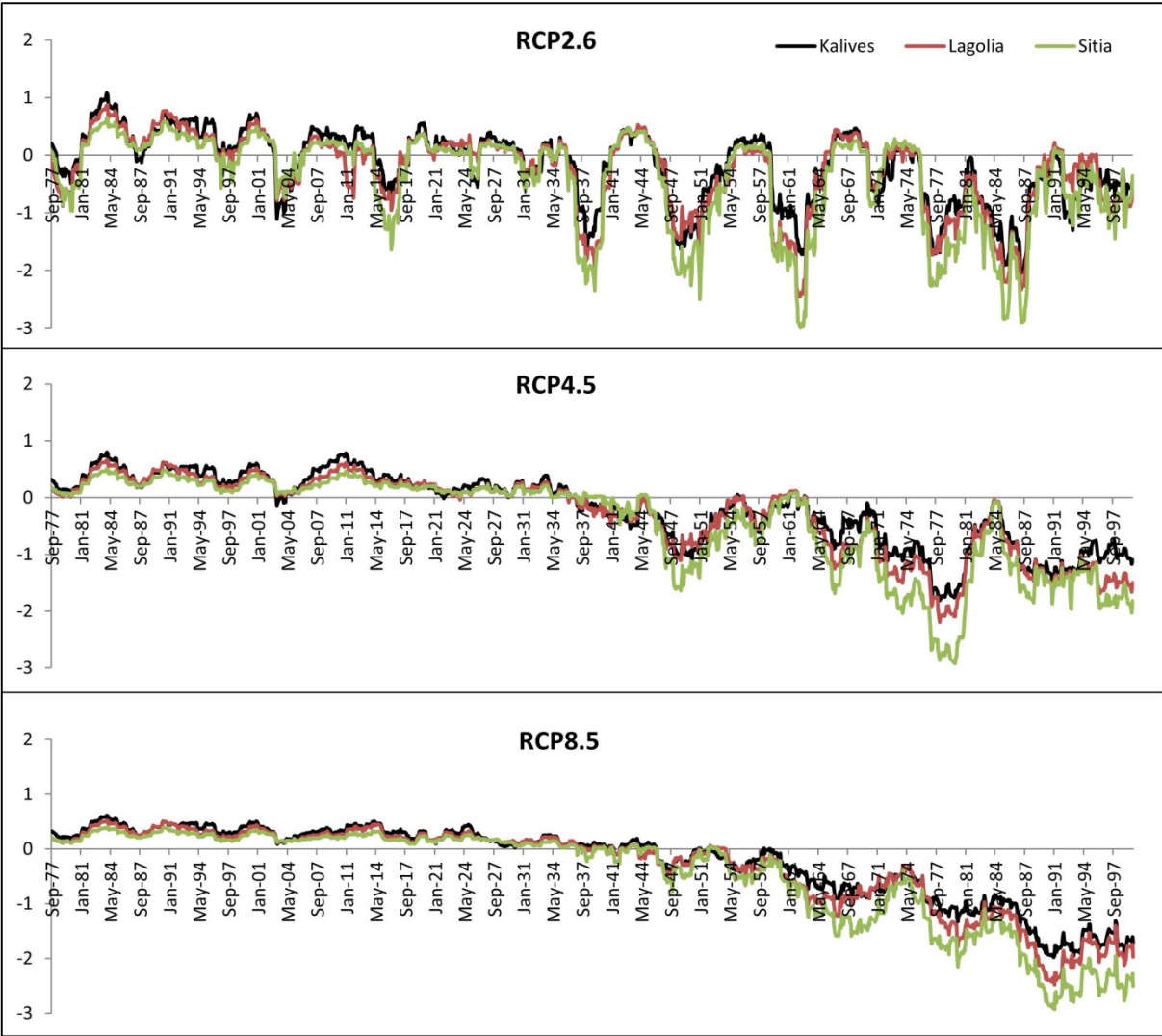


**Figure 4-10:** SN-SPI for three representative stations concerning all RCPs during the period 1973-2099.

Passing from a RCP to another, it is worth mentioning that there is a 10-year shift on the beginning of extreme drought events and the wet conditions become even milder. Furthermore, the period 1973-2035 as mildly wet is apparently juxtaposed with the extreme drought occurrence of the period 2035-2099. Regarding the last future period, one can deduce that drought phenomena become more intense, as mean precipitation is projected to decrease, whereas wet conditions are completely absent. There is clear indication of a spatial drought variation from the west to the east, thereby characterized the eastern part as the most vulnerable area in drought events.

## 5. Conclusions and recommendations for future research

---

### 5.1 Conclusions

#### *Precipitation distribution impacts on droughts*

Results of spatio-temporal precipitation analysis for the period 1974–2005 for the island of Crete revealed valuable information within the context of drought occurrence. A positive rate between precipitation and elevation comprises a fact, whereas a negative correlation lies between precipitation and longitude. It is then deduced that amongst many topographic and geographic factors, elevation and longitude strongly determine the spatial association in precipitation variations. The multiple linear regression method has been used to develop correlations to estimate the spatial distribution of orographic precipitation for complex territory such as that of the island of Crete in Greece using the parameters of elevation and longitude. The two-variable model is more reliable and realistic, especially when dealing with a relatively small number of rain gauges. The coefficient of determination  $R^2$  is lower when the one-variable model is used, whereas  $R^2$  is higher for precipitation when both dependent variables, e.g. elevation and longitude are used. Spatially, it was obvious that precipitation is of orographic type (precipitation is strongly correlated with elevation).

The SN-SPI was selected for the drought assessment as a variant of the common tool of drought assessment SPI, but represents a more suitable means of comparing drought conditions between neighboring areas of differing precipitation heights because the SN-SPI expands the meaning of the temporal character of drought to its spatial relativity. It appears that these new drought index

values are reasonably comparable in their local significance both in space and time, in contrast with SPI. The proposed methodology can evaluate the precipitation deficit and thus can become a practical tool for the assessment of regional drought events. Accordingly, the SN-SPI was successfully evaluated in 6 representative stations in the island of Crete the period 1974 – 2005. The SN-SPI analysis revealed that Crete has faced a main drought period across the whole island and an additional drought period at the southern and eastern parts. The additional drought period at the southern and eastern part is then justified by the combination of the regional atmospheric patterns and the morphological variability among different parts of the island. Cluster analysis confirmed the negative correlation between drought events and elevation, a fact that unifies the precipitation impact assessment on droughts. The selected clustering method proved to be effective, giving the opportunity to perform multiple runs until the optimum cluster set is achieved.

The statistical tools that were used proved to be very effective in the evaluation of the spatio-temporal variability of precipitation and accordingly of drought in the island of Crete. The combination of multiple methods, such as multiple linear regression, cluster and SN-SPI analysis offers a complete study that could be used in the context of climate change impact assessments.

Finally, the results signal an urgent need for the development of strategic water management and preparedness plans in all drought-prone areas in order to help mitigate most of the effects. Water resources could be seriously affected by shorter rainy periods, with wide-ranging consequences for local human societies and ecosystems. The impact of these precipitation changes at station level is required in order to develop strategies in long-term water supply and demand, and thus to attain sustainable water resources management. A specific policy framework on droughts is provided by the EU Water Framework Directive, which in combination with the presented methodology, could be used for assessing the impact of climate change on water resources and, hence, developing strategies dealing with the predictability of the phenomenon.

#### *The impact of hydrometeorological parameters on droughts*

The results obtained from this study show that significant changes in hydrological parameters are expected in Platis basin. The production of simulated flow, soil moisture and lower groundwater reservoir volume for the period 1974-2100 through the input of temperature and precipitation of

the observed and WFD datasets to the HBV model, revealed valuable information within the context of drought occurrence. It was concluded that the simulation with WFD better reproduces the observed flow than the simulated local forcing data. The forcing of the WFD calibrated HBV model with the bias corrected GCM output from 1974 to 2100 for the SRES A2 and B1 future climate-change scenarios, offered significant information for both quantitative and qualitative variable status. Both scenarios exhibit a decrease in precipitation and an increase in temperature average compared to past climate data; comparing to WFD, A2 scenario provides -56% decrease for flow, -34% for soil moisture and -65% for groundwater over 2076-2100, whereas B1 scenario demonstrates a -18% change for flow, -15% for soil moisture and -22% for groundwater.

Apart from the hydrological regime estimation, projections from the three climate models were used for the drought identification with the aid of the threshold level method. It was found that the GCMs results underestimate the number of drought events in comparison with observed dataset results (up to -7% for CNCM, -18% for ECHAM5 and -15% for IPSL) while mean drought duration is overestimated (up to 18% for CNCM, 29% for ECHAM5 and 67% for IPSL).

For A2 scenario, it was found that drought events number increases up to 98%, 109% and 81% for flow, soil moisture and groundwater respectively. B1 scenario provided “milder” conditions, with a drought events number increase of 56%, 92% and 34% in flow, soil moisture and groundwater respectively. The drought duration difference between scenarios reaches up to 33%, 89% and 34% for simulated flow, soil moisture and groundwater respectively till 2100. Changes in drought deficit volume were defined with an estimated maximum increase of 19%, 33% and 22% in flow, soil moisture and groundwater involving A2 scenario, whereas B1 scenario predicted 10%, 2% and 26% maximum increase in the former parameters. The predicted precipitation (30% and 7% decrease for A2 and B1 respectively) and temperature (5.3°C and 3.4°C increase for A2 and B1 respectively) is consistent with the evolution of the hydrological parameters.

The proposed methodology proved to be effective in the evaluation of the parameters variability at basin scale and accordingly of droughts. As shown in this study, the impact of hydrological variable changes in drought propagation can be substantial at a basin scale. The assessment of potential impacts of climate change on water resources and droughts can be carried out via a

framework of resources management national policies. The ensemble results from models forced under multi- climate models results offer a complete picture of probable hydrological trends thereby reviewing and enabling the development of drought management plans. It seems reasonable to assume that large scale forcing data (WFD) can effectively be used for drought analysis at small scale basins. The WATCH Sixth Framework Programme includes the applied data as results that are provided online. Most data of this study (test basin data) was used to enrich the WATCH database. Generally, the study comprises a wide range of predicted changes in important hydrologic parameters, and therefore in drought forecasting, featuring the advantage of modeling approach in assessing climate-change impacts at basin scale.

#### *Drought assessment based on multi-model projections*

Results of precipitation and temperature output of 13 GCMs analysis for the island of Crete between 1973 and 2099 provide a complete picture of climate prediction. The examination of three RCPs showed that the bias corrected annual precipitation follows a negative trend (decrease of 6%, 17% and 26% up to 2099 for RCP2.6, 4.5 and 8.5 respectively) , while temperature will increase (8%, 12% and 21% for RCP2.6, 4.5 and 8.5 respectively). Taking into consideration three representative stations, less mean precipitation (decrease of 7%, 18% and 30%) is expected for Sitia (eastern part) regarding RCP2.6, 4.5 and 8.5.

Apart from the precipitation status estimation, projections were carried out for drought identification through an ensemble of the percentages of the models for each station. The SN-SPI methodology has been used for the drought assessment and successfully evaluated the spatial and temporal character of drought. It was found that the period 2065-2099 will display severe and extreme droughts for 32% of time concerning RCP8.5. The analysis on 3 representative stations revealed that the eastern part suffers significantly from drought events; all scenarios provide the mildest conditions for Kalives, despite the fact that extreme drought events are present in a fluctuated pattern. A continuous drought development with a total absence of wet conditions after 2060 is defined using RCP8.5 for all stations. The SN-SPI proved to be effective in evaluating drought conditions offering a reliable scheme as based on a multimodel dataset; this index enables the spatial comparison between neighboring areas of differing precipitation heights

in terms of drought status and offers an appropriate picture of drought conditions according to the corresponding precipitation patterns of each station.

The models used were shown to skillfully capture past trends, suggesting that they can provide valuable information about the future trends. As shown in this study, the impact of precipitation changes in drought propagation can be meaningful at a spatial and temporal scale. As global climate change is depicted on meteorological variables, it is fundamental to pay attention to their evolution analysis. Therefore, probable precipitation trends from GCM outputs can enable the development of drought management plans and provide an additional clue in climate change investigation.

## **5.2 Recommendations for future research**

The thesis provides a clear overview of the effect of hydrological and meteorological parameters on drought. A useful extension would be to examine the time series of other drought indices and correlate them with the SN-SPI. Furthermore, an analysis of further model results could be assessed with the application of other climatic scenarios. The use of an alternative hydrological model – as the HBV used in this study – might lead to notable findings through comparison.

Future research might be directed at investigating the effects of drought occurrence on crop production and agricultural activities. In agricultural drought, the establishment of a functional relationship between the crop yield, soil moisture deficit and drought, is of paramount importance; a correlation between Crop Moisture Index (Palmer, 1968) and SN-SPI could be developed and might prove to be interesting.

To improve our knowledge about the spatial behavior of droughts, a possible approach would be to use regionalization tools in order to refine climatic information produced by Atmosphere General Circulation Models (AGCMs – Cubasch et al., 1995) as well as to apply other statistical downscaling methods. Moreover, a noteworthy extension of the present thesis could comprise the linkage between drought and desertification with the aid of Desertification Risk Index (DRI – Feoli et al., 2000) and Normalized Difference Vegetation Index (NDVI – Rouse et al., 1973).

It is important to stress the deficiency of rain gauges network on the western part of the island of Crete. Therefore, the densification of rain gauges network will result to a more detailed and complete study in terms of spatial variability providing uniformity in results. It would be also useful to attempt a performance of socio-economical analysis of water availability and demand as well as an evaluation of water balance under specific climatic scenarios and adaption strategies.

# Bibliography

---

- Abramowitz, M., Stegun, I.A., 1965. Handbook of mathematical function. Dover: Editora, 1046.
- Ali, A. and Lebel, T., 2009. The Sahelian standardized rainfall index revisited. *Int. J. Climatol.*, 29, 1705-1714.
- Allamano, P., Claps, P., Laio, F., and Thea, C., 2009. A data-based assessment of the dependence of short-duration precipitation on elevation. *Physics and Chemistry of the Earth*, 34, 635-641.
- American Meteorological Society (AMS), 2004. Statement on meteorological drought. *Bull. Am. Meteorol. Soc.* 85, 771-773.
- Aswathanarayana, U., 2001. *Water Resources Management and the Environment*, Balkema, Rotterdam, The Netherlands.
- Bacanli, U., Dikbas, F., Baran, T., 2008. Drought analysis and a sample study of Aegean Region. Sixth International Conference on Ethics and Environmental Policies, Ethics and Climate Change, Scenarios for Justice and Sustainability. Padova.
- Barry, R.G., and Chorley, R.J., 2003. *Atmosphere, weather, and climate*, eighth ed. Routledge, London, ISBN 0-415-27170-3.
- Basist, A., Bell, G., and Meentmeyer, V., 1994. Statistical relationships between topography and precipitation patterns. *Journal of Climate*, 7, 1305-1315.

- Berdowski, J., Guicherit, R., Heij, B., 2001. *The Climate System*. Balkema Publishers, Rotterdam, the Netherlands.
- Bergström, S., 1995. The HBV model. In: Singh, V.P. (Ed.), *Computer Models of Watershed Hydrology*. Water Resources Publications, Highlands Ranch, CO, USA. ISBN: 0-918334-91-8.
- Bergström, S., Carlsson, B., Grahn, G., Johansson, B., 1997. A More Consistent Approach to Catchment Response in the HBV Model. *Vannet i Norden*, No. 4.
- Blaney, H.F., Criddle, W.D., 1950. Determining Water Requirements in Irrigated Area from Climatological Irrigation Data. US Department of Agriculture, Soil Conservation Service, Tech. Pap. No. 96, 48.
- Bonaccorso, B., Bordi, I., Cancelliere, A., Rossi, G., and Sutera, A., 2003. Spatial Variability of Drought: An Analysis of the SPI in Sicily. *Water Resour. Man.* 17, 273–296.
- Booij, M.J., Tollenaar, D., van Beek, E., Kwadijk, J.C., 2011. Simulating impacts of climate change on river discharges in the Nile basin. *Physics and Chemistry of the Earth, Parts A/B/C* 36 (13), 696-709.
- Boorman, D.B., Sefton, C.E.M., 1997. Recognizing the uncertainty in the quantification of the effects of climate change on hydrological response. *Climatic Change* 35 (4), 415–434.
- Boyer, C., Chaumont, D., Chartier, I., Roy, A.G., 2010. Impact of climate change on the hydrology of St. Lawrence tributaries. *Journal of Hydrology* 384, 65–83.
- Bras, R.L., Rodriguez-Iturbe, I., 1985. *Random Functions and Hydrology*. Addison-Wesley: Reading.
- Brázdil, R., Trnka, M., Dobrovolný, P., Chromá, K., Hlavinka, P., and Žalud, Z., 2008. Variability of droughts in the Czech Republic, 1881–2006. *Theor Appl Climatol.* doi: 10.1007/s00704-008-0065-x.

- Briffa, K. R., Jones, P.D., and Hulme, M., 1994. Summer moisture variability across Europe, 1892-1991: An analysis based on the Palmer Drought Severity Index. *Int. J. Climatol.*, 14, 475-506.
- Chakravarti, I.M., Laha, R.G., Roy, J., 1967. Handbook of methods of applied statistics. Volume 1, John Wiley and Sons, 392-394.
- Chartzoulakis, K. and Psarras, G., 2005. Global change effects on crop photosynthesis and production in Mediterranean: the case of Crete, Greece. *Agriculture, Ecosystems and Environment*, 106, 147–157.
- Chavoshi, S. and Soleiman, W.N.A., 2009. Delineating Pooling Group for Flood Frequency Analysis Using Soft Computing. *European Journal of Scientific Research*, 181-187, 35(2).
- Christensen, J.H., Christensen, O.B., 2003. Climate modeling: severe summertime flooding in Europe. *Nature* 421, 805–806.
- Christensen, J.H., Hewitson, B., Busuioc, A., Chen, A., Gao, X., et al., 2007. Regional climate projections. In: Solomon S, Qin D, Manning M, Chen Z, Marquis M, et al. eds. *Climate Change 2007: The Physical Science Basis. Contribution of Working Group I to the Fourth Assessment Report of the Intergovernmental Panel on Climate Change*. Cambridge and New York: Cambridge University Press.
- Christensen, J.H., Boberg, F., Christensen, O.B., Lucas-Picher, P., 2008. On the need for bias correction of regional climate change projections of temperature and precipitation. *Geophys. Res. Lett.* 35, L20709, doi:10.1029/2008GL035694.
- Cramer, H., Leadbetter, M.R., 1967. *Stationary and Related Stochastic Processes : Sample Function Properties and their Applications*. Wiley, New York.
- Crossman, J., Futter, M.N., Oni, S.K., Whitehead, P.G., Jin, L., Butterfield, D., Baulch, H.M., Dillon, P.J., 2013. Impacts of climate change on hydrology and water quality: Future proofing management strategies in the Lake Simcoe watershed, Canada. *Journal of Great Lakes Research* 39, 19-32.

- Cubasch, U., Waszkewitz, J., Hegerl, G., Perlwitz, J.P., 1995. Regional climate changes as simulated in time-slice experiments. *Climatic Change* 31, 273-304, doi:10.1007/BF01095150.
- Dai, A., Trenberth, K. E., and Karl, T.R., 1998. Global variations in droughts and wet spells: 1900–1995. *Geophys. Res. Lett.*, 25, 3367–3370.
- Dai, A., Trenberth, K. E., and Qian, T., 2004. A global data set of Palmer Drought Severity Index for 1870–2002: relationship with soil moisture and effects of surface warming. *Journal of Hydrometeorology*, 5, 1117–1130.
- Deng, H., Luo, Y., Yao, Y., Liu, C., 2013. Spring and summer precipitation changes from 1880 to 2011 and the future projections from CMIP5 models in the Yangtze River Basin, China. *Quaternary International* 304, 95-106.
- Deque, M., Marquet, P., Jones, R.G., 1998. Simulation of climate change over Europe using a global variable resolution general circulation model. *Clim. Dyn.* 14, 173–189.
- Dessai, S., Van der Sluijs, J.P., 2007. Uncertainty and climate change adaptation: A scoping study. Copernicus Institute for Sustainable Development and Innovation, Utrecht University, Utrecht.
- Dibike, Y.B., Coulibaly, P., 2005. Hydrologic impact of climate change in the Saguenay watershed: comparison of downscaling methods and hydrologic models. *Journal of Hydrology* 307 (1–4), 145–163.
- Dickinson, R.E., Errico, R.M., Giorgi, F., Bates, G.T., 1989. A regional climate model for western United States. *Clim Change* 15, 383–422.
- Dracup, J.A., Lee, K.S., Paulson, E.G., 1980. On the definition of droughts. *Water Resources Research* 16 (2), 297-302.
- Draper, N. R., Smith, H., 1998. *Applied regression analysis*, Wiley, New York.

- Drogue, G., Humbert, J., Deraisme, J., Mahr, N., Freslon, N., 2002. A statistical-topographic model using an omnidirectional parameterization of the relief for mapping orographic rainfall. *Int. J. Climatol.*, 22, 599-613.
- Dubrovský, M., Svoboda, M.D., Trnka, M., Hayes, M.J., Wilhite, D.A., Žalud, Z., Hlavinka, P., 2009. Application of relative drought indices in assessing climate change impacts on drought conditions in Czechia. *Theoretical and Applied Climatology*, 96, 155-171.
- European Environment Agency (EEA), 2012. Climate change, impacts and vulnerability in Europe 2012. An indicator-based report, No 12/2012, Copenhagen, doi:10.2800/66071.
- Feoli, E., Giacomich, P., Mignozzi, K., Ozturk, M., Scimone, M., 2000. The use of GIS and remote sensing in monitoring desertification risk in coastal areas of Turkey. *Proceedings of AGROENVIRON 2000, 2nd International Symposium on New Technologies for Environmental Monitoring and Agro-Application*, 18-20 October, Tekirdag, Turkey.
- Ficklin, D.L., Luo, Y., Luedeling, E., Zhang, M., 2009. Climate change sensitivity assessment of a highly agricultural watershed using SWAT. *Journal of Hydrology* 374, 16–29.
- Fowler, H.J., Blenkinsop, S., Tebaldi, C., 2007. Linking climate change modelling to impacts studies: recent advances in downscaling techniques for hydrological modelling. *Int. J. Climatol.* 27, 1547–1578.
- Fu, T.C., Chung, F.L., Ng, V., Luk, R., 2001. Pattern discovery from stock time series using self-organizing maps. In *Proceedings of the Seventh ACM SIGKDD International Conference on Knowledge Discovery and Data Mining*, San Francisco, CA, 27–37.
- Gibbs, W.J., Maher, J.V., 1967. Rainfall deciles as drought indicators. *Bureau of Meteorology Bulletin no. 48*. Commonwealth of Australia, Melbourne.
- Giorgi, F., 2006. Climate change Hot-spots. *Geophys. Res. Lett.* 33, L08707.
- Giorgi, F., Mearns, L.O., 1991. Approaches to the simulation of regional climate change: A review. *Rev. Geophys.* 29, 191–216.

- Giorgi, F., Mearns, L.O., 1999. Introduction to special section: regional climate modeling revisited. *J. Geophys. Res. (Atmospheres)* 104, 6335–6352, doi:10.1029/98JD02072.
- Giorgi, F., Mearns, L.O., 2002. Calculation of average, uncertainty range, and reliability of regional climate changes from AOGCM simulations via the “reliability ensemble averaging” (REA) method. *J. Climate*. 15, 1141–1158.
- Giorgi, F., Bi, X., Pal, J.S., 2004. Mean interannual variability and trends in a regional climate change experiment over Europe. Part I: present day climate (1961–1990). *Clim. Dyn.* 22, 733–756.
- Giorgi, F., Lionello, P., 2008. Climate change projections for the Mediterranean region. *Global and Planetary Change* 63, 90-104.
- Goodess, C.M., 2013. How is frequency, location and severity of extreme events likely to change up to 2060? *Environmental Science and Policy* 27S, S4-S14.
- Grillakis, M.G., Koutroulis, A.G., Tsanis, I.K., 2011. Climate change impact on the hydrology of Spencer Creek watershed in Southern Ontario, Canada. *Journal of Hydrology* 409, 1–19.
- Grillakis, M.G., Koutroulis, A.G., Tsanis, I.K., 2013. Multisegment statistical bias correction of daily GCM precipitation output. *Journal of Geophysical Research* 118, 1-13.
- Guan, H., Wilson, J., Makhin, O., 2005. Geostatistical mapping of mountain precipitation incorporating autosearched effects of terrain and climatic characteristics. *Journal of Hydrometeorology*, 6, 1018–1030.
- Gutin, G., Yeo, A., Zverovich, A., 2002. Traveling salesman should not be greedy: domination analysis of greedy-type heuristics for the TSP. *Discrete Applied Mathematics* 117, 81-86.
- Guttman, N.B., 1998. Comparing the Palmer Drought Index and the Standardized Precipitation Index. *J. Amer. Water Resour. Assoc.*, 34, 113-121.

- Haerter, J.O., Hagemann, S., Moseley, C., Piani, C., 2011. Climate model bias correction and the role of timescales. *Hydrol. Earth Syst. Sci.*, 15, 1065-1079, doi:10.5194/hess-15-1065-2011.
- Hagemann, S., Arpe, K., Bengtsson, L., 2005. Validation of the hydrological cycle of ERA-40. ERA-40 Project Rep. Ser. no. 24. ECMWF (available at: [www.ecmwf.int/publications/library/do/reference/list/192](http://www.ecmwf.int/publications/library/do/reference/list/192)).
- Harris, D., Menabde, M., Seed, A., Austin, G., 1996. Multifractal characterization of rain fields with a strong orographic influence. *Journal of Geophysical Research*, 101, 26405–26414.
- Hayward, D., Clarke, R.T., 1996. Relationship between rainfall, altitude and distance from the sea in the Freetown Peninsula, Sierra Leone. *Hydrological Sciences*, 41(3), 377-384.
- Heim, Jr. R.R., 2002. A review of twentieth-century drought indices used in the United States. *Bull. Am. Meteor. Soc.*, 83 (8), 1149–1165.
- Hisdal, H., Tallaksen, L.M., 2000. Drought event definition, ARIDE Technical Report No. 6, University of Oslo, Oslo, Norway.
- Hourdin, F., Musat, I., Bony, S., Braconnot, P., Codron, F., Dufresne, J.L., Fairhead, L., Filiberti, M. A., Friedlingstein, P., Grandpeix, J.Y., Krinner, G., LeVan, P., Li, Z.X., Lott, F., 2006. The LMDZ4 general circulation model: Climate performance and sensitivity to parametrized physics with emphasis on tropical convection. *Climate Dyn.* 27, 787–813. doi: 10.1007/s00382-006-0158-0.
- Intergovernmental Panel on Climate Change, (IPCC), *Climate Change*, 2001. The Scientific Basis. Cambridge: Cambridge University Press.
- Intergovernmental Panel on Climate Change, (IPCC) *Climate Change*, 2007. The physical science basis, contribution of working group I to the fourth assessment report of the intergovernmental panel on climate change. Synthesis report, Cambridge: Cambridge University Press.

- Jacob, D., Barring, O.B., Christensen, J.H., Christensen, M., De Castro, M., Deque, M, Giorgi, F., Hagemann, S., Lenderink, G., Rockel, E., Sanchez, E., Schar, C., Seneviratne, S.I., Somot, S., van Ulden, A., van der Hurk, B., 2007. An inter-comparison of regional climate models for Europe: model performance in present-day climate. *Climatic Change* 81, 31-52.
- Jevrejeva, S., Moore, J.C., Grinsted, A., 2012. Sea level projections to AD2500 with a new generation of climate change scenarios. *Global and Planetary Change* 80-81, 14-20.
- Jiang, T., Su, B., Hartmann, H., 2007. Temporal and spatial trends of precipitation and river flow in the Yangtze River Basin, 1961–2000. *Geomorphology* 85, 143–154.
- Kalpakis, K., Gada, D., Puttagunta, V., 2001. Distance measures for effective clustering of ARIMA time series. In *Proceedings of the 2001 IEEE International Conference on Data Mining, San Jose, CA*, 273–280.
- Kaufman, L., Rousseuw, P.J., 1990. *Finding groups in data: An introduction to cluster analysis*. New York: John Wiley and Sons, Inc.
- Kerkhoven, E., Gan, T.Y., 2011. Unconditional uncertainties of historical and simulated river flows subjected to climate change. *Journal of Hydrology* 396 (1–2), 113–127. doi: 10.1016/j.jhydrol.2010.10.042.
- Keyantash, J.A., Dracup, J.A., 2004. An Aggregate Drought Index: Assessing drought severity based on fluctuations in the hydrologic cycle and surface water storage. *Water Resources Res.* 40, W09304.
- Kim, J., Choi, J., Choi, C., Park, S., 2013. Impacts of changes in climate and land use/land cover under IPCC RCP scenarios on streamflow in the Hoeya River Basin, Korea. *Science of the Total Environment* 452-453, 181, 195.
- Kirono, D.G.C., Kent, D.M., Hennessy, K.J., Mpelasoka, F., 2011. Characteristics of Australian droughts under enhanced greenhouse conditions: Results from 14 global climate models. *Journal of Arid Environments* 75, 566-575.

- Koutroulis, A.G., Vrochidou, A.-E.K., Tsanis, I.K., 2011. Spatiotemporal characteristics of meteorological drought for the island of Crete. *Journal of Hydrometeorology* 12 (2), 206-226, doi:10.1175/2010JHM1252.1.
- Koutroulis, A.G, Tsanis, I.K, Daliakopoulos, I.N., 2010. Seasonality of floods and their hydrometeorologic characteristics in the island of Crete. *Journal of Hydrology*. doi:10.1016/j.jhydrol.2010.04.025.
- Krause, P., Boyle, D.P., Base, F., 2005. Comparison of different efficiency criteria for hydrological model assessment. *Advances in Geosciences* 5, 89-97.
- Kysely, J., Beguería, S., Beranová, R., Gaál, L., López-Moreno, J.-I., 2012. Different patterns of climate change scenarios for short-term and multi-day precipitation extremes in the Mediterranean. *Global and Planetary Change* 98-99, 63-72.
- Lindström, G., Johansson, B., Persson, M., Gardelin, M., Bergström, S., 1997. Development and test of the distributed HBV-96 hydrological model. *Journal of Hydrology* 201, 272–288.
- Livada, I., Assimakopoulos, V.D., 2007. Spatial and temporal analysis of drought in Greece using the Standardized Precipitation Index (SPI). *Theor. Appl. Climatol.* 89, 143-153.
- Lettenmaier, D.P., McCabe, G., Stakhiv, E.Z., 1996. Global climate change: effects on hydrologic cycle, L.W. Mays, Editor, *Water Resources Handbook, Part V*, McGraw-Hill, New York.
- Lloyd-Hughes, B., Saunders, M., 2002. A drought climatology for Europe. *Int. J. Climatol.*, 22, 1571–1592.
- Loukas, A., Vasiliades, L., 2004. Probabilistic analysis of drought spatiotemporal characteristics in Thessaly region, Greece. *Natural Hazards and Earth System Sciences*, 4: 719–731, 2004.
- Loukas, A., Vasiliades, L., Tzabiras, J., 2007. Evaluation of climate change on drought impulses in Thessaly, Greece. *European Water* 17/18, 17-28.

- Love, D., Uhlenbrook, S., van der Zaag, P., 2011. Regionalising a meso-catchment scale conceptual model for river basin management in the semi-arid environment. *Physics and Chemistry of the Earth, Parts A/B/C* 36 (14-15), 747-760.
- Manios, T., Tsanis, I., 2006. Evaluating water resources availability and wastewater reuse importance in the water resources management of small Mediterranean municipal districts. *Resources, Conservation and Recycling* 47, 245–259.
- Matondo, J.I., Peter, G., Msibi, K.M., 2004. Evaluation of the impact of climate change on hydrology and water resources in Swaziland: Part II. *Physics and Chemistry of the Earth* 29, 1193–1202.
- McGregor, J.L., 1997. Regional climate modelling. *Meteorol. Atmos. Phys.* 63, 105–117.
- McKee, T., Doesken, N., Kleist, J., 1993. The relationship of drought frequency and duration to time scales. In *Proceedings of the 8<sup>th</sup> Conference on Applied Climatology*, Boston, Am. Met. Soc., 179–184.
- McMahon, T.A., Peel, M.C., Lowe, L., Srikanthan, R., McVicar, T.R., 2012. Estimating actual, potential, reference crop and pan evaporation using standard meteorological data: a pragmatic synthesis. *Hydrol. Earth Syst. Sci. Discuss.* 9, 11829-11910, doi:10.5194/hessd-9-11829-2012.
- McQueen, J.B., 1967. Some Methods for classification and Analysis of Multivariate Observations. In *Proceedings of the 5<sup>th</sup> Berkeley Symposium on Mathematical Statistics and Probability*, Berkeley, University of California Press, 1, 281-297.
- Meehl, G.A., Stocker, T.F., Collins, W.D., Friedlingstein, P., Gaye, A.T., et al., 2007. Global climate projections. In: Solomon S, Qin D, Manning M, Chen Z, Marquis M, et al. eds. *Climate Change 2007: The Physical Science Basis. Contribution of Working Group I to the Fourth Assessment Report of the Intergovernmental Panel on Climate Change*. Cambridge and New York: Cambridge University Press.
- Middelkoop, H., Daamen, K., Gellens, D., Grabs, W., Kwadijk, J.C.J., Lang, H., Parmet, B. W.A.H., Schadler, B., Schulla, J., Wilke, K., 2001. Impact of climate change on

- hydrological regimes and water resources management in the Rhine basin. *Climatic Change* 49, 105–128.
- Mishra, A.K., Singh, V.P., 2010. A review of drought concepts. *Journal of Hydrology* 391, 202–216.
- Mohan, S., Arumugam, N., 1995. An intelligent front-end for selecting evapotranspiration estimation methods. *Computers and Electronics in Agriculture* 12, 295–309.
- Monteith, J.L., 1965. Evaporation and environment. *Symposia of the Society for Experimental Biology* 19: 205–224. *Forest Hydrology and Watershed Management – Hydrologie Forestiere et Amenagement des Bassins Hydrologiques (Proceedings of the Vancouver Symposium, August 1987, Actes du Colloque de Vancouver, Aout 1987)*, IAHS-AISH Publ. no. 167, 1987, 319–327.
- Moss et al., 2008. Towards new scenarios for analysis of emissions, climate change, impacts and response strategies. Intergovernmental panel on Climate Change, Geneva.
- Moss et al., 2010. The next generation of scenarios for climate change research and assessment. *Nature* 463 (7282), 747–756.
- Murphy, J.M., Sexton, D.M.H., Barnett, D.N., Jones, G.S., Webb, M.J., Collins, M., Stainforth, D.A., 2004. Quantification of modelling uncertainties in a large ensemble of climate change simulations. *Nature* 430, 768–772.
- Nakićenović, N., Davidson, O., Davis, G., Gróbler, A., Kram, T., Rovere, E., Metz, M., Morita, T., Pepper, W., Pitcher, H., Sankovski, A., Shukla, P., Swart, R., Watson, R., Dadi, Z., 2000. Special Report on Emissions Scenarios. A Special Report of Working Group III of the Intergovernmental Panel on Climate Change. Cambridge University Press, Cambridge, 599.
- Naoum, S., Tsanis, I.K., 2003. Temporal and spatial variation of annual rainfall on the island of Crete, Greece. *Hydrological Processes*, 17(10), 1899–1922.

- Naoum, S., Tsanis, I.K., 2004. Orographic precipitation modeling with multiple linear regression. *Journal of Hydrologic Engineering*, 9(2), 79-102.
- Nash, J.E., Sutcliffe, J.V., 1970. River flow forecasting through conceptual models. *Journal of Hydrology* 10, 282–290.
- Normand, S., Konz, M., Merz, J., 2010. An application of the HBV model to the Tamor Basin in Eastern Nepal. *Journal of Hydrology and Meteorology* 7 (1), 49-58.
- Oates, T., Firoiu, L., Cohen, P.R., 1999. Clustering time series with Hidden Markov Models and Dynamic Time Warping. In *Proceedings of IJCAI-99 Workshop on Neural, Symbolic and Reinforcement Learning Methods for Sequence Learning*, Stockholm, Sweden, 17–21.
- Oosterwijk, J., van Loon, A.F., Machlica, A, Horvat, O., van Lanen, H.A.J., Fendekova, M., 2009. Hydrological drought characteristics of the Nedožery sub catchment, Upper Nitra, Slovakia, based on HBV modeling. WATCH Project, Technical Report No. 20.
- Ouyang, R., Ren, L., Cheng, W., Zhou, C., 2010. Similarity search and pattern discovery in hydrological time series data mining. *Hydrological Processes*, 24, 1198-1210.
- Palmer, W.C., 1965. Meteorological drought. Research Paper No 45, US Weather Bureau, Washington, DC.
- Palmer, W.C., 1968. Keeping track of crop moisture conditions, nationwide: The new Crop Moisture Index. *Weatherwise* 21: 156-161.
- Panu, U.S., Sharma, T.C., 2002. Challenges in drought research: some perspectives and future directions. Special Issue: Towards Integrated Water Resources Management for Sustainable Development, *Hydrological Sciences - Journal des Sciences Hydrologiques* 47(S), 19-30.
- Parry, M.L., Rosenzweig, C., Iglesias, A., Livermore, M., Fischer, G., 2004. Effects of climate change on global food production under SRES emissions and socio-economic scenarios. *Global Environmental Change* 14 (1), 53–67.

- Pavlakis, P., 2004. Hydrological study of Platis basin. Organisation for the development of Western Crete.
- Pereira, A.R., Pruitt, W.O., 2004. Adaptation of the Thornthwaite scheme for estimating daily reference evapotranspiration. *Agric. Water Manag* 66, 251-257, ISSN: 0378- 3774.
- Peters, E., 2003. Propagation of drought through groundwater systems - Illustrated in the Pang (UK) and Upper-Guadiana (ES) catchments. Ph.D. Dissertation, Wageningen University.
- Peters, E., van Lanen, H.A.J., Torfs, P.J.J.F., Bier, G., 2005. Drought in groundwater - drought distribution and performance indicators. *Journal of Hydrology* 306, 302–317.
- Piani, C., Haerter, J., Coppola, E., 2010. Statistical bias correction for daily precipitation in regional climate models over Europe. *Theoretical and Applied Climatology* 99(1-2), 187-192. doi: 10.1007/s00704-009-0134-9.
- Primožič, M., Kobold, M., Brilly, M., 2008. The implementation of the HBV Model on the Sava River Basin. XXIVth Conference of the Danubian Countries, Earth and Environmental Science. doi: 10.1088/1755-1307/4/1/012004.
- Prudhomme, C., Parry, S., Hannaford, J., Clark, D.B., Hagemann, S., Voss, F., 2011. How well do large-scale models reproduce regional hydrological extremes in Europe? *Journal of Hydrometeorology* 12, 1181-1204. doi: 10.1175/2011JHM1387.1.
- Qi, S., Sun, G., Wang, Y., McNulty, S.G., Moore Myers, J.A., 2009. Streamflow response to climate and landuse changes in a coastal watershed in North Carolina. *Trans ASABE* 52, 739–749.
- Räisänen. J., 2007. How reliable are climate models? *Tellus A* 59, 2–29  
<http://dx.doi.org/10.1111/j.1600-0870.2006.00211.x>.
- Ramirez-Villegas, J., Challinor, A., 2012. Assessing relevant climate data for agricultural applications. *Agricultural and Forest meteorology* 161, 26-45.

- Reihan, A., Kovalenko, O., 2000. Experience of an application of the HBV model for runoff computation in Estonia. Proceedings of the Symposium dedicated to the 40<sup>th</sup> Anniversary of Institute of the Environmental Engineering at Tallinn Technical University, 126-134.
- Region of Crete, 2002. Sustainable management of water resources in Crete. Region of Crete Information Bull., pp. 24 (in Greek).
- Riahi, K., Gumbler, A., Nakicenovic, N., 2007. Scenarios of long-term socio-economic and environmental development under climate stabilization. *Technological Forecasting and Social Change* 74 (7), 887-935.
- Riahi, K., Rao, S., Krey, V., Cho, C., Chirkov, V., Fischer, G., 2011. RCP 8.5 — a scenario of comparatively high greenhouse gas emissions. *Climatic Change* 109, 33–57.
- Rice, S.O., 1954. Mathematical analysis of random noise. In Wax N (ed) *Selected Papers on Noise and Stochastic Processes*, Dover, New York. 133-294.
- Roeckner, E., Bäuml, G., Bonaventura, L., Brokopf, R., Esch, M., Giorgetta, M., Hagemann, S., Kirchner, I., Kornblueh, L., Manzini, E., Rhodin, A., Schlese, U., Schulzweida, U., Tompkins, A., 2003. Max-Planck-Institute for Meteorology, Report No. 349.
- Rossi, G., 2000. Drought mitigation measures: A comprehensive framework. *Drought and Drought Mitigation in Europe*, J. Voght, F. Somma, Eds., Kluwer Academic Publishers, 233–246.
- Rouse, J.W., Haas, R.H., Schell, J.A., Deering, D.W., 1973. Monitoring vegetation systems in the Great Plains with ERTS, *Third ERTS Symposium*, NASA SP-351 I, 309 - 317.
- Royer, J.F., Cariolle, D., Chauvin, F., Déqué, M., Douville, H., Hu, R.M., Planton, S., Rascol, A., Ricard, J.L., Salas-Mélia, D., Sevault, F., Simon, P., Somot, S., Tyteca, S., Terray, L., Valcke, S., 2002. Simulation des changements climatiques au cours du 21-ème siècle incluant l'ozone stratosphérique (Simulation of climate changes during the 21-st century including stratospheric ozone). *C. R. Geoscience* 334, 147-154.

- Rumman, M. A, Hiyasat, M., Sweis, G. J, and Sweis, R.J., 2009. Assessment of droughts in Jordan: The Yarmouk and Zarqa basins. *Management of Environmental Quality*, 20 (6), 696-711.
- Semmler, T., Jacob, D., 2004. Modeling extreme precipitation events — a climate change simulation for Europe. *Glob. Planet. Change* 44, 119–127.
- Shafer, B.A., Dezman, L.E., 1982. Development of a Surface Water Supply Index (SWSI) to assess the severity of drought conditions in snowpack runoff areas. In: *Proceedings of the Western Snow Conference*, Reno (NV), 19-23 April 1982. Colorado State Univ., Fort Collins (CO), pp. 164-175.
- Sharma, D., Das Gupta, A., Babel, M.S., 2007. Spatial disaggregation of bias-corrected GCM precipitation for improved hydrologic simulation: Ping River Basin, Thailand, *Hydrol. Earth Syst. Sci.* 11, 1373–1390, doi:10.5194/hess-11-1373-2007.
- Silberstein, R.P., 2006. Hydrological models are so good, do we still need data? *Environmental Modelling & Software* 21, 1340-1352, doi:10.1016/j.envsoft.2005.04.019.
- Sluiter, R., 2009. Interpolation methods for climate data. Literature review, KNMI report. De Bilt, The Netherlands.
- Smakhtin, V.U., Hughes, D.A., 2007. Automated estimation and analyses of meteorological drought characteristics from monthly rainfall data. *Environmental Modelling and Software* 22, 880-890.
- SMHI, 2006. *Integrated Hydrological Modelling System. Manual Version 5.10.* Swedish Meteorological and Hydrological Institute.
- Soltani, S., Modarres, R., 2006. Classification of Spatio -Temporal Pattern of Rainfall in Iran Using A Hierarchical and Divisive Cluster Analysis. *Journal of Spatial Hydrology* 6(2), 1-12.

- Sönmez, K., Kömüscü, Ü., Erkan, A., Turgu, E., 2005. An analysis of spatial and temporal dimension of drought vulnerability in Turkey using the Standardized Precipitation Index. *Natural Hazards* 35, 243-264. doi: 10.1007/s11069-004-5704-7.
- Sperna Weiland, F.C., van Beek, L.P.H., Weerts, A.H., Bierkens, M.F.P., 2012. Extracting information from an ensemble of GCMs to reliably assess future global runoff change. *Journal of Hydrology* 412-413, 66-75.
- Struyf, A., Hubert, M., Rousseeuw, P.J., 1997. Integrating robust clustering techniques in S-PLUS. *Computational Statistics and Data Analysis*, 26, 17-37.
- Szep, I. J, Mika, J., Dunkel, Z., 2005. Palmer drought severity index as soil moisture indicator: physical interpretation, statistical behavior and relation to global climate. *Physics and Chemistry of the Earth*, 30, 231–243.
- Tallaksen, L.M., Hisdal, H., 1997. Regional analysis of extreme streamflow drought duration and deficit volume. FRIEND '91 - Regional Hydrology: Concepts and Models for Sustainable Water Resource Management, Proceedings of the Postojna, Slovenia, Conference, September-October 1997, IAHS Publ. 246, 141-150.
- Tallaksen, L.M., Hisdal, H., van Lanen, H.A J., 2009. Space-time modeling of catchment scale drought characteristics. *Journal of Hydrology* 375, 363–372.
- Tallaksen, L.M., van Lanen, H.A.J., 2007. Key aspects of low flow and drought. In: *Book of Abstracts, International CHR-Workshop – Expert Consultation, Würzburg, Germany, 25-26 September 2007*, 13-18.
- Tan, P.N., Steinbach, M., Kumar, V., 2006. *Introduction to Data Mining*. Chapter 8. Cluster Analysis: Basic Concepts and Algorithms, Michigan State University and University of Minnesota.
- Taylor, K.E., Stouffer, R.J., Meehl, G.A., 2012. An Overview of CMIP5 and the experiment design. *Bull. Amer. Meteor. Soc.* 93, 485-498, doi:10.1175/BAMS-D-11-00094.1.

- Thom, H.C.S., 1966. Normal degree days above any base by the universal truncation coefficient. *Monthly Weather Review* 94, 461-465.
- Thorntwaite, C. W.: An approach towards a rational classification of climate. *Geogr Rev* 38: 55–94, 1948.
- Tsakiris, G., Vangelis, H., 2004. Towards a Drought Watch System based on spatial SPI. *Water Resour. Man.*, 18, 1–12.
- Tsakiris, G., Vangelis, H., 2005. Establishing a Drought Index incorporating evapotranspiration. *European Water*, 9-10, 3-11.
- Tsakiris, G., Pangalou, D., Tigkas, D., Vangelis, H., 2007. Assessing the areal extent of drought. *Water Resources Management, New Approaches and Technologies*, European Water Resources Association, Chania, Crete-Greece.
- Tsakiris, G., Pangalou, D., Vangelis, H., 2007. Regional drought assessment based on the Reconnaissance Drought Index (RDI). *Water res. Manage.* 21 (5), 821-833.
- Tsanis, I.K., Naoum, S., 2003. The effect of spatially distributed meteorological parameters on irrigation water demand assessment. *Advances in Water Resources*, 26, 311-324.
- Uppala, S.M., Kållberg, P.W., Simmons, A.J., Andrae, U., Da Costa Bechtold, V., et al., 2005. The ERA-40 re-analysis. *Quart. J. Meteo. Soc.* 131, 2961-3012.
- Van der Linden P., Mitchell, J.F.B. (eds.), 2009. *ENSEMBLES: Climate Change and its Impacts: Summary of research and results from the ENSEMBLES project*. Met Office Hadley Centre, FitzRoy Road, Exeter EX1 3PB, UK. 160pp.
- Van Der Schrier, G., Briffa, K. R., Jones, P. D., Osborn, T.J., 2006. Summer moisture variability across Europe. *J. Climate*, 19, 2818–2834.
- Van Lanen, H.A.J., Tallaksen, L.M., 2007. Hydrological drought, climate variability and change. In: Heinonen, M. (Ed.) *Climate and Water. Proc. of the third Int. Conf. on Climate and Water*, Helsinki, Finland, 3-6 September 2007, 488-493.

- Van Vuuren, D.P., Edmonds, J., Thomson, A., Riahi, K., Kainuma, M., Matsui, T., Hurtt, G.C., Lamarque, J.F., Meinshausen, M., Smith, S., 2011. Representative Concentration Pathways: An overview. *Climatic Change* 109 (1), 5-31.
- Varis, O., Kajander, T., Lemmelä, R., 2004. Climate and water: from climate models to water resources management and vice versa. *Climatic Change* 66, 321-344.
- Vicente-Serrano, S.M., Beguería, S., 2003. Estimating extreme dry-spell risk in the middle Ebro valley (Northeastern Spain): a comparative analysis of partial duration series with a General Pareto distribution and annual maxima series with a Gumbel distribution. *Int. J. Climatol.* 23, 1103–1118.
- Vidal, J.-P., Wade, S.D., 2008. Multimodel projections of catchment-scale precipitation regime. *Journal of Hydrology* 353, 143-158.
- Vrochidou, A.-E.K., Tsanis, I.K., 2012. Assessing precipitation distribution impacts on droughts on the island of Crete. *Natural Hazards and Earth System Sciences* 12, 1159-1171.
- Vrochidou, A.-E.K., Tsanis, I.K., Grillakis, M.G., Koutroulis, A.G., 2013. The impact of climate change on hydrometeorological droughts at a basin scale. *Journal of Hydrology* 476, 290-301.
- Wang, Y., Leung, L.R., McGregor, J.L., Lee, D.-K., Wang, W.-C., et al., 2004. Regional climate modelling: Progress, Challenges, and Prospects. *J. Meteorol. Soc. Japan* 82, 1599–1628.
- Wardekker, J.A., 2011. Climate change impact assessment and adaptation under uncertainty. PhD dissertation. Utrecht University, Utrecht.
- Weedon, G.P., Gomes, S., Viterbo, P., Shuttleworth, W.J., Blyth, E., Osterle, H., Adam, J.C., Bellouin, N., Boucher, O., Best, M., 2011. Creation of the WATCH Forcing Data and Its Use to Assess Global and Regional Reference Crop Evaporation over Land during the Twentieth Century. *Journal of Hydrometeorology*, Special WATCH collection. doi: 10.1175/2011JHM1369.1.

- Weghorst, K., 1996. The reclamation drought index: Guidelines and practical applications. Bureau of Reclamation, Denver (CO), 6 pp.
- Wells, N., Goddard, S., Hayes, M.J., 2004. A self-calibrating Palmer Drought Severity Index. *J. Climate*, 17, 2335–2351.
- Wilhite, D.A., 2000. Drought as a natural hazard: Concepts and definitions. *Drought: A Global Assessment, Natural Hazards and Disasters Series 2*, Routledge Publishers, 3–18.
- Wilhite, D.A., Glantz, M.H., 1985. Understanding the drought phenomenon: The role of definitions, *Water Int.* 10(3), 111-120.
- Wotling, G., Bouvier, Ch., Danloux, J., Fritsch, J.-M., 2000. Regionalization of extreme precipitation distribution using the principal components of the topographical environment. *Journal of Hydrology*, 233, 86-101.
- Wu, H., Svoboda, M., Hayes, M., Wilhite, D., Wen, F., 2007. Appropriate application of the Standardized Precipitation Index in arid locations and dry seasons. *Int. J. Climatol.*, 27: 65–79.
- Xu, C.Y., Singh, V.P., 2002. Cross comparison of empirical equations for calculating potential evapotranspiration with data from Switzerland. *Water Resources Management* 16, 197-219.
- Xystrakis, F., Matzarakis, A., 2011. Evaluation of 13 empirical reference Potential Evapotranspiration equations on the island of Crete in Southern Greece. *Journal of Irrigation and Drainage Engineering* 137, 211-222.
- Yahiaoui, A., Touaïbia, B., Bouvier, C., 2009. Frequency analysis of the hydrological drought regime. Case of oued Mina catchment in western of Algeria. *Revue Nature et Technologie* 1, 3-15.
- Yevjevich, V., 1967. An objective approach to definition and investigations of continental hydrologic droughts. *Hydrology Papers* 23, Colorado State University, Fort Collins.

Yevjevich, V., 1983. Methods for determining statistical properties of droughts, in: Coping with droughts, edited by: Yevjevich, V., da Cunha, L., and Vlachos, E., Water Resources Publications, Colorado, 22–43.

Zhang, H., Ho, T.B., Lin, M.S., 2004. A non-parametric wavelet feature extractor for time-series classification. In Proceedings of the Eighth Pacific-Asia Conference on Knowledge Discovery and Data Mining, Sydney, Australia, 595–603.

Zunz, V., Goose, H., Massonnet, F., 2012. How does internal variability influence the ability of CMIP5 models to reproduce the recent trend in Southern Ocean sea ice extent? The Cryosphere Discuss. 6, 3539-3573, doi:10.5194/tcd-6-3539-2012.

*Websites:*

[www.noaa.gov](http://www.noaa.gov)

# Publication list

---

## Peer reviewed conference proceedings

- Koutroulis, A.G., **Vrochidou, A.-E.K.**, Tsanis, I.K., Jacob, D., 2010. Meteorological drought patterns and climate change for the island of Crete. EGU2010-8782, Vienna.

## Peer reviewed journal articles

- Koutroulis, A.G., **Vrochidou A.-E.K.**, Tsanis, I.K., 2011. Spatiotemporal characteristics of meteorological drought for the island of Crete. *Journal of Hydrometeorology* 12 (2), 206-226, doi: 10.1175/2010jhm1252.1.
- **Vrochidou, A.-E.K.**, Tsanis, 2012. I.K., Assessing precipitation distribution impacts on droughts on the island of Crete. *Nat. Hazards Earth Syst. Sci.*, 12, 1159–1171, doi:10.5194/nhess-12-1159-2012
- **Vrochidou, A.-E.K.**, Tsanis, I.K., Grillakis, M.G., Koutroulis, A.G., 2012. The impact of climate change on hydrometeorological droughts at a basin scale. *Journal of Hydrology* 476, 290-301, doi: 10.1016/j.jhydrol.2012.10.046.
- **Vrochidou, A.-E.K.**, Grillakis, M.G., Tsanis, I.K., 2013. Drought assessment based on multi-model precipitation projections. *Journal of Earth Science and Climatic Change* 4 (6), 158, doi:10.4172/2157-7617.1000158.